

University of Windsor

Scholarship at UWindor

Electronic Theses and Dissertations

Theses, Dissertations, and Major Papers

2008

Synergistic effect of PST and Tamoxifen in inducing apoptosis by targeting the mitochondria and insights into novelty of PST induced apoptosis

Peter Siedlakowsk
University of Windsor

Follow this and additional works at: <https://scholar.uwindsor.ca/etd>

Recommended Citation

Siedlakowsk, Peter, "Synergistic effect of PST and Tamoxifen in inducing apoptosis by targeting the mitochondria and insights into novelty of PST induced apoptosis" (2008). *Electronic Theses and Dissertations*. 8026.

<https://scholar.uwindsor.ca/etd/8026>

This online database contains the full-text of PhD dissertations and Masters' theses of University of Windsor students from 1954 forward. These documents are made available for personal study and research purposes only, in accordance with the Canadian Copyright Act and the Creative Commons license—CC BY-NC-ND (Attribution, Non-Commercial, No Derivative Works). Under this license, works must always be attributed to the copyright holder (original author), cannot be used for any commercial purposes, and may not be altered. Any other use would require the permission of the copyright holder. Students may inquire about withdrawing their dissertation and/or thesis from this database. For additional inquiries, please contact the repository administrator via email (scholarship@uwindsor.ca) or by telephone at 519-253-3000ext. 3208.

NOTE TO USERS

This reproduction is the best copy available.

UMI[®]

Synergistic Effect of PST and Tamoxifen in Inducing Apoptosis by
Targeting the Mitochondria and Insights into Novelty of PST Induced
Apoptosis

By: Peter Siedlakowski

A thesis

Submitted to the Faculty of Graduate Studies
through the Department in Chemistry and Biochemistry
in Partial Fulfillment of the Requirements for
the Degree of Master of Science at the
University of Windsor

Windsor, Ontario, Canada

2008

© 2008 Peter Siedlakowski



Library and
Archives Canada

Bibliothèque et
Archives Canada

Published Heritage
Branch

Direction du
Patrimoine de l'édition

395 Wellington Street
Ottawa ON K1A 0N4
Canada

395, rue Wellington
Ottawa ON K1A 0N4
Canada

Your file *Votre référence*
ISBN: 978-0-494-47006-0
Our file *Notre référence*
ISBN: 978-0-494-47006-0

NOTICE:

The author has granted a non-exclusive license allowing Library and Archives Canada to reproduce, publish, archive, preserve, conserve, communicate to the public by telecommunication or on the Internet, loan, distribute and sell theses worldwide, for commercial or non-commercial purposes, in microform, paper, electronic and/or any other formats.

The author retains copyright ownership and moral rights in this thesis. Neither the thesis nor substantial extracts from it may be printed or otherwise reproduced without the author's permission.

AVIS:

L'auteur a accordé une licence non exclusive permettant à la Bibliothèque et Archives Canada de reproduire, publier, archiver, sauvegarder, conserver, transmettre au public par télécommunication ou par l'Internet, prêter, distribuer et vendre des thèses partout dans le monde, à des fins commerciales ou autres, sur support microforme, papier, électronique et/ou autres formats.

L'auteur conserve la propriété du droit d'auteur et des droits moraux qui protègent cette thèse. Ni la thèse ni des extraits substantiels de celle-ci ne doivent être imprimés ou autrement reproduits sans son autorisation.

In compliance with the Canadian Privacy Act some supporting forms may have been removed from this thesis.

Conformément à la loi canadienne sur la protection de la vie privée, quelques formulaires secondaires ont été enlevés de cette thèse.

While these forms may be included in the document page count, their removal does not represent any loss of content from the thesis.

Bien que ces formulaires aient inclus dans la pagination, il n'y aura aucun contenu manquant.


Canada

Declaration of Co-Authorship / Previous Publication

II. Declaration of Previous Publication

This thesis includes 1 original paper that have been previously published/submitted for publication in peer reviewed journals, as follows:

Thesis Chapter	Publication title/full citation	Publication status*
<i>Chapter 3</i>	Siedlakowski P., McLachlan-Burgess A., Griffin C., Tirumalai S., McNulty J., Pandey S. Synergy of pancratistatin and tamoxifen on breast cancer cells in inducing apoptosis by targeting mitochondria. <i>Cancer Biology and Therapy</i> : 2008; 7(3):376-84.	<i>Published</i>

I certify that I have obtained a written permission from the copyright owner(s) to include the above published material(s) in my thesis. I certify that the above material describes work completed during my registration as graduate student at the University of Windsor.

I declare that, to the best of my knowledge, my thesis does not infringe upon anyone's copyright nor violate any proprietary rights and that any ideas, techniques, quotations, or any other material from the work of other people included in my thesis, published or otherwise, are fully acknowledged in accordance with the standard referencing practices. Furthermore, to the extent that I have included copyrighted material that surpasses the bounds of fair dealing within the meaning of the Canada Copyright Act, I certify that I have obtained a written permission from the copyright owner(s) to include such material(s) in my thesis.

I declare that this is a true copy of my thesis, including any final revisions, as approved by my thesis committee and the Graduate Studies office, and that this thesis has not been submitted for a higher degree to any other University of Institution.

ABSTRACT:

Cancer is a devastating disease, affecting millions of individuals every year. Though no cure exists for cancer at present, countless years of research have given rise to promising treatments such as Trastuzumab, Taxol, Tamoxifen, VP-16 and cisplatin. The majority of these treatments are non-selective thus affecting both normal and cancerous cells. Pancratistatin, a natural compound obtained from the Hawaiian spider lily, is known to be specific and selective in inducing apoptosis in multiple cancer cell lines through selectively targeting the mitochondria. In this study it was discovered that PST induced increased levels of cytosolic pro-apoptotic protein Bad in the cytoplasm as well as localization of Bax to the mitochondrial membrane. Release of Cytochrome *c* due to membrane permeabilization indicating the activation of the mitochondrial (intrinsic) pathway of apoptosis was initiated.

Tamoxifen is a known anti-estrogen compound, which has the capability to induce apoptosis in estrogen receptor dependent breast cancers selectively. This compound is relatively non-toxic to normal cells. Recently, it was reported that Tamoxifen has the capability of destabilizing mitochondrial membrane potential. In combination with the anti-estrogen Tamoxifen, PST had a synergic effect in both estrogen receptor positive as well as estrogen receptor negative cells at lower doses than previously reported. Furthermore, whole cell reactive oxygen species levels were increased and mitochondrial destabilization was observed. Thus the present work provides evidence to support the observation that Tamoxifen might work through mechanisms distinct from the canonical estrogen receptor antagonism and act synergistically with PST.

DEDICATION:

I would like to dedicate this thesis to all the lives that have been touched by cancer, not just the ones who suffer directly, but those who live on without a mother, father, sister, or brother.

ACKNOWLEDGMENTS

I would like to first and foremost thank Dr. Pandey for giving me the opportunity to work in his lab. The knowledge, experience, and wisdom gained through his influence will be with me all my life. I would like to thank Mallika for all her exhaustive efforts to help me out over the years. Carly, thanks for all the help in lab related protocols and of course spelling and grammar. Katrina and Daneijla, thank you for your support, but most importantly your friendship. The undergrads that have worked with us, past and present: Aditya, Brandon, Dennis, Sudipa, Pamala, Kristen, Ed, Natasha Rafo, Natasha Sharda, Divya, Subitha and Cynthia, for all there help and above all friendship.

Also, I would like to thank all the professors in the Department of Chemistry and Biochemistry who helped me out over the years. Thanks to: Dr. Vacratsis, Dr. Mutus, Dr. Lee, Dr. Ananvoranich for there generosity in allowing access to there lab equipment. A special thank you to Dr. Swan and Dr. Vacratsis for being on my committee.

Special thanks to Dr. Sridhar for his philosophical and practical input in the matters of scientific research. As well as thank you to Dr. McNulty for providing PST.

A special thank you to the Gail Rosenbaum Foundation, the Lott and John Hetch Memorial Foundation, and the St. Clair Beach Chapter Knights of Columbus for their financial support.

TABLE OF CONTENTS

DECLARATION OF PREVIOUS AUTHOR/CO-AUTHORSHIP	iii
ABSTRACT	iv
DEDICATION:	v
ACKNOWLEDGMENTS	vi
LIST OF FIGURES:	x
LIST OF ABBREVIATIONS	xii
CHAPTER 1: INTRODUCTION	1
1.1 Cancer	1
1.1.1 Cancer Statistics.....	1
1.1.2 Causes of Cancer.....	2
1.2 Breast Cancer	3
1.2.1 Breast Cancer Development	3
1.3 Apoptosis	5
1.3.1 Necrosis and Apoptosis.....	5
1.3.2 Extrinsic pathway.....	7
1.3.3 Intrinsic Pathway	9
1.4 Pro/Anti Apoptotic Proteins.....	12
1.5 Mitochondria.....	14
1.5.1 Mitochondria in Cancer Therapy	17
1.6 Current Chemotherapy Options	19
1.7 Pancratistatin and Tamoxifen	21
1.8 Objectives.....	25
CHAPTER 2: MATERIALS AND METHODS	26
2.1 Cell culture.....	26
2.1.1 Cell lines	26
2.1.2 Media and Supplements.....	26
2.2 Pancratistatin and Tamoxifen	26
2.3 Antibodies.....	27
2.4 Apparatus and Instrumentation.....	27
2.5 <i>In-vitro</i> Proliferation of Cell Lines	28
2.6 Sub-culturing of Cells.....	29
2.7 Treatment of Cells with Anti-Cancer Drugs: PST and Tamoxifen.....	29
2.8 Data Collection and Analysis.....	29
2.9 Nuclear Staining and Phase Microscopy.....	30
2.10 Trypan Blue Staining.....	30
2.11 Flow Cytometry analysis.....	30
2.11.1 Annexin-V Binding Assay.....	31
2.11.2 Tunel Assay.....	31
2.12 Total and Cytosolic Cell Lysate.....	32
2.13 Mitochondrial isolation.....	33
2.14 ROS Detection in Isolated Mitochondria.....	33

2.15 Whole Cell ROS.....	34
2.16 Western Blot.....	34
2.16.1 Protein Estimation.....	34
2.16.2 SDS-PAGE and Gel Transfer.....	35
2.16.3 Immunoblotting Analysis	35
2.17 Whole Cell Caspase-8 Activation Assay.....	36
2.18 Long-term drug resistance and viability study.....	36
2.19 JC-1 Staining.....	37
2.20 In- vivo Treatment Preparation.....	37
2.21 RAG 2M Mouse Care, Xenograft Transplantation and Treatment.....	37
2.22 Tissue Preparation for Histochemical Analysis.....	38
2.23 Tissue Preparation Revision.....	39
2.24 TUNEL Assay With DAPI on Tissue Sections.....	39
2.25 Haematoxylin and Eosin.....	40
2.26 Tissue Preparation for Biochemical Analysis.....	41
CHAPTER 3: RESULTS.....	42
3.1 <i>In-vitro</i> Apoptotic Synergy Exhibited by PST and Tamoxifen.....	42
3.1.1 Susceptibility of MCF-7 Cells to Apoptosis by PST Treatment.....	42
3.1.2 Synergistic Action of PST and Tamoxifen in ER+ MCF-7 Cells.....	43
3.1.3 Induction of Apoptosis in ER- Hs578-T Cells by PST Treatment.....	47
3.1.4 Synergistic Action of PST and Tamoxifen in ER- Hs578-T Cells.....	47
3.1.5 NHF Cells Un-effected by Combined PST and Tamoxifen Treatment.....	50
3.1.6 Quantitative Analysis of Apoptotic Synergy in MCF-7 Cells.....	52
3.1.7 Whole Cell ROS Increases upon PST and Tamoxifen Treatment.....	54
3.1.8 Mitochondrial Membrane Potential Collapse upon Treatment of PST and Tamoxifen.....	57
3.1.9 Mitochondria as the Target for PST and Tamoxifen Induced Apoptosis.....	61
3.1.10 PST and Tamoxifen Cause Release of Cytochrome c Synergistically in Isolated MCF-7 Mitochondria.....	66
3.2 Insights into the Mechanism of PST Induced Apoptosis.....	68
3.2.1 Pro/Anti-apoptotic Protein Expression and Localization upon PST Treatment...	69
3.2.2 Hs-578-T and MCF-7 Cells Exhibit Late Caspase-8 Activation.....	73
3.2.3 MCF-7 Cells do not Exhibit Resistance to PST.....	76
3.3 Preliminary Study of <i>In-vivo</i> PST and Tamoxifen Induced Apoptosis.....	78
3.3.1 Breast Cancer Tumors Successfully Generated in RAG 2M Mice.....	78
3.3.2 TUNEL and DAPI Staining Reveal No Toxicity to Kidney and Liver.....	81
3.3.3 TUNEL and DAPI staining reveal Toxicity to Treated Tumor Samples.....	82
3.3.4 Histological Analysis of Tissues Using Hemotoxalyn and Eosin.....	85
3.3.5 Western Blot Analysis: Kidney, Liver and Tumor Samples.....	89
CHAPTER 4: DISCUSSION.....	94
4.1 Synergy Between PST and Tamoxifen is Estrogen Receptor Pathway Independent..	94
4.2 Role of Mitochondria in Synergistic Response.....	95
4.3 PST and Tamoxifen Treatment Does Not Induce Apoptosis in Normal Cells.....	97
4.4 Localization of Key Apoptotic Factors in PST Induced Apoptosis.....	98

4.5 MCF-7 Cells Do Not Become Resistant to PST Treatment.....100
4.6 *In-vivo* Study of PST and Tamoxifen Synergy.....101

CHAPTER 5: FUTURE PROSPECTS.....103
CHAPTER 6: CONCLUSIONS.....105
REFERENCES.....106
VITA AUCTORIS.....121

LIST OF FIGURES:

Figure 1-1: The Extrinsic Pathway of Apoptosis.....	8
Figure 1-2: The Intrinsic Pathway of Apoptosis.....	11
Figure 1-3a: The Intrinsic Pathway of Apoptosis	16
Figure 1-3b: Opening of the Permeability Transition Pore Complex Mediating Mitochondrial Membrane Permeabilization	16
Figure 1-4a: Chemical Structure Tamoxifen Citrate	24
Figure 1-4b: Chemical Structure Pancratistatin.....	24
Figure 3-1: Apoptotic Index: Dose Response of MCF-7 cells to Pancratistatin and Tamoxifen.....	45
Figure 3-2a: Synergistic response of MCF-7 cells to Pancratistatin and Tamoxifen Treatment MCF-7	45
Figure 3-2b: Apoptotic Index: Synergy of PST and Tamoxifen at High dose PST	46
Figure 3-2c: Apoptotic Index: Synergy of PST and Tamoxifen at Low dose PST	46
Figure 3-3a: Synergistic Response of Hs578-T Cells to PST and Tamoxifen Treatment for 72 Hours	49
Figure 3-3b: Apoptotic Index: Synergistic response of Hs578-T cells to PST and Tamoxifen Treatment.....	49
Figure 3-4a: Combinatorial Treatment of PST and Tamoxifen in NHF Cells	51
Figure 3-4b: Apoptotic Index: Combinatorial Treatment of NHF Cells to PST and Tamoxifen for 72 Hours.....	51
Figure 3-5a: Flow Cytometry: Annexin-V Analysis of PST and Tamoxifen Synergy in MCF-7 Cells.....	53
Figure 3-5b: Flow Cytometry: TUNEL Analysis of PST and Tamoxifen Synergy in MCF-7 Cells.....	53
Figure 3-6a: Whole Cell ROS of MCF-7 Cells Treated With PST and Tamoxifen.....	55
Figure 3-6b: Whole Cell ROS of Hs578-T Cells Treated With PST and Tamoxifen	55
Figure 3-6c: Whole Cell ROS of NHF Cells Treated With PST and Tamoxifen.....	56
Figure 3-7a: : Mitochondrial Membrane Permeability in MCF-7 Cells Treated by PST and Tamoxifen: JC-1 Staining	58
Figure 3-7b: : Mitochondrial Membrane Permeability in Hs578-T Cells Treated by PST and Tamoxifen: JC-1 Staining	59
Figure 3-7c: : Mitochondrial Membrane Permeability in NHF Cells Treated by PST and Tamoxifen: JC-1 Staining	60
Figure 3-8a: Mitochondrial ROS Measurement Isolated From MCF-7 Cells.....	63
Figure 3-8b: Mitochondrial ROS Measurement Isolated From Hs578-T Cells.....	64
Figure 3-8c: Mitochondrial ROS Measurement Isolated From NHF Cells.....	65
Figure 3-9a: : Retention of Cytochrome <i>c</i> Upon Treatment of PST Directly on Isolated MCF-7 Mitochondria.....	67
Figure 3-9b: Retention of Cytochrome <i>c</i> Upon the Combinatorial Treatment of PST and Tamoxifen Directly on Isolated MCF-7 Mitochondria.....	67
Figure 3-10a: Cytosolic Fraction of MCF-7 Cells Treated With 1 μ M PST	70
Figure 3-10c: Mitochondrial Fraction of MCF-7 Cells Treated With 1 μ M PST	70
Figure 3-11a: Cytosolic Fraction of Hs578-T Cells Treated With 1 μ M PST	71
Figure 3-11b: Mitochondrial Fraction of Hs578-T Cells Treated With 1 μ M PST.....	71

LIST OF ABBREVIATIONS

AIF	apoptosis inducing factor
ANT	adenine nucleotide translocase
APAF-1	apoptosis activating factor 1
ATP	adenosine triphosphate
BH(1-4)	bcl-2 homology domains 1-4
BRCA1	breast cancer susceptibility gene 1
BSA	bovine serum albumin
CARD	caspase recruitment domain
Cyp D	cyclophilin D
DAPI	4',6-diamidino-2-phenylindole
Diablo	direct IAP binding protein with low pI
DIGE	2-dimensional in gel electrophoresis
DISC	death inducing signaling complex
DMEM	dulbecco's modified eagle's medium
DMSO	dimethyl sulfoxide
DNA	deoxyribonucleic acid
EDTA	ethylenediamine-tetraacetic acid
EGFR	epidermal growth factor receptor
EGTA	ethylene glycol-bis(2-aminoethylether)- <i>N,N,N',N'</i> -tetraacetic acid
ER	estrogen receptor
FADD	fas associated death domain
FBS	fetal bovine serum
GFP	green fluorescent protein
GTP	guanine triphosphate
H ₂ DCFCA	dichlorofluorescein diacetate
HEPES	N-(2-Hydroxyethyl)piperazine-N'-(2-ethanesulfonic acid)
HRP	horseradish peroxidase
HK	hexokinase
Hs578-T	mammary fibroblast carcinoma
IAP	inhibitors of apoptosis
IR	ionizing radiation
JC-1	5',6,6'-tetrachloro-1,1',3,3'-tetraethylbenzimidazolylcarbocyanine iodide
MAPK	mitogen activated protein kinase
MCF-7	mammary adenocarcinoma
MIM	mitochondrial inner membrane
MMP	mitochondrial membrane potential
MOM	mitochondrial outer membrane
MOMP	mitochondrial outer membrane permeabilization
NADH	nicotinamide adenine dinucleotide
NHF	normal human fibroblast
NR	nuclear receptor
PBS	phosphate buffer saline
PR	progesterone receptor

PST	pancratistatin
PTP	permeability transition pore
RAG 2M	disrupted recombinase activating gene-2
ROS	reactive oxygen species
SDH	succinate dehydrogenase
SDS-PAGE	sodium dodecyl sulphate- polyacrilamide gel electrophoresis
Smac	secondary mitochondrial derived activator of caspases
SRM	selective receptor modulators
TAM	tamoxifen
TBST	Tris-Buffered Saline Tween-20
TGFR	transforming growth factor receptor
TNFR	tumor necrosis factor receptor
TRAIL	TNF related apoptosis inducing ligand
TUNEL	Terminal uridine deoxynucleotidyl transferase dUTP Nick End Labelling
VDAC	voltage dependent anionic channel

CHAPTER 1: INTRODUCTION

1.1 Cancer

Our bodies are immensely complicated machines made up of trillions of cells, each cell containing billions of base pair DNA. This DNA codes for proteins which carry out the roles necessary to maintain normal function and homeostasis within the cell. Protein function is dictated by the structure, which is in turn governed by the genetic code that serves as a blueprint for life. It is therefore mutations in a small group of critical genes (oncogenes) that results in uninhibited cell growth which ultimately leads to tumor development (Kliensmith 2006). The effects of the tumor as felt by the individual can be categorized as invasive; in which the cancer affects surrounding tissue or metastatic; in that the tumor moves to other regions of the body (Kliensmith 2006). These factors lead to interference of normal bodily functions and if left untreated may lead to death.

1.1.1 Cancer Statistics

Cancer is a disease which has continuously plagued societies for thousands of years and even today it remains as one of the most frequently diagnosed and deadly diseases despite exhaustive efforts in cancer research. In 2008 it was projected by the Canadian Cancer Society that new cancer cases will reach 166,000 and cancer related mortality will approach 73,000 in Canada alone (www.cancer.ca). The most common types of cancers differ in males and females. In particular in males the most frequently diagnosed form of cancers include: prostate (20,400 new cases), lung (11,900 new cases) and colorectal (10,600 new cases). In Females the most highly diagnosed forms include:

breast (19,300 new cases), lung (9,300 new cases) and colorectal (9,100 new cases) (www.cancer.ca).

1.1.2 Causes of Cancer

Cancer is caused by a variety of factors including: diet, lifestyle, family health history and exposure to industrial chemicals (Ames *et. al.* 1995). It is therefore adequate to point out that cancer is not a disease with one cause; instead cancer is a heterogeneous disease, which arises from a life-time accumulation of mutations in very specific regions of DNA. This factor influences cancer cell development by causing mutations in the DNA of genes critical to cell growth, cell cycle maintenance and apoptosis inducing genes (tumor suppressor genes). Mutated versions of such genes are termed oncogenes.

Proto-oncogenes are normal genes responsible for inhibition of apoptosis and propagation of cellular growth. When proto-oncogenes become mutated and become oncogenes they resume normal function, however, they do not respond to inhibitory stimuli leading to increased cell division, and inhibition to cell suicide stimulating factors (Osborne *et. al.* 2004, Weinberg 1996). Tumor suppressor genes in normal cells induce apoptosis when the conditions for growth are not met. These genes when mutated to oncogenes lack the normal function and thus prevent the initiation of apoptosis in cancer cells which contributes to cancer cell formation (Chabner, Roberts 2005, Weinberg 1996).

It has been found that lifestyle, environment and diet are immensely tied into cancer cell development and is responsible for approximately 80% of all cancers cases (Ames *et. al.* 1995). Compounds which reduce the body's capacity to dealing with

oxidative stress increase the propensity of oxidative damage to cellular DNA. The most common cause of such DNA mutation in cancer is smoking cigarettes. Tobacco products consumed by individuals are responsible for one third of all cancer cases. The exact mechanism of cancer cell development by these products is unknown, however it is postulated that these compounds reduce the amount of natural anti-oxidants circulating the body, thereby sensitizing individuals to oxidative stress induced DNA mutation (Ames *et. al.* 1995).

1.2 Breast Cancer

Breast cancer is the most highly diagnosed carcinoma in women, new cases of this disease are projected to reach 19,300 in 2008 (www.cancer.ca). For this reason it has been one of the most fiercely researched forms of cancer. Due to such research efforts great progress has been made in the understanding of this disease and its progression.

1.2.1 Breast Cancer Development

Breast cancer like all cancers is a genetically and clinically heterogeneous disease. The specific causes of this disease have been significantly studied and it has been shown to arise primarily as a result from the malignant transformation of mammary stem and/or progenitor cells (LaMarca, Rosen 2008). Post natal mammary gland development is coordinated by both systemic hormones and growth factors. In particular hormones such as progesterone and estrogen drive the development of mammary tissue through the actions of their respective receptors: progesterone receptor (PR) and estrogen receptor (ER) respectively (LaMarca, Rosen 2008). However, up-regulation of the proto-oncogene

estrogen receptor has been shown to increase the probability of breast tumor development (Mense *et. al.* 2008). Furthermore specific genes have been found to have a high frequency of mutation in breast cancer increasing the probability of disease development. In particular, it has been found that mutations in tumor suppressor genes: p53 and BRCA1 increases the propensity of breast cancer development (Gayther *et. al.* 1995).

Estrogen receptors (ER's) are members of the nuclear receptor superfamily (NR's) and induce the pleiotropic effects of estrogen (Shao, Brown 2003). The effect of the estrogen receptor plays a critical role in the physiology and developmental processes of normal breast tissue by inducing expression of specific genes. At present two types of estrogen receptors have been discovered ER α and ER β which have distinctly opposite roles. Estrogen receptor α (ER α) plays a pivotal role in mammary cell development by acting as a transcription factor of key genes responsible for growth such as transforming growth factor receptor (TGF) and epidermal growth factor receptor (EGFR) (Mandlekar, Kong 2001). Interestingly it was found that ER α is antagonistic to the functions of ER β which primarily acts to suppress growth of the cell (Mandlekar, Kong 2001). Therefore the growth of ER α positive breast cancers has been shown to be accelerated in presence of estrogen (Mense *et. al.* 2008).

Mutation in genes responsible for programmed cell death has been linked to breast cancer development. In particular, the tumor suppressor gene p53 has been shown to be mutated in approximately 30-50% of all breast cancer cases (Halder *et. al.* 1994). Normal p53 when activated is responsible for inhibition of cell cycle propagation and initiation of cell suicide via apoptosis. However, in breast cancer cells this mechanism is

inhibited by the lack of functioning p53 (mutated p53) and therefore genetic mutations propagate into daughter cells potentially leading to tumorigenesis (Halder *et. al.* 1994).

Also, mutations in the tumor suppressor gene termed breast cancer susceptibility gene 1 (BRCA1) have been shown to increase the incidents of developing breast cancer (Gayther *et. al.* 1997). BRCA1 is a DNA damage response protein involved in DNA repair caused by ionizing radiation (Hongtae, Junjie 2008). Mutations in this gene therefore reduce the cells potential in DNA repair increasing incidence of further mutations and tumor development. In particular, germ line mutations in BRCA1 gene have been shown to occur in 80-90% of familial cases of breast cancer (Gayther *et. al.* 1995).

1.3 Apoptosis

The cell consists of complex biochemical machinery that is critical to the normal homeostasis and survival of the organism as a whole. When a cell no longer suits the need of the organism it undergoes a suicide program termed apoptosis. Apoptosis was first discovered in 1972 by Kerr *et. al.* who found that cell death processes can be categorized into two distinct forms: necrosis and apoptosis.

1.3.1 Necrosis and Apoptosis

Necrosis can be defined as pathological, inappropriate and passive. It is brought about by physical or chemical factors such as heat, pressure, injury and chemical damage (Szabo *et. al.* 2005). The changes within the cell upon such stimuli are random and do not exhibit any distinct pattern because they are not controlled by any internal biochemical

mechanism. Instead they bring about random damage to the many different organelles that are integrated within the cellular environment. Such damage causes inflammatory responses within the organism through the facilitated action of immune cells like macrophages (Haslett 1992).

Apoptosis by contrast to necrosis can be defined as a physiological, appropriate and active process which simply acts to activate a complex biochemical pathway that acts to initiate cell suicide and remove the damaged cell from the organism. Initiation of this process can be activated by factors such as cellular receptors, DNA damage, growth factor deprivation and cell cycle arrest (Hickey *et. al.* 2001).

Once initiated this process requires the input of energy in the form of ATP and the activation of proteases named caspases to orderly deconstruct the cell into very distinct and visible components. In general the process involves the ordered destruction of cells and phosphatidyl serine flipping which acts to recruit phagocytes which exhibit non-inflammatory responses (Pandey *et. al.* 2000, Green, Reed 1998). Due to this order, distinct apoptotic features can be visualized under a light and fluorescent microscope including: DNA fragmentation, phosphatidyl serine flipping, membrane blebbing and mitochondrial membrane potential collapse (Duke *et. al.* 1996).

Two distinct pathways exist in which a particular stimulus can induce apoptosis. The two pathways are termed intrinsic and extrinsic, however the ultimate effect of both pathways is the depolarization of mitochondrial membrane potential leading to permeabilization and the release of apoptogenic factors such as AIF, cytochrome C, and SMAC Diablo.

1.3.2 Extrinsic Pathway

Apoptosis can be initiated by a specific group of death receptors on the surface of the cellular membrane termed TNF receptor (tumor necrosis factor). The TNF receptor family includes Fas receptor, TNF and TRAIL (TNF related apoptosis inducing ligand) (Degterev *et. al.* 2003). Apoptosis by the extrinsic method is initiated by ligands that bind to the receptor and induce a conformational change on the receptor which induces apoptotic events. One key event induced by ligand binding to “death receptors” is the recruitment of key proteins which form a death induced signaling complex (DISC) (Ashkenzai, Dixit 1998). Once formed, the DISC complex acts to activate caspase-8 through cleavage of the zymogen procaspase-8 (**figure 1-1**). Caspase-8 then processes Bid to truncated Bid (tBid) which in turn acts to destabilize the mitochondrial membrane which releases apoptogenic factors that cause activation of caspase-3 (Ashkenzai, Dixit 1998). Therefore, Bid activation into tBid links the extrinsic pathway of apoptosis to that of the intrinsic pathway (Chou *et. al.* 1999, McDonnell *et. al.* 1999, Korsmeyer *et. al.* 2000).

Figure 1-1: The Extrinsic Pathway of Apoptosis

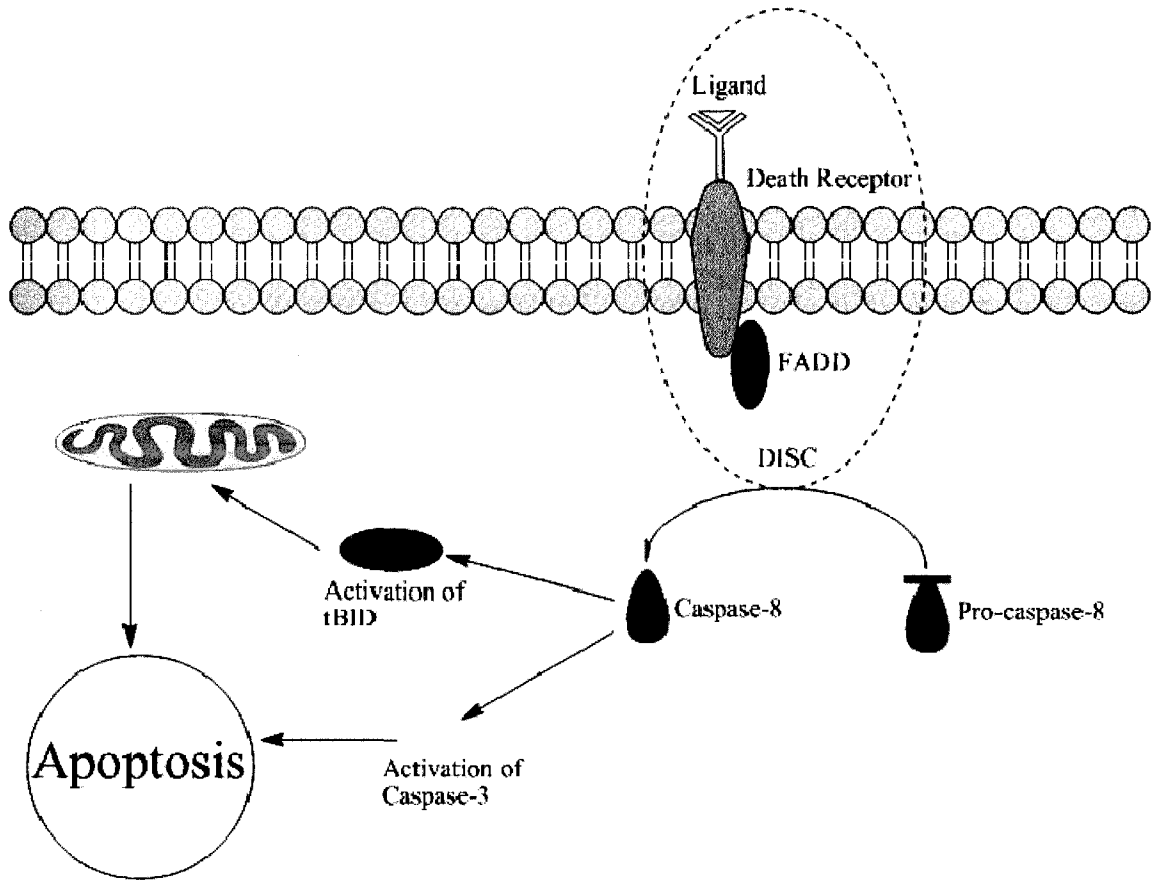


Figure 1-1: The extrinsic pathway of apoptosis

In the extrinsic pathway of apoptosis, the death receptors are activated by ligand binding, which leads to the formation of DISC (death inducing signaling complex) and the activation of caspase-8. Active caspase-8 causes the activation of caspase-3 and the formation of tBid, both of which lead to apoptosis.

1.3.3 Intrinsic Pathway

Intrinsic pathway begins with cellular stress induced internally such as DNA damage induced by DNA damaging agents such as: radiation, chemotherapies and reactive oxygen species (Kroemer, Reed 2000). The intrinsic process of apoptosis is centered on destabilization of mitochondrial membrane potential by pro-apoptotic proteins.

When a DNA damaging agent is presented to a cell, the general intrinsic pathway which is followed includes activation of p53 transcription factor, which up-regulates pro-apoptotic proteins including Bax. Bax, when activated, will localize to the outer mitochondrial membrane and induce mitochondrial destabilization. Bax can induce destabilization directly or indirectly. Direct mitochondrial pore formation through Bax is thought to occur by Bax homodimerization (**figure 1-3a**). Indirect Bax induced mitochondrial pore formation is believed to occur mainly through the interaction with the PTP (protein transition pore) complex on the outer mitochondrial membrane (**figure 1-3b**). Bax binding to the PTP induces opening of the PTP (Reed 2000). Depolarization of mitochondrial membrane potential leads to the release of apoptogenic factors such as cytochrome *c*, SMAC Diablo and AIF (Green and Reed 1998).

Cytochrome *c*, once released from the mitochondria, forms an ATP dependent complex with APAF-1 (apoptosis activating factor-1) and caspase-9 termed the apoptosome (Ashkenazi, Dixit 1998). The apoptosome then serves the role of inducing activation of caspase-3 through cleavage of a zymogen procaspase-3 (**figure 1-2**). Caspase-3 is an enzyme which is a part of a broad family of enzymes termed aspartyl specific cystienyl protease, which act via proteolysis through the cleavage of specific

recognition amino acid sequence (DEVD). Caspase-3 translocates to the nucleus when activated and targets key proteins for proteolysis such as ICAD (inhibitor of caspase-activated DNase), once activated ICAD acts to cleave DNA in an ATP dependent manner and causes chromatin condensation (Li *et. al.* 1997).

Smac/DIABLO (direct IAP binding protein with low pI) was found to be released from the mitochondrial membrane along with cytochrom C (Verhagen *et. al.* 2000). This protein was found to promote apoptosis by binding to and inhibiting IAP (inhibitor of apoptosis protein). IAP acts to inhibit caspases necessary to propagate the apoptotic signal cascade (Verhagen *et. al.* 2000).

It was observed that a key apoptogenic factor exists which can bypass the caspase cascade all together and directly induce the effects of caspases. Apoptosis inducing factor (AIF) was found to translocate to the nucleus once released from the mitochondrial membrane and induce chromatin condensation and DNA degradation (Susin *et. al.* 1999).

Figure 1-2: The Intrinsic Pathway of Apoptosis

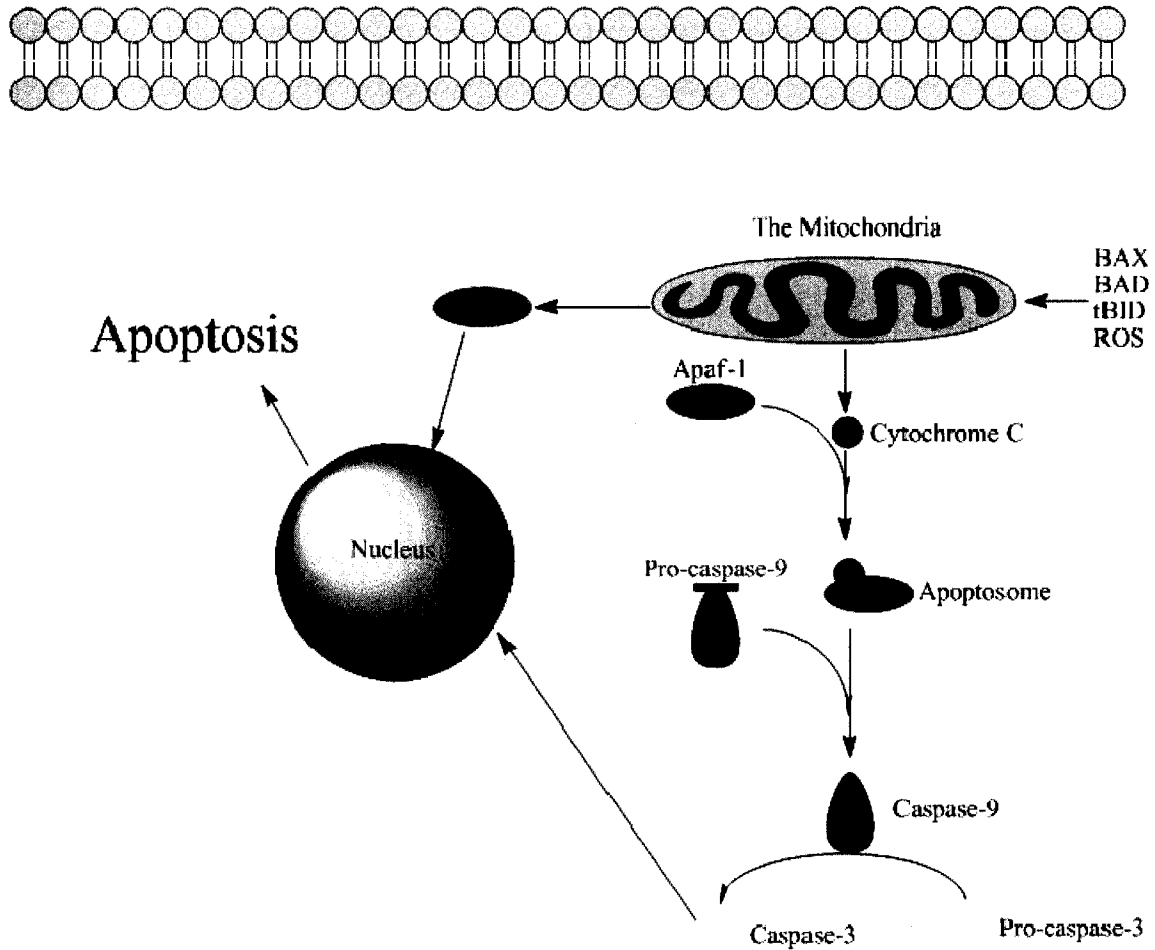


Figure 1-2: The intrinsic pathway of apoptosis, outer mitochondrial membrane permeabilization by pro-apoptotic proteins (tBid, Bax, Bok) leads to the release of cytochrome c forming the apoptosome and activating caspase-9, leading to caspase-3 activation. Simultaneously, AIF are released and trans-locates to the nucleus, where it induces DNA fragmentation. As well, Smac/Diablo is released which inhibits inhibitors of apoptosis proteins leading to prolonged caspase activation.

1.4 Pro/Anti-apoptotic Proteins

Bcl-2 is a family of pro and anti-apoptotic proteins which contain homologous domains; these domains are termed Bcl-2 homologous domains (BH domains) which range from BH1-BH4 (Hunter *et. al.* 1996, Chinnadurai, Lutz 1995). Interaction of pro/anti-apoptotic proteins involved in apoptotic regulation mainly involves the BH domain. Currently, there are approximately 15 known pro/anti-apoptotic proteins. Bcl-2-family members share one or more Bcl-2 homologous (BH) domain and are divided into two main groups according to whether they promote (pro-apoptotic) or inhibit (anti-apoptotic) apoptosis. The pro-apoptotic family members are further classified according to whether they contain multiple BH domains or BH3 only. The BH3-only proteins are pro-apoptotic and require the co-operation of their multidomain relatives to induce apoptosis (Kuwana, Newmeyer 2003).

Anti-apoptotic proteins include: Bcl-2, Bcl-xl, Bcl-w, Mcl-1, and A1. These proteins act to protect the cell mitochondria against permeabilization by sequestration of pro-apoptotic proteins. All anti-apoptotic proteins contain some variation of BH1 and BH2 domain, however the proteins Bcl-2 and Bcl-xl contain all four (BH1-BH4) conserved domains (Levine *et. al.* 2008). The protein Bcl-2 acts to protect the mitochondria by binding to Bax and forming Bax/Bcl-2 heterodimers inhibiting the localization of Bax to the mitochondria and subsequently protecting against permeabilization of the outer mitochondrial membrane (Goping *et. al.* 1998). Also, anti-apoptotic proteins such as Bcl-2 and Bcl-xl reside on the outer mitochondrial surface inhibiting mitochondrial membrane potential collapse caused by the pro-apoptotic proteins Bax and Bak (Levine *et. al.* 2008).

Pro-apoptotic proteins containing BH1-BH3 domains include: Bax, Bak and Bok. Bax and Bak have the ability to destabilize the mitochondrial membrane directly. Work by Wolter *et. al* 1997 showed that localization of GFP fused Bax from the cytosol to mitochondria is a crucial event during apoptosis leading to mitochondrial destabilization. Investigations by Kuwana *et. al.* 2002 showed that Bax in presence of Bid has the ability to form pores on the mitochondrial membrane directly, thus allowing the release of apoptogenic factors from the inter-mitochondrial membrane space. Furthermore, work by Shimizu *et. al.* 1999 suggests that Bax and Bak have the ability to interact with voltage dependent anionic channels (VDAC) on the mitochondrial membrane and thus permeabilize the mitochondrial membrane allowing molecules such as Cytochrome *c* to be released (**figure 1-3b**).

Other pro-apoptotic proteins contain only BH3 domain and are comprised of only alpha helix structure with no mitochondrial membrane binding domain, these include: Bad, Bid, Bik, Bcl-2, BNIP3 and BimL (Kuwana Newmeyer 2003). BH3 only proteins are believed to play two distinct roles which are: localize pro-apoptotic proteins from cytosolic compartments to the mitochondrial membrane (Bid) and sequestering anti-apoptotic proteins (Bad) (Levine *et. al.* 2008). The BH3 only peptides Bid and Bim activate Bax and Bak directly, whereas the Bad and Bik BH3 peptides act indirectly by inactivating Bcl-xL or Bcl-2, thus allowing Bax and Bak to act unopposed (Kuwana Newmeyer 2003). Therefore the pro-apoptotic mechanism primarily involves the destabilization of the mitochondrial membrane.

1.5 Mitochondria

Mitochondria play an integral role in energy metabolism through oxidative phosphorylation, which generates energy in the form of ATP that is essential for the various biochemical reactions inside a cell (Leist *et. al.* 1997). Energy metabolism in the mitochondria involves reduction of O_2 into H_2O by electron transfer mechanisms through redox reaction in the electron transport chain. There are many internal factors within the mitochondria which when released activate the cellular processes involved in the induction of apoptosis. Therefore, mitochondria play a central role in both the intrinsic and extrinsic apoptotic pathways. The key outcome of both processes is induction of mitochondrial membrane collapse and release of the key mitochondrial apoptogenic factors such as Cytochrome *c*, AIF, and Smac/DIABLO (Green, Kroemer 2004, Yuan *et. al.* 2001 Kroemer, Reed 2000, Zoratti, Szabo 1997).

As described earlier the release of the apoptogenic factors within the mitochondria is guided by one of two potential mechanisms that lead to mitochondrial membrane potential (MMP) collapse. The first is by direct pore formation through the localization of pore forming pro-apoptotic proteins such as Bax and Bak (**figure 1-3a**) (Green, Kroemer 2004) and the second is by opening of the mitochondrial protein transition pore complex.

The opening of mitochondrial permeability transition pore complex (MPTP) is a crucial event in apoptosis. This complex includes the voltage dependent anionic channels (VDAC) which detects a change in mitochondrial membrane potential ($\Delta\Psi_m$) and thus opens the MPTP complex allowing molecules of up to 5000 Daltons to pass through (Harris, Thompson 2000, Zoratti, Szabo 1997). Other integral components of the MPTP

include adenine nucleotide transporter (ANT), benzodiazepine receptor, hexokinase (HK) and cyclophilin D (**figure 1-3b**). The MPTP complex can be opened directly through interaction with pro-apoptotic proteins such as Bax, partial failure of electron transport chain, cellular increases in reactive oxygen species and increases in the intra Ca^{2+} concentrations (Zoratti, Szabo 1997).

Figure 1-3a: Bax/Bak Mediated Mitochondrial Membrane Permeabilization

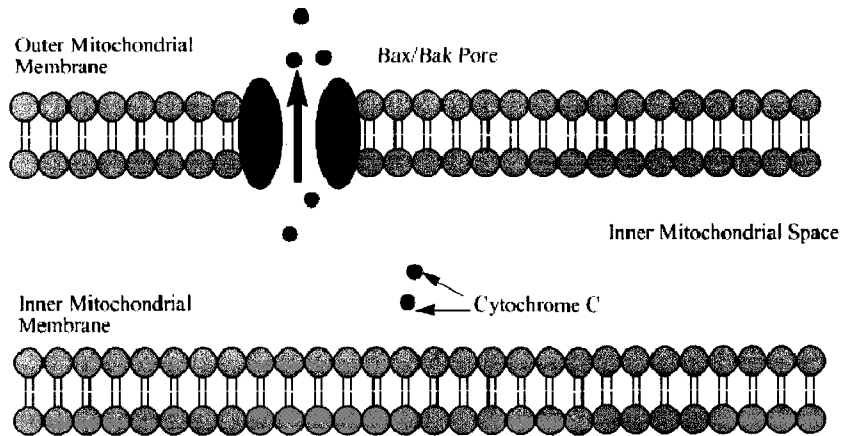


Figure 1-3a: Bax/Bak mediated mitochondrial membrane permeabilization. Upon induction of apoptotic pathway, Bax and Bak migrate to the outer mitochondrial membrane where they homodimerize and form pores. This pore leads to the release of Cytochrome c, as well as other apoptogenic factors (Smac/DIABLO, AIF).

Figure 1-3b: Opening of the Permeability Transition Pore Complex Mediating Mitochondrial Membrane Permeabilization

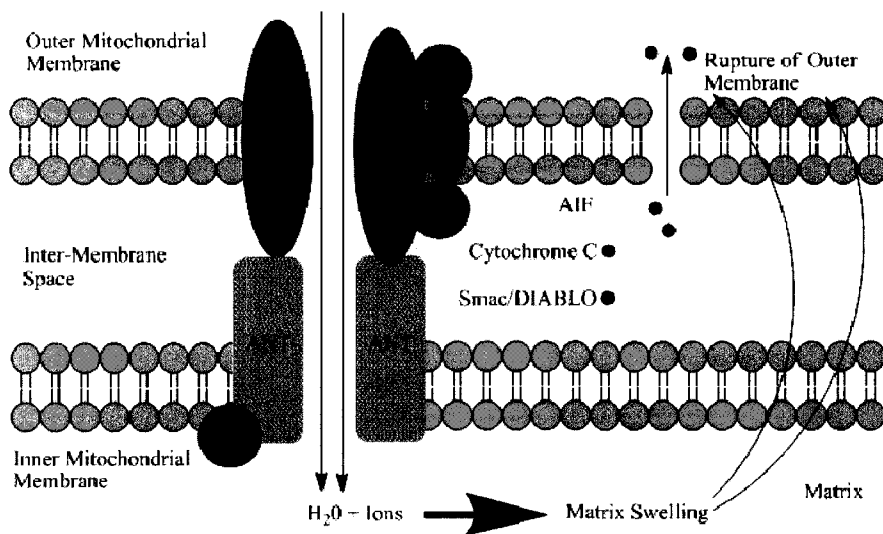


Figure 1-3b: Opening of the permeability transition pore complex mediating mitochondrial membrane permeabilization. Upon induction of apoptotic pathway, BAX interacts with VDAC on the PTP where it leads to the opening of the PTP complex. Rapid in flow of H₂O and ions leads to swelling of the mitochondrial matrix and rupture of the outer mitochondrial membrane releasing apoptogenic factors such as cytochrome C, AIF and Smac/DIABLO.

1.5.1 Mitochondria in Cancer Therapy

Cancer cells have devised mechanisms that inhibit mitochondrial dysfunction and prolong life of the cell in presence of various stresses. Recent advances in cancer research have uncovered key differences between cancer and normal cell mitochondria such as: mitochondrial membrane potential, metabolism, mitochondrial DNA mutations and mitochondrial integrity due to rapid cell division. It is therefore possible to exploit these key differences in cancer cell mitochondria to induce apoptosis in cancer cells selectively.

A key difference in cancer cell metabolism over that of normal cells is the use of anaerobic metabolism as opposed to aerobic metabolism (Modica-Napolitano, Singh 2002). This phenomenon has been named the “Warburg phenomena” where the reliance on anaerobic metabolism aids in the protection of cancer cells from mitochondrial induced apoptosis by reducing the risk of reactive oxygen species induced opening of the MPTP complex (Green, Kroemer 2004). Despite this phenomena, it has been observed that cancer cells have an increase in mitochondrial membrane potential ($\Delta\Psi_m$) (Modica-Napolitano, Singh 2002, 2004) as observed by localization of the cell membrane permeable cationic dye Rh123. Experiments show that this dye accumulates in the mitochondria of cancers including: kidney, ovary, pancreas, lung, adrenal cortex, skin, breast, prostate, cervix, vulva, colon, liver and testis in greater extent than the normal cell counterparts (Don, Hogg 2004). The hydrophobic nature of the compound is believed to affect electron transport chain and ATP synthesis causing mitochondrial dysfunction. This result indicates that the increase in mitochondrial membrane potential in cancer cells

is driving the accumulation of the molecule into the mitochondria and also causing toxic effects specifically in cancer cells (Don, Hogg 2004).

Mitochondrial DNA accounts for only 1% of expressed DNA inside a cell. However the expression of genes from mitochondrial transcript DNA (mtDNA) is imperative for normal cellular function (Modica-Napolitano, Singh 2004). Unlike mammalian DNA, mtDNA has no introns, and no protective histones. Furthermore, mtDNA is continuously exposed to oxidative stress due to oxidative phosphorylation reactions. Work by Selvanayagam *et. al.* 2004 revealed that mutations in mtDNA of NADH dehydrogenase subunit III is a phenotype associated with renal cell carcinoma.

Rapid cell cycle progression due to over-expression of genes responsible for cellular growth is a phenomenon commonly observed in cancer cells. Due to this occurrence, additional mitochondrial differences have been observed in cancer cells when compared to normal cell mitochondria. It was recently postulated that cancer cell mitochondria are unable to properly ensure proper formation of mitochondrial membrane components during mitosis (Modica-Napolitano, Singh 2002, 2004). This lack of proper mitochondrial replication during mitosis has the potential to cause the development of mitochondria with altered inner and outer mitochondrial membrane compositions (Villa, Doglia 2004).

These differences between cancer and normal cell mitochondria have the potential to give rise to novel targets for chemotherapeutics research. A new class of compounds termed “mitocans” has been proposed which have the ability to exploit the vulnerability of cancer cell mitochondria (Neuzil *et. al.* 2007). Vitamin E analogues have recently shown promise to target cancer cell mitochondria. One such compound which shows

selectivity in inducing apoptosis through mitochondrial destabilization in cancer cells at concentrations that is tolerated by normal cells is the vitamin E analogue α -tocopheryl succinate (Neuzil *et. al.* 2007). Another compound, lonidamine, has been shown to cause opening of the mitochondrial transition pore complex through binding to the adenine nucleotide transporter site (Neuzil *et. al.* 2007). Therefore the mitochondria can provide novel targets for selective apoptosis induction (Kroemer 2003).

1.6 Current Chemotherapy Options

Current cancer treatment strategies depend on the severity of the disease. Upon diagnosis of cancer, the treatment methods available include systemic and local intervention. New techniques and compounds have led to prolonged life and sometimes complete inhibition of cancer re-occurrence. Unfortunately no cure exists and drugs used as chemotherapies can have drastic side effects which in turn have the potential to do more harm than good to the patient.

Local therapies include surgical intervention and ionizing radiation (IR). Removal of the cancerous growth is accomplished by surgical intervention along with supplemental drugs to prevent reoccurrence of the disease. Radiation therapy is given to approximately 70% of cancer patients (Martin 2001). This treatment involves inducing oxidative stress leading to DNA damage on cancerous tissue through focused beams of ionizing radiation (Jeremic 2004). Unfortunately the ionizing beam of radiation also affects nearby normal cells, increasing the probability of DNA damage in normal tissue potentially leading to formation of secondary tumors (Zhang *et. al.* 2001).

Nearly 50% of all newly diagnosed cancer patients will receive some form of systemic chemotherapy (Martin 2001). Systemic therapies vary in the way that they target a particular cancer cell however the overall desired effect of these therapies remains the inhibition of growth and the induction of apoptosis. These therapies work simply by the fact that cancer cells divide rapidly and therefore are more vulnerable to stresses that are imposed to replication machineries. Specific targets of systemic therapies include: cell surface receptors, hormonal receptors, DNA, and cell cycle machinery.

Immunotherapy's act on specific protein targets on the cancer cell membrane. They induce immunological responses and activate internal cellular processes that lead to apoptosis. This type of chemotherapeutic strategy is used in the treatment of breast and leukemic cancers (Kim 2005). One such immunotherapy named Trastuzumab is a monoclonal antibody therapy which targets breast cancers that expresses HER-2 which is an epidermal growth factor responsible for cellular growth (Duffy 2005). Once bounded to HER-2 Trastuzumab causes down modulation of HER-2 leading to: cell cycle arrest through p27, immune response, and inhibition of angiogenesis (Duffy 2005). Unfortunately, treatment with Trastuzumab is limited to cancers expressing HER-2 and current research indicates that even when HER-2 expression is high the effect of Trastuzumab is limited to the duration of therapy (Albanell, Baselga 2001).

Hormonal therapies include a class of drugs termed Selective Receptor Modulators (SRM's). These compounds are selective for certain types of breast, ovarian and thyroid cancers which exhibit specific cellular receptors (Kleinsmith 2006). Tamoxifen is the prototypic SRM, which acts antagonistically on the estrogen receptor

(Smith *et. al.* 2004). Estrogen receptor as previously mentioned is a transcription factor involved in expressing proteins critical for maintaining cell growth and survival (Shao, Brown 2003). Therefore the antagonistic effect of Tamoxifen acts by sequestering the estrogen receptor so that it cannot bind to estrogen and therefore cutting off vital receptor mediated growth mechanisms. The benefit of this therapy is that it is selective only towards cells that exhibit estrogen receptor and therefore has little toxic effects towards normal cells. However, the downside is that it is limited to cancers expressing the estrogen receptor.

Cell cycle inhibitory drugs act by reducing the rate of mitosis thereby leading to apoptosis. The class of drugs called Taxanes, isolated from the pacific yew tree, works in such a way. In particular, one such compound called Taxol, acts to induce apoptosis by microtubule stabilization during mitosis. Taxol binds to pockets in β -Tubulin inhibiting GTP hydrolysis of the other side of the polymer (Yeung *et. al.* 1999). Inhibition of microtubule depolymerization in G2-M phase leads to bcl-2 phosphorylation which inhibits bcl-2's normal anti-apoptotic activity, therefore leading to apoptosis (Yeung *et. al.* 1999). Unfortunately, taxol is non-specific and exhibits toxicity to normal cells leading to drastic side-effects to the patient. For this reason selective targeting of cancer cells is a priority in novel therapeutic strategies in cancer therapy research.

1.7 Pancreatistatin and Tamoxifen

The vast amount of research in cancer therapeutics has given rise to many compounds which target many biochemical processes in cancer cells. All the research in such compounds have made great strides in therapeutic options to patients, however the

limitations of each individual treatment remains with respect to unwanted and drastic side effects. Therefore, the current focus is in the development of compounds which are toxic and selective towards cancer cells.

Previous investigations with Tamoxifen (**figure 1-4a**) have established the antagonistic action of this drug on the estrogen receptor. Current advances in Tamoxifen research have shown that it plays roles outside the normal estrogen receptor antagonism, which induces apoptosis in ER⁺ cancer cells. Tamoxifen induced apoptosis involves biochemical pathways involving: Protein kinase C induced apoptosis, binding to calmodulin, induction of c-Myc, mitogen activated protein kinases (MAPK) and mitochondrial dysfunction (Mandlekar, Kong 2001). In particular, work by Moreire *et. al.* 2006, has shown that Tamoxifen has binding affinity to complex 1 of the electron transport chain, which in turn causes destabilization of mitochondrial membrane potential and increases levels of reactive oxygen species. Also, work done by Kallio *et. al.* 2005, showed that MCF-7 (mammary adenocarcinoma) cells treated with 5-7 μ M Tamoxifen in serum free media exhibited mitochondrial dysfunction, reactive oxygen species increases and Cytochrome *c* release.

There is a clear link between consumption of natural compounds and decreased susceptibility to disease. Epidemiological research has proven that consumption of phytochemicals from fruits and vegetables results in reduced risk of cancer development over the lifetime of an individual (Reedy *et. al.* 1997). Therefore, isolating natural substances which show promise as anti-cancer compounds, is an approach used by many researchers and has thus opened the window to current chemotherapeutics (taxol) and future promising compounds (pancratistatin).

Pancratistatin (**figure1-4b**) is a natural compound that was originally isolated from the spider lily *Pancreatum Litorale* in 1993 by Pettit *et. al.* Early work with PST revealed the potential to act as an anti-neoplastic and anti-fungal agent (Luduena *et. al.* 1992). Pharmacological work with PST has been limited due to the low yield obtained from extraction of this compound from the spider-lily, therefore, surprisingly little *in-vivo* and *in-vitro* work has been completed in PST related research. Previous results from our lab demonstrated the ability of PST to induce apoptosis in cancer cells (McLachlan *et. al.* 2005). Importantly, the effects of PST induced apoptosis were found to be selective towards cancer cells and having no toxic effects towards normal cell lines. (McLachlan *et. al.* 2005). The exact biochemical mechanism of action in PST induced apoptosis is unknown, however recent advances in our lab demonstrate that this drug has potential targets existing directly on the mitochondria of cancer cells leading to selective induction of apoptosis. Therefore, research is currently being undertaken in our lab to exploit this feature of cancer selectivity, and understand the mechanism of how this phenomenon occurs.

Figure 1-4a: Chemical Structure Tamoxifen Citrate

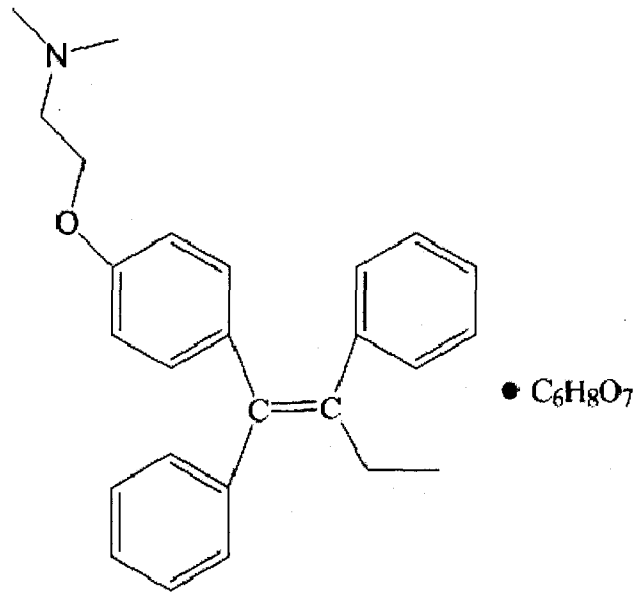


Figure 1-4a: Chemical structure of tamoxifen citrate

Tamoxifen citrate ($C_{32}H_{37}NO_8$) has a molecular weight of 563.32g/mol. The molecular structure is shown here

Figure 1-4b: Chemical Structure of Pancratistatin

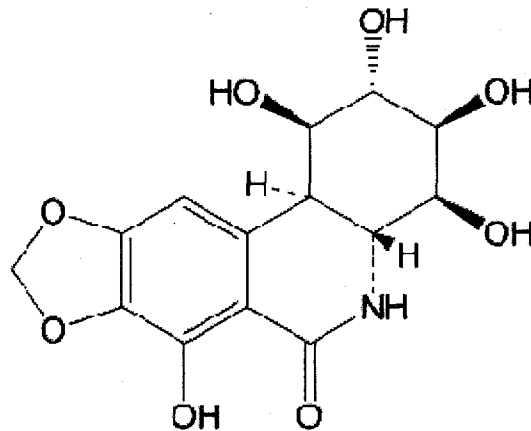


Figure 1-4b: Chemical structure of pancratistatin

Pancratistatin ($C_{14}H_{15}NO_8$) has a molecular weight of 325.28g/mol. The molecular structure is shown here.

1.8 Objectives

The present study expands upon the previous work completed on PST which established this compound as a selective inducer in apoptosis by targeting the mitochondria. The objectives of this investigation include:

1. Study combinatorial treatment of cancer cells with PST and Tamoxifen in both ER negative and ER positive breast cancer cells as well as determine the level of toxicity to normal cells *in-vitro*.
2. Investigate biochemical features in PST induced apoptosis in both Hs578-T and MCF-7 cell lines in order to gain key insights into the biochemical mechanism induced by PST treatment.
3. Establish a mouse breast cancer model in order to investigate the *in-vivo* response of PST and Tamoxifen treatment.

CHAPTER 2: MATERIALS AND METHODS

2.1 Cell Culture

2.1.1 Cell lines

Normal human fibroblast (NHF) cells (AG09309) were obtained from Coriell Institute for Medical Research, Camden, NJ, USA. Mammary gland adenocarcinoma (MCF-7) cells were obtained as a gift from Dr. Hubberstey and Dr. Porter, University of Windsor as well as purchased from American Type Culture Collection (ATCC). Mammary gland carcinoma (Hs-578T) cells were obtained from the American Type Culture Collection (ATCC), Manassas, VA, USA.

2.1.2 Media and Supplements

Dulbecco's modified Eagle's medium (DMEM) / nutrient mixture Ham's F-12 medium modified with 2 mM L-glutamine obtained from Sigma Chemical Company, Mississauga, Ontario, Canada. L-Glutamine and Gentamycin were purchased from Invitrogen Canada Inc., Burlington, Ontario, Canada. Fetal bovine serum (FBS), glucose, bovine insulin, sodium bicarbonate and sodium pyruvate were purchased from Sigma Chemical Company, Mississauga, Ontario, Canada.

2.2 Pancratistatin and Tamoxifen

Pancratistatin (PST) was obtained from our collaborator, Dr. James McNulty, McMaster University, Hamilton, Ontario, Canada. PST was isolated from the bulb of the *Hymenocallis littoralis*, a spider lily native to the islands of Hawaii, following a previously

published method (Pettit *et al.* 1993). Tamoxifen Citrate was purchased from Sigma Chemical Company, Mississauga, Ontario, Canada.

2.3 Antibodies

Monoclonal primary antibodies raised in mouse were purchased from Sigma Chemical Company, Mississauga, Ontario, Canada these consisted of: anti-Bax, anti-Bcl-xl and anti-Bcl-2. Polyclonal primary antibodies raised in rabbit were purchased from Sigma Chemical Company, Mississauga, Ontario, Canada and consisted of: anti-Actin and anti-Bad. Furthermore polyclonal primary raised in rabbit anti-Succinate Dehydrogenase B and monoclonal primary raised in mouse anti-Cytochrome c antibodies were purchased from Santa-Cruz Biotechnology Inc., Santa-Cruz, CA. Secondary anti-rabbit and secondary anti-mouse conjugated antibodies to HRP were purchased from Sigma Chemical Company, Mississauga, Ontario, Canada.

2.4 Apparatus and Instrumentation

The Leica DM IRB fluorescent microscope was obtained from Lieca, Wetzlar Germany. The multi-well plate reader, Spectra Max Gemini XS, was obtained from Molecular Devices, Sunnyvale, California and the UV-Visible Spectrophotometer was purchased from Thermo Technologies. Chemi-Imager v5.5 (Alphatech Inovations) was used to visualize westernblots. A Becton Dickinson FACSCalibur flow cytometer was used at Wayne State University.

Cell culture was conducted under sterile conditions in a class-II type A/B3 Biosafety cabinet (NuAire Inc., Plymouth, MN, USA), and all cultures were maintained in a CO₂ incubator containing a HEPA filter (Thermo Forma Scientific, Inc, Marietta, OH, USA)

Centrifugation was conducted using a low speed Jouan CR3-I centrifuge (Jouan by Thermo Electron Corporation, Waltham, MA, USA) and a MC2 DESAGA centrifuge (Sarstedt-Gruppe, Montreal, Quebec). Other general laboratory equipment included the following: a pH Meter (VWR, Model 8100) with buffer solutions from VWR, Adventurer balance (OHAUS, Ontario, Canada), Vortex Jr. Mixer from Scientific Industries Inc, 1296-002 DELFIA plate shaker from Wallac, Rocking platform model 200 from VWR, and Corning stirrer from Fisher Scientific. Additionally, a Dounce homogenizer from Kontes Glass Company (NJ, USA), freezer vials (VWR), and Eppendorf pipettes (Fisher Scientific) were used.

2.5 *In-vitro* Proliferation of Cell Lines

MCF-7 cells were grown at 37°C and 5% CO₂ in DMEM / Nutrient Mixture Ham's F-12 medium modified to contain 2mM L-glutamine, 1.5g/L sodium bicarbonate, and 10mg/mL Gentamycin supplemented with 10% fetal bovine serum (FBS).

NHF cells were grown at 37°C and 5% CO₂ in DMEM modified to contain 2mM L-glutamine, 1.5g/L sodium bicarbonate and 10mg/L Gentamycin supplemented with 15% FBS, 1X essential and 1X non-essential amino acids, and 1X vitamins.

Hs578-T cells were grown at 37°C and 5% CO₂ in DMEM with 4 mM L-glutamine adjusted to contain 1.5g/L sodium bicarbonate, 10mg/L Gentamycin, and 4.5g/L glucose supplemented with 0.01mg/mL bovine insulin and 10% fetal bovine serum

2.6 Sub-culturing of Cells

Cells were sub-cultured by removing the culture medium by aspiration and rinsing the cells with a 0.25% (w/v) trypsin - 0.53mM EDTA solution or Puck's solution (140mM NaCl, 5mM KCl, 5.5mM glucose, 4mM NaHCO₃, 0.8mM ethylenediamine tetraacetic acid (EDTA)) in order to remove all traces of serum (serum contains a trypsin inhibitor). Additional 20% (w/v) trypsin solution was added and the cells were incubated at 37°C until the cell layer began to disperse (usually within 5 to 10 minutes). Additional appropriate complete media was added, cells were aspirated, and appropriate aliquots of the cell suspension were added to new culture flasks or plates.

2.7 Treatment of Cells with Anti-Cancer Drugs: PST and Tamoxifen

Cells were grown to 70% confluence and treated with the indicated concentration of Pancratistatin (PST) and Tamoxifen by the addition directly to fresh complete medium for varying time periods.

2.8 Data Collection and Analysis

All fluorescent and phase contrast pictures were taken using Improvision's OpenLab 3.1.5 Software on a Leica DM IRB fluorescent microscope. All pictures were processed using Adobe Photoshop software and Microsoft Powerpoint software. Fluorescence measurements were collected using SoftMax PRO 3.1.2 software and a SpectraMax Gemini XS fluorescent plate reader. Microsoft Excel software was used for data representation and statistical analysis.

2.9 Nuclear Staining and Phase Microscopy

In order to examine nuclear morphological changes induced by treatment of PST and Tamoxifen, cancerous and non-cancerous cells were grown and treated with PST and Tamoxifen, followed by staining with 10 μ M of Hoechst-33342 (Sigma Chemical Company, Mississauga, Ontario, Canada). The fluorescent dye was directly added to the culture media at a final concentration of 1 μ M and incubated for 10 minutes. Cells were examined under a fluorescent microscope and phase contrast and fluorescence pictures were taken.

2.10 Trypan Blue Staining

The Trypan blue exclusion test (Sigma Chemical Company, Mississauga, Ontario, Canada) is a common method to measure the number of viable cells in a given sample. Cells were trypsinized as previously described, except that floating cells were spun down and added to the cell suspension. Fresh media was added and 10 μ L of the cell suspension was added to 10 μ L of 0.4% Trypan blue stain. Cells were counted using a hemacytometer and the number of cells per volume unit of sample was calculated.

2.11 Flow Cytometry Analysis

Flow cytometry was carried out at Wayne State University by a trained specialist (Dr. Kim Zukowski). A Becton Dickinson FACSCalibur equipped with two lasers: a standard Argon laser at 488 nm and a red diode laser at 635 nm which measures forward scatter (cell size) and side scatter (granularity, complexity). The FACSCalibur is controlled by a FACStation which consists of a Macintosh Power PC 7600 loaded with

Becton Dickinson Immunocytometry Systems acquisition and analysis software including CellQuest, ModFit, FACSCComp, FACSCConvert, Attractors, and Paint-A-Gate. Cells were analyzed for annexin binding and tunnel labeling.

2.11.1 Annexin-V Binding Assay

The cells were grown and treated with varying combination of drugs (PST and Tamoxifen). After various treatment times, an annexin-V binding assay (Sigma Chemical Company, Mississauga, Ontario, Canada) was conducted using a purchased kit and the manufacturer's protocol. Cells were harvested via trypsinization, washed twice using phosphate buffer saline (PBS) (0.137mM NaCl, 2.7mM KCl, 8.0mM Na₂HPO₄, 1.47mM KH₂PO₄) and then re-suspended in annexin-V binding buffer (10mM HEPES and NaOH pH 7.5, 140mM NaCl, 2.5mM CaCl₂) at a concentration of $\sim 10^6$ cells/mL. 100 μ L of each solution was transferred to eppendorf tubes, 5 μ L of annexin-V-FITC conjugate was added, and the mixture was incubated for 15 minutes at room temperature. After incubation, the cells were re-suspended in 400 μ L of fresh binding buffer. Cells were then put into eppendorfs and taken to Wayne State for flow cytometry analysis.

2.11.2 TUNEL Assay

In order to observe DNA fragmentation, an APO-BrdU TUNEL (terminal uridine-derivatized nick end labeling) assay was performed using the manufacturer's protocol (Sigma Chemical Company, Mississauga, Ontario, Canada). Cells were grown and treated as previously described. Approximately $\sim 1 \times 10^6$ cells were washed with PBS and incubated in 5mL of 1% (w/v) paraformaldehyde in PBS on ice for 15 minutes. The cells

were washed twice with PBS and re-suspended in 0.5mL of PBS. Cells were added to 5mL of ice-cold 70% (v/v) ethanol and set at -20°C overnight (at least 12 hours).

The next day, ethanol was removed by centrifugation and washed twice using the wash buffer, provided in the kit. 50µL of DNA labeling solution was prepared for each sample (10µL of reaction buffer, 0.75µL of TdT enzyme, 8.0µL of BrdUTP and 31.25µL of dH₂O) and cells were incubated for 60minutes in DNA labeling solution at 37°C in a temperature controlled bath (shaken every 15 minutes). At the end of the incubation time, 1.0mL of Rinse Buffer (provided in the kit) was added to each tube followed by centrifugation. The cells were washed twice with Rinse Buffer and incubated in 100µL of antibody staining solution (5µL Alexa Fluor 488 dye labeled anti-BrdU antibody, 95µL Rinse Buffer) for 30minutes at room temperature. The samples were then re-suspended in a total volume of 400µL (rinse buffer) put in eppendorf tubes and taken for flow cytometry analysis.

2.12 Total and Cytosolic Cell Lysate

Cells were harvested by mechanical dislodging using a rubber policeman and centrifuged at 500xg for 5 minutes. The supernatant was removed and the pellet was washed twice with 1X PBS pH 7.4 and centrifuged again at 500xg for 5 minutes. The supernatant was removed and the pellet was re-suspended in 0.4 ml of extraction buffer (25mM HEPES pH 7.25, 5mM MgCl₂, 1mM EGTA, 0.1% Triton X 100). The cell suspension buffer was transferred into a Dounce cell homogenizer. Cells were homogenized with ~20 strokes to produce the total cell lysate. Cytosolic cell lysates

were obtained by an additional centrifugation at 200xg. The supernatant was collected as the cytosolic cell lysate.

2.13 Mitochondrial Isolation

Intact mitochondria were isolated from cells using a previously published method (Li *et. al.* 2003). Cells were collected by centrifugation at 500xg for 5 minutes. The pellet was washed twice with ice cold PBS and centrifuged at 250xg. The pellet was re-suspended in isolation buffer containing 1mM EDTA, 10mM HEPES (pH 7.4) and 250mM sucrose. Cells were homogenized and the disrupted cells were centrifuged for 5 minutes at 600xg at 4°C. The supernatant was collected and centrifuged at 15 000xg at 4°C for 5 minutes and the resulting pellet was considered to be crude mitochondria. The pellet was re-suspended in isolation buffer without EDTA. Mitochondrial suspensions were kept on ice and all of the experiments were performed within 2 hours of centrifugation.

2.14 ROS Detection in Isolated Mitochondria

Isolated mitochondria from untreated cells were subjected to direct incubation with 0.5µM PST and 5µM Tamoxifen. Also, 100µM paraquate was added to mitochondrial preparations as a positive control. Mitochondrial ROS generation was measured using Amplex Red dye (Sigma Chemical Company, Mississauga, Ontario, Canada), increase in the fluorescence due to oxidized Amplex Red fluorescence was approximated to be due to mitochondrial destabilization. This assay utilized horseradish peroxidase (HRP) to couple Amplex Red oxidation with peroxide reduction. In a 96-well

micro-titer plate, 0.25mg of mitochondrial suspension was added to a 100µl reaction mixture containing 0.25M sucrose, 1mM MgCl₂, 10mM HEPES, 100mM succinate, 5µM Amplex Red and 1 unit of HRP per well. Fluorescence of oxidized Amplex Red was measured at excitation 560nm and emission 590nm using the Spectra Max Gemini XS which was set to read the wells every 2 min over a total time of 2 hours.

2.15 Whole Cell ROS

Cells were grown on 24-well clear bottom plates until 70% confluence was established. Cells were treated with varying concentrations of drugs mentioned (PST and Tamoxifen) and incubated for a period of 48 hrs. Following incubation, 10µM 2'-7'-dichlorofluorescein diacetate (H₂DCFCA; Molecular Probes, Eugene, OR) was added to each well and cells were monitored overnight for 18 hrs with readings taken in 10 min intervals using SoftMax PRO 3.1.2 software on a SpectraMax Gemini XS fluorescent plate reader at excitation 495nm and emission 530nm. Microsoft Excel software was used for data representation and statistical analysis.

2.16 Western Blot

2.16.1 Protein Estimation

The concentration of proteins present in cytosolic or mitochondrial cell lysate samples was estimated using a protocol from BioRad Laboratories. Protein estimation was conducted by adding 10µL aliquots of each cell lysate sample, 790 µL of water and 200µL of BioRad protein assay reagent into 1mL plastic cuvettes. The mixtures were vortexed and allowed to stand for 10 minutes at room temperature. The absorbance was

then measured a UV-Visible Spectrophotometer and analyzed at 595 nm. A standard curve was prepared by using various amounts of a standard protein solution (1mg/ml bovine serum albumin).

2.16.2 SDS-PAGE and Gel Transfer

Protein samples were separated using either 10% or 12% SDS-PAGE (sodium dodecyl sulphate polyacrylamide gel electrophoresis). A total of 40 µg of protein was loaded into the gel and run in running buffer (1.44g Glycerine, 0.1g SDS, 0.3g Tris-HCl in 1L of distilled water, pH=8.9) for one hour at a constant 30 mAmps and 200V. The gel was then transferred to a nitrocellulose membrane in transfer buffer (20% methanol, 25mM Tris Base, 0.2M Glycine, pH<8) for one hour at 200mAmps and 80V. The membrane was then stained with Ponceau S for rapid reversible detection of protein loaded and an image was scanned.

2.16.3 Immunoblotting Analysis

The membrane was blocked in 5% milk in TBST for one hour at 25°C. The membrane was then incubated with primary antibody solution (2% milk in TBST, 1:1000 dilution) and incubated for one hour. Then the membrane was washed 3 times with TBST for 15 min. The membrane was then incubated for one hour with secondary antibody (2% milk in TBST and a 1:1000 dilution) consisting of anti-mouse conjugated to HRP or anti-rabbit conjugated HRP. As before, the membrane was subjected to three 15 minute TBST washes. The chemiluminescent peroxidase substrate reagent and buffer (Sigma Chemical Company, Mississauga, Ontario, Canada) was prepared and the blot was visualized using the

Chemi-Imager v5.5 (Alphatech Inovations) in Dr. Ananvoranich's lab. Spot analyses was carried out using image J software downloaded directly from the internet.

2.17 Whole Cell Caspase-8 Activation Assay

Whole cell caspase-8 detection assay was purchased from Cell Technology Inc. Mountain View, CA. As per protocol, treated and un-treated cells were placed in 96 well black fluorescent plates in 300 μ L of media. A total of 10 μ L of the 30 X caspase detection reagents (FAM-LETD-FMK) was added directly to 300 μ L of cell suspension. Cells were incubated for 1 hour at 37°C. After the incubation time the media was decanted by spinning the plates in a centrifuge and gently flicking the plate. Approximately 300 μ L of 1X Wash Buffer (provided in kit) was added to each well, centrifuged and removed. After the final wash 100 μ L of Wash Buffer was added at which point the plate was ready for analysis. The plate was read using a fluorimeter at an excitation of 515nm and emission of 590nm.

2.18 Long-term Drug Resistance and Viability Study

MCF-7 breast cancer cells were grown and maintained using sub-culturing techniques, however, 25nM and 50nM PST was added to the media after each culture splitting for a period of 20 days. After 20 days of 25nM and 50nM PST treatment the cells were treated with 1 μ M PST for 72 hours. At this time 1 μ M Hoechst 33342 dye was added to observe positive nuclear staining as mentioned before.

2.19 JC-1 Staining

Mitochondrial membrane permeability was visualized using 5,5',6,6'-tetrachloro-1,1',3,3'-tetraethylbenzimidazolylcarbocyanine iodide (JC-1) dye purchased from Sigma Chemical Company, Mississauga, Ontario, Canada and used according to the manufacturer's protocol and a previously published method (Olichon *et. al.* 2003). The cells were grown and treated as previously described. The cells were incubated in media containing 1 μ M of JC-1 dye for 15 minutes and the media was replaced by PBS (floating cells were re-added after centrifugation). The cells were examined under a fluorescent microscope and pictures were taken.

2.20 *In-vivo* Treatment Preparation

Intraperitoneal Placebo treatment consisted of 250 μ L of sterile peanut oil. PST treatments were intratumoural and consisted of 5 μ L of 10mM PST stock solution in a total volume of 250 μ L of sterile PBS this was calculated to be approximately 3mg/kg concentration. Tamoxifen treatments consisted of 20 μ L of 10mM Tamoxifen stock added to 250 μ M steril peanut oil, which was calculated to be approximately 25mg/kg. Peanut oil was used based on previously published method of Tamoxifen injection (Paine-Murrietta *et. al.* 1997).

2.21 RAG 2M Mouse Care, Xenograft Transplantation and Treatment

For this study, a total of 10 male immunodeficient RAG 2M mice were purchased from Taconic, Cambridge City, IN. Mice were injected with 60 day slow release 17 β -estradiol pellets using a trochar device, both purchased from Innovative Research of

America, Sarasota, FL. The mice were housed in autoclaved cages and fed irradiated food and autoclaved water. All of the mice were injected sub-cutaneously with 6×10^6 human MCF-7 breast cancer cells and visible tumours formed after 10-14 days. The mice were then divided into 4 groups: 3 received intraperitoneal Placebo treatment; 2 received intratumoral PST treatment; 3 received intraperitoneal Tamoxifen treatment; and 2 received intratumoural PST + intraperitoneal Tamoxifen treatment. The PST treated mice were given approximately 3mg/kg PST twice weekly and Tamoxifen treated mice were given 25 mg/kg Tamoxifen 3 times a week for 5 weeks. Periodically, the mice were weighed and the tumour volume was measured using callipers. One week after the last treatment, all mice were sacrificed by CO₂ asphyxiation according to ethical care committee protocol.

2.22 Tissue Preparation for Histochemical Analysis

The tissues stored in 10% formalin were moved to 70% ethanol within 24hours and then processed through a dehydration gradient being put into paraffin-wax blocks. The tissues were moved through an increasing ethanol gradient and then submerged in xylene and wax. The following times and concentrations were used: 70% EtOH overnight; 1 hour 95% EtOH; 1 hour absolute EtOH; 90 minutes xylene; 1 hour xylene/wax (50:50); wax overnight at 60°C. Wax blocks were assembled by placing a piece of tumour, liver and kidney from one mouse at the bottom of the mould and then pouring wax to fill the mould. The mould is then placed in -20°C overnight before it is ready to be sectioned using a microtome. Microtome sections of 8 microns were cut into ribbons, which were laid in a 40°C water bath and allowed to stretch out before being

mounted on a superfrost slide. About 3-4 sections were placed on each slide. The slides were left overnight on a hot plate at about 55°C. The slides were then ready for histochemical analysis.

2.23 Tissue Preparation Revision

When the tissues were prepared and sectioned, it was found that the liver tissues were over dehydrated. The dehydration of the tissues is irreversible, thus the protocol was optimized for future work. The revised method is identical to the previous method but the tissue is subjected to a shorter time in xylene to reduce the amount of dehydration caused to the tissues. The optimum xylene incubation time was found to be 30 minutes compared to the 90 minute incubation in the previous method.

2.24 TUNEL Assay With DAPI on Tissue Sections

The Terminal uridine deoxynucleotidyl transferase dUTP Nick End Labelling (TUNEL) assay was purchased from Sigma Chemical Company Mississauga Ontario . This assay detects the presence of nicks in the DNA which can be identified by terminal deoxynucleotidyl transferase, an enzyme that catalyzes the addition of dUTPs that are secondarily labelled with a marker. These nicks are typically observed in cells that have undergone apoptosis. DAPI (4',6-diamidino-2-phenylindole) is a fluorescent stain that intercalates into the minor groove of DNA. Chromatin condensation is consistent with apoptosis and can be visualized by a concentrated and brighter fluorescence than the surrounding non-apoptotic nuclei.

This assay begins with the slide being rehydrated according to the following procedure: 2x5 min xylene; 2x5min absolute EtOH; 3 min 95% EtOH; 3 min 80% EtOH; 3 min 70% EtOH; 3 min H₂O; 3 min PBS. The slides were incubated in primary antibody solution (40µL Reaction buffer, 3µL TdT enzyme, 24µL BrdUTP, 125µL dH₂O) overnight at 4°C. The slides were then washed with Rinse Buffer and incubated in Alexa Fluor 488 secondary antibody solution (10µL Alexa Fluor, 190µL Rinse Buffer) for 1 hour at 25°C. The slides were then washed with PBS and mounted using mounting media containing DAPI nuclear stain.

2.25 Haematoxylin and Eosin

This stain is performed to visualize the morphology of the tissue. The nucleus stains blue and the cytoplasm stains pink, which gives an overall morphological view of the tissue. The slides were dewaxed/rehydrated, stained with Harris Haematoxylin (Fischer Scientific, Kalamazoo MI), dehydrated, and then stained with Eosin Y (EMD Chemicals Inc., Darmstadt Germany) according to the following procedure: 10 min xylene; 10 min absolute EtOH; 5 min 95% EtOH; 5 min 70% EtOH; dipped in 50% EtOH; dipped in 30% EtOH; dipped in H₂O; 3 min Haematoxylin stain; dipped in H₂O; dipped in 30% EtOH; dipped in 50% EtOH; dipped in 70% EtOH; dipped in 95% EtOH; 3 min Eosin stain; 10 min absolute EtOH; 10 min xylene. These last two steps are done to completely dehydrate the tissues. The slides were then mounted with coverslips using Cytoseal 60 and viewed on a light microscope.

2.26 Tissue Preparation for Biochemical Analysis

The flash-frozen tissue samples were unfrozen at 4°C and homogenized in 3 volumes of homogenization buffer (50mM Tris-HCl, 150mM NaCl, 1mM EDTA, 1mM PMSF, 1mM benzamide, 10µg/ml pepstatin A and 10µg/ml leupeptin, 2% beta mercaptoethanol) using a Sorvall Omni-Mixer at 4°C.¹⁵ The samples were centrifuged at 2700 x g for 10min at 4°C to separate the nuclear and cell debris from the supernatant. The supernatant was then centrifuged at 10,000xg for 10 minutes at 4°C to obtain the mitochondrial pellet and the post-mitochondrial cytoplasmic supernatant. The mitochondrial pellet was resuspended in the homogenisation buffer; both fractions were used for biochemical analysis using western blot procedure.

CHAPTER 3: RESULTS

3.1: *In-vitro* Apoptotic Synergy Exhibited by PST and Tamoxifen

Pancratistatin has been shown to have the ability of activating apoptosis in cancer cells specifically through the destabilization of cancer cell mitochondria. Tamoxifen which is primarily an anti-estrogen treatment for breast cancer, has recently been discovered to induce apoptosis through biochemical pathways unrelated to the estrogen receptor (Mandlekar, Kong 2001). The electron transport chain of cancer cell mitochondria has been found to be disrupted by Tamoxifen through binding of Tamoxifen to the flavomononucleotide binding site in complex 1 (Moreira *et. al.* 2006). Due to these observations PST and Tamoxifen were considered as a potential combination therapy in both estrogen receptor +/- breast cancers.

3.1.1 Susceptibility of MCF-7 Cells to Apoptosis by PST Treatment

Several cancer cell lines are susceptible to PST-induced apoptosis at 1 μ M concentration including: Jurkat (B-cell lymphoma), SHSY-5Y (neuroblastoma), 5123 (rat hepatoma) as reported by our laboratory (Pandey *et. al.* 2001, McLachlan *et. al.* 2005). Furthermore, we have shown that PST specifically induces apoptosis in cancer cells with minimal effect on normal cell lines (McLachlan *et. al.* 2005).

To evaluate the effect of PST on estrogen dependent breast cancer cells, we treated MCF-7 (adenocarcinoma) with concentrations of 1 μ M and 500nM PST for a period of 72 hours. Following treatment we stained the cells with cell permeable Hoechst 33342 dye to semi-quantitatively determine the number of cells exhibiting the hallmark

feature of apoptosis: nuclear condensation. Figure 3-1 shows that 0.5 μ M PST concentration caused approximately 45% apoptosis at 72 hours and 1 μ M PST at this time point caused 60% apoptosis in MCF-7 cells.

3.1.2 Synergistic Action of PST and Tamoxifen in ER+ MCF-7 Cells

Research from as early as the 1970's shows that 50-70% of invasive breast cancer expresses estrogen receptor, based on pooled analysis of 400 patients (McGuire *et. al.* 1975). Of these estrogen receptor positive breast cancer patients 50-60% responded well to endocrine therapy (McGuire *et. al.* 1975). Tamoxifen as a therapy has selectivity for the estrogen receptor and therefore shows little toxicity to normal cells (Duffy 2005). This initially sparked our interest in examining combinatorial therapy of Tamoxifen and PST on estrogen receptor positive breast cancer (MCF-7). We aimed to determine the effect of adding PST and Tamoxifen in combination to the estrogen receptor positive MCF-7 cell line to evaluate the apoptotic response to combination therapy relative to each compound separately.

Breast adenocarcinoma positive for ER was treated with Tamoxifen at 1 μ M, 5 μ M, and 10 μ M concentrations for 72 hours and stained with Hoechst 33342 dye to generate relative apoptotic indices. As shown in figure 3-1 and 3-2a 5 μ M Tamoxifen treatment did not cause apoptosis as compared to control; only the higher concentration of 10 μ M Tamoxifen causes significant apoptosis in this cell line. We then treated MCF-7 cells with low dose of 0.5 μ M PST in combination with 1 μ M, 5 μ M and 10 μ M Tamoxifen and the effective dose of 1 μ M PST in combination with 1, 5, 10 μ M Tamoxifen for a period of 72 hours. Figure 3-2b shows the result of combinatorial treatment of 5 μ M

Tamoxifen and 1 μ M PST after 72 hours: a significant increase in apoptosis is evident when compared to Tamoxifen and PST on their own (figure 3-1). The apoptotic index of combined treatment of 1 μ M PST and 5 μ M Tamoxifen increased by approximately 20% when compared to 1 μ M PST alone (figure 3-1, 3-2b). Similar results were observed when MCF-7 cells were treated with 0.5 μ M PST in combination with 5 μ M Tamoxifen. A concentration of 0.5 μ M PST on its own induced approximately 45% apoptosis after of 72 hours treatment; however, in combination with 5 μ M Tamoxifen (the concentration were no effect was observed), the apoptotic index increased to 65% apoptosis, which corresponds to an apoptotic increase of 20% (figure 3-1, 3-2a, 3-2c).

Figure 3-1: Apoptotic Index: Dose Response of MCF-7 cells to Pancreatistatin and Tamoxifen

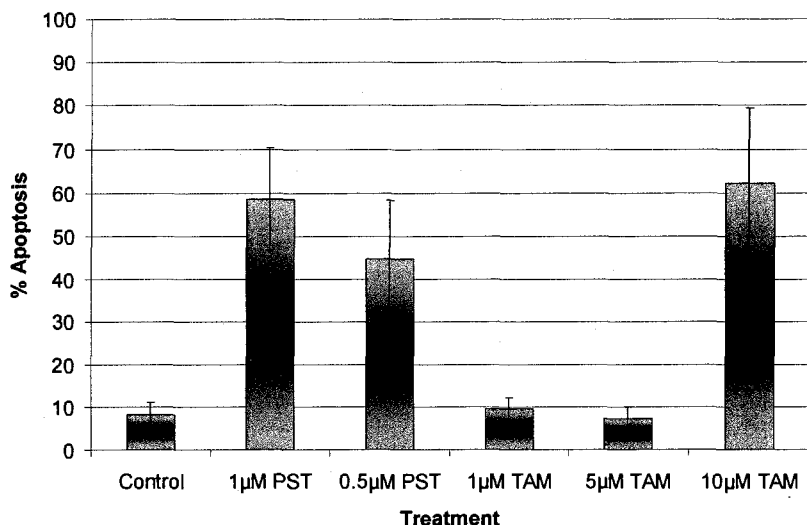


Figure 3-1: Apoptotic Index: Dose response of MCF-7 cells to Pancreatistatin and Tamoxifen. MCF-7 cells were treated with PST and Tamoxifen for 72 hours and stained with Hoechst 333423 dye. The number of apoptotic nuclei was counted and the average percentage of apoptotic cells was calculated from a minimum of 500 cells. Standard error was calculated using data from a minimum of three separate experiments.

Figure 3-2a: Synergistic response of MCF-7 cells to Pancreatistatin and Tamoxifen Treatment MCF-7

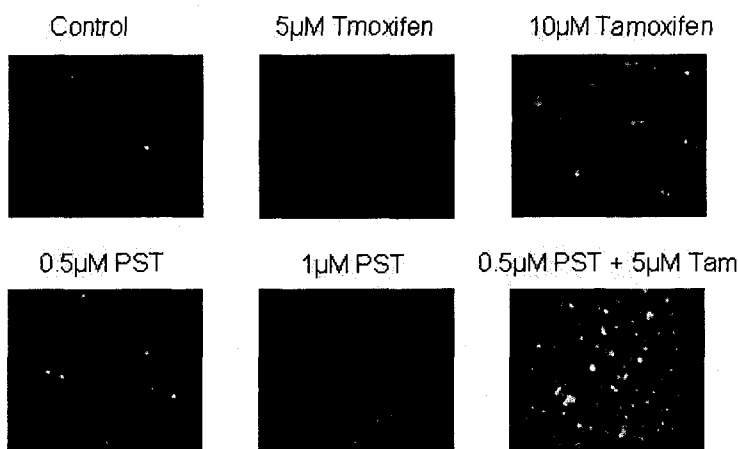


Figure 3-2a: Synergistic response of MCF-7 cells to Pancreatistatin and Tamoxifen treatment MCF-7. MCF-7 cells were treated with PST and tamoxifen for 72 hours and stained with Hoechst 33342 dye to examine nuclear morphology. Fluorescent pictures were taken at 400x magnification. Nuclear condensation is evident in cells with bright, condensed, and rounded nuclei.

Figure 3-2b: Apoptotic Index: Synergy of PST and Tamoxifen at High Dose PST

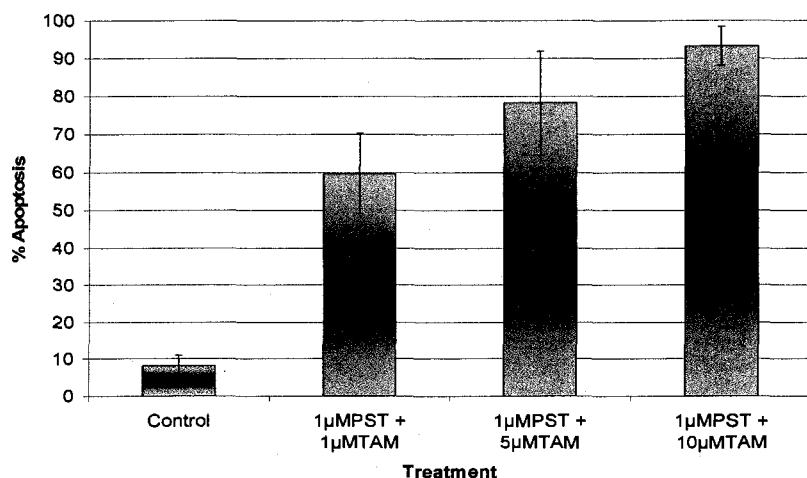


Figure 3-2b: Apoptotic Index: Synergy of PST and Tamoxifen at high dose PST. MCF-7 cells were treated in combination with 1 μM PST and various concentrations of Tamoxifen for 72 hours and stained with Hoechst 33342 dye. The number of apoptotic nuclei was counted and the average percentage of apoptotic cells was calculated from a minimum of 500 cells. Standard error was calculated using data from a minimum of three separate sets of experiments.

Figure 3-2c: Apoptotic Index: Synergy of PST and Tamoxifen at Low Dose PST

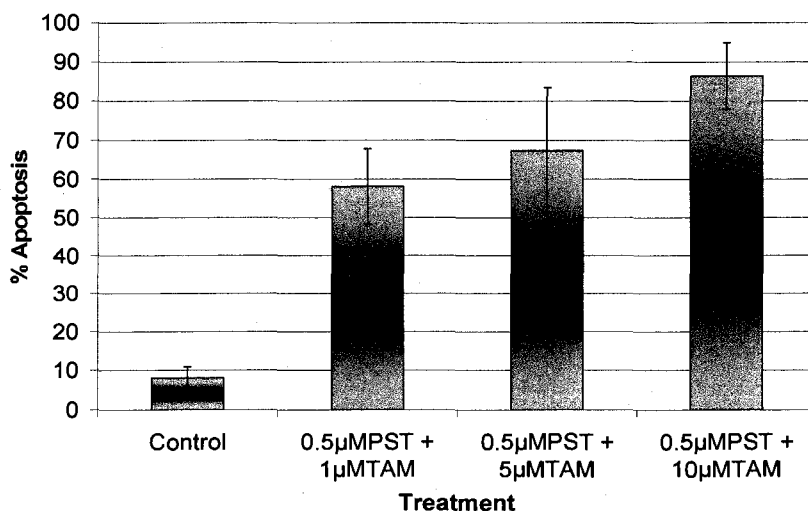


Figure 3-2c: Apoptotic Index: Synergy of PST and Tamoxifen at low dose PST. MCF-7 cells were treated in combination with 0.5 μM PST and various concentrations of Tamoxifen for 72 hours and stained with Hoechst 33342 dye. The number of apoptotic nuclei was counted and the average percentage of apoptotic cells was calculated from a minimum of 500 cells. Standard error was calculated using data from a minimum of three separate sets of experiments.

3.1.3 Induction of Apoptosis in ER- Hs578-T Cells by PST Treatment

Estrogen receptor negative Hs578-T cells were treated with 0.5 μ M and 1 μ M PST treatment for 72 hours and quantified by Hoechst-33342 dye in order to examine nuclear condensation and develop apoptotic indexes to establish the relative apoptotic effect as compared to a control. Apoptotic nuclear morphology was observed upon the addition of 0.5 μ M and 1 μ M PST in the form of condensed bright nuclei (figure 3-3a). As observed in figure 3-3b, 0.5 μ M PST treatment caused 20% apoptosis while 1 μ M PST treatment exhibited approximately 45% apoptosis for 72 hours.

3.1.4 Synergistic Action of PST and Tamoxifen in ER- Hs578-T Cells

Tamoxifen, an estrogen receptor antagonist, has been recently observed to induce apoptosis by directly destabilizing cancer cell mitochondria through the flavomononucleotide (FMN) binding site on complex 1 of the electron transport chain (Moreira *et. al.* 2006). Here, the effect of Tamoxifen was considered in estrogen receptor negative cells in combination with PST in order to observe a potential to exploit the Tamoxifen targeted mitochondrial membrane dysfunction. To examine whether a synergistic relationship exists between these agents, various concentrations of PST and Tamoxifen were combined and incubated with Hs578-T cells for 72 hours and quantitatively analyzed by Hoechst 33342 staining as per protocol. Figure 3-3a shows that the addition of 10 μ M Tamoxifen over 72 hours exhibited little apoptotic nuclear morphology when compared to control; however, the addition of 0.5 μ M PST in combination with 10 μ M Tamoxifen increased the apoptotic response of the 0.5 μ M PST treatment.

Furthermore, apoptotic indices were established from counting the number of cells which demonstrate condensed apoptotic nuclei. As observed in figure **3-3b** Hs578-T cells treated with 10 μ M Tamoxifen for 72 hours exhibited minimal apoptotic morphology. The combined treatment of 0.5 μ M PST and 10 μ M Tamoxifen for 72 hours exhibited approximately 40% apoptosis which corresponds to a 20% increase from 0.5 μ M PST on its own (figure **3-3b**).

Figure 3-3a: Synergistic Response of Hs578-T Cells to PST and Tamoxifen Treatment for 72 Hours

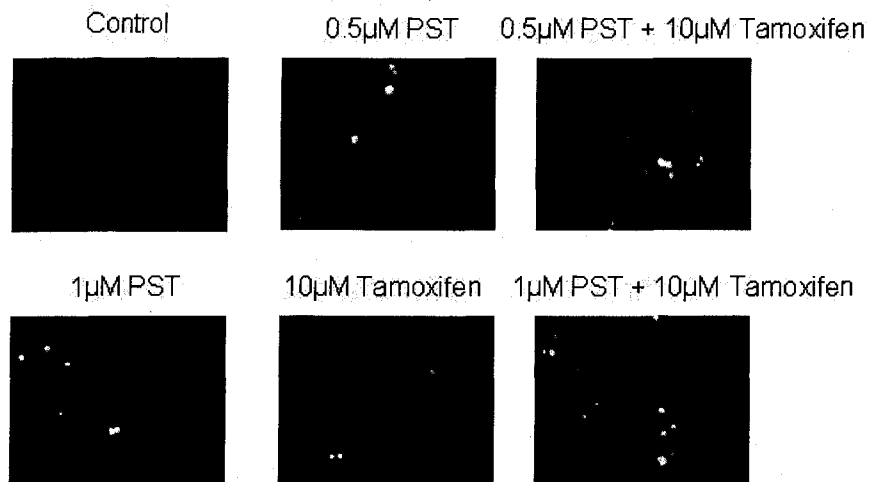


Figure 3-3a: Synergistic response of Hs578-T cells to Pancratistatin and Tamoxifen treatment. Hs578-T cells were treated with various concentrations of PST and Tamoxifen for 72 hours and stained with Hoechst 33342 dye to examine nuclear morphology. Fluorescent pictures were taken at 40x magnification. Nuclear condensation is evident in cells with bright, condensed, and rounded nuclei.

Figure 3-3b: Apoptotic Index: Synergistic response of Hs578-T cells to PST and Tamoxifen Treatment

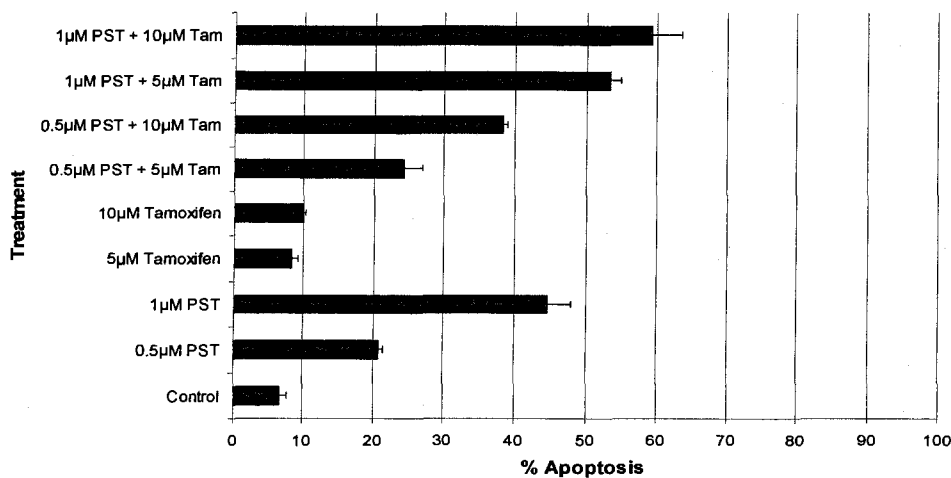


Figure 3-3b: Apoptotic Index: Synergistic response of Hs578-T cells to Pancratistatin and Tamoxifen treatment. Hs578-T cells were treated in combination with various PST and Tamoxifen concentrations for 72 hours and stained with Hoechst 33342 dye. The number of apoptotic nuclei was counted and the average percentage of apoptotic cells was calculated from a minimum of 500 cells. Standard error was calculated using data from a minimum of three separate sets of experiments.

3.1.5 NHF Cells Un-effected by Combined PST and Tamoxifen Treatment

Minimal toxicity to normal cells is an important characteristic in novel chemotherapeutic strategies to avoid the harsh side effects that arise from current cancer therapies. Toxicity to normal cells due to current chemotherapies such as taxol and topoisomerase II inhibitors has been attributed with re-occurrence of disease and establishment of secondary tumors (Cunha *et. al.* 2001, Boos, Stopper 2000). Therefore compounds which reduce the risk of side-effects are the focus of modern research. As previously mentioned PST has been shown to exhibit no toxic effect to normal tissue (Pandey *et. al.* 2001, McLachlan *et. al.* 2005). Furthermore, Tamoxifen has been reported to exhibit minimal toxicity to normal tissue (Duffy 2005). Therefore the combinatorial treatment of both compounds was considered in a normal non-cancerous cell line to examine the potential for toxicity.

To determine the effect of combined PST and Tamoxifen treatment on normal cell lines we chose to treat normal human fibroblasts (NHF). There was no evidence suggesting toxicity of combination treatment to these cells after 72 hours. Figure 3-4a and 3-4b shows that combinatorial treatments of 10 μ M Tamoxifen and 1 μ M PST did not induce significant nuclear condensation when compared to untreated NHF cells.

Figure 3-4a: Combinatorial Treatment of PST and Tamoxifen in NHF Cells

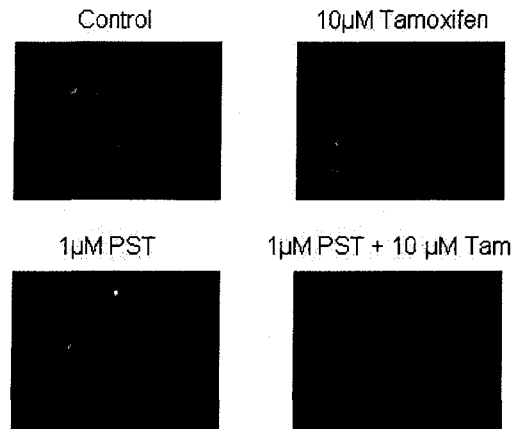


Figure 3-4a: Combinatorial Treatment of PST and Tamoxifen in NHF. Cells NHF cells were treated with various concentrations of PST and tamoxifen for 72 hours and stained with Hoechst 33342 dye to examine nuclear morphology. Fluorescent pictures were taken at 400x magnification. Nuclear condensation is evident in cells with bright, condensed, and rounded nuclei.

Figure 3-4b: Apoptotic Index: Combinatorial Treatment of NHF Cells to PST and Tamoxifen for 72 Hour

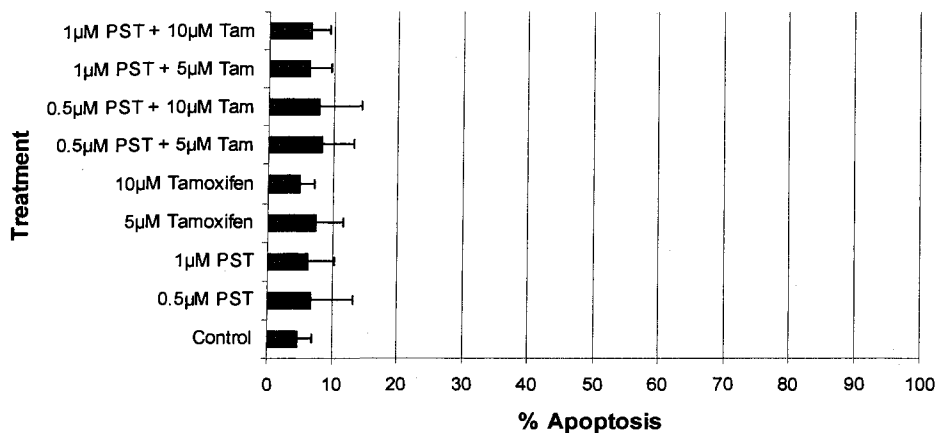


Figure 3-4b: Apoptotic Index: Combinatorial Treatment of NHF Cells to PST and Tamoxifen for 72 Hour. treated for 72 hours and stained with Hoechst 33342 dye. The number of apoptotic nuclei was counted and the average percentage of apoptotic cells was calculated from a minimum of 500 cells. Standard error was calculated using data from a minimum of three separate sets of experiments.

3.1.6 Quantitative Analysis of Apoptotic Synergy in MCF-7 Cells

The synergistic effect in MCF-7 cells was quantitatively analyzed by flow cytometry utilizing Annexin-V FITC conjugate binding. MCF-7 cells were treated with 0.5 μ M PST and/or 5 μ M Tamoxifen for a period of 72 hours and incubated with Annexin-V FITC conjugate. Percent positive staining was obtained from a population of 20 000 cells. Figure 3-5a shows that treatment with 5 μ M Tamoxifen resulted in 14.27% positive Annexin-V staining, which is not a significant increase over control cells which stained 13.88% Annexin-V positive. Furthermore figure 3-5a shows that treatment with 0.5 μ M PST resulted in 34.45% positive Annexin-V staining in MCF-7 cells and the combined treatment of 0.5 μ M PST and 5 μ M Tamoxifen resulted in 52.63% Annexin-V positive staining which corresponds to a 20% increase from the single treatment with PST.

The level of DNA fragmentation was investigated by TUNEL assay and quantified by flow cytometry. MCF-7 cells were treated with 0.5 μ M PST and/or 5 μ M Tamoxifen for 72 hours upon which the TUNEL assay was performed as per manufacturer's protocol. Cells were properly gated and 20 000 cells were analyzed. Figure 3-5b shows that 11.85% of untreated MCF-7 cells were positively stained for DNA fragmentation and 5 μ M Tamoxifen treatment resulted in 15.78% positive staining. Furthermore, figure 3-5b demonstrates that MCF-7 cells treated with 0.5 μ M PST resulted in 44.29% positive staining, while the combination of 0.5 μ M PST and 5 μ M Tamoxifen resulted in 48.88% of cells to stain positively.

Figure 3-5a: Flow Cytometry: Annexin-V Analysis of PST and Tamoxifen Synergy in MCF-7 Cells

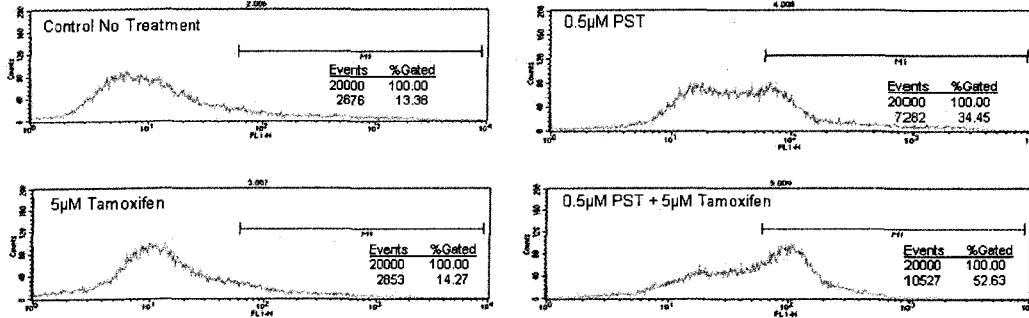


Figure 3-5a: Flow Cytometry: Annexin-V analysis of PST and Tamoxifen synergy in MCF-7 cells. MCF-7 cells were treated with 0.5µM PST, 5µM Tamoxifen and a combination of both for 72 hours. Total cell counts of 20,000 were gated and analyzed by flow cytometry operator. Annexin V-FITC positive cells were then taken as % Gated.

Figure 3-5b: Flow Cytometry: TUNEL Analysis of PST and Tamoxifen Synergy in MCF-7 Cells

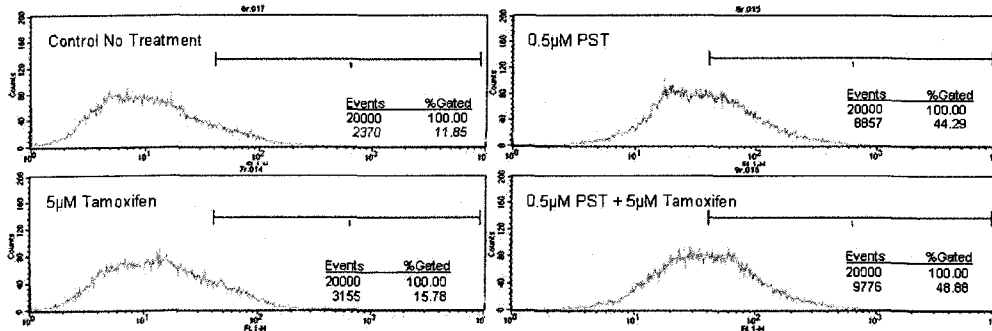


Figure 3-5b: Flow Cytometry: TUNEL analysis of PST and Tamoxifen synergy in MCF-7 cells. MCF-7 cells were treated with 0.5µM PST, 5µM Tamoxifen and a combination of both for 72 hours. Total cell counts of 20,000 were gated and analyzed by flow cytometry operator. TUNEL positive cells were then taken as % Gated.

3.1.7 Whole Cell ROS Increases upon Combinatorial PST and Tamoxifen Treatment

Increase in whole cell ROS is attributed to the dysfunction of the mitochondrial membrane and eminent apoptosis (Somayajulu *et. al.* 2005). Whole cell ROS was measured by the fluorometric assay using H₂DCFDA fluorophore. Cancerous and non-cancerous cell lines were treated with PST and Tamoxifen upon which relative whole cell ROS was measured.

MCF-7 (ER+) and Hs578-T (ER-) were grown on 24-well culture plates and treated with 0.5 μ M PST, 5 μ M Tamoxifen or a combination of both for a period of 24 hours, upon which whole cell ROS was measured as per protocol. As observed in figure **3-6a**, the combined treatment of 0.5 μ M PST and 5 μ M Tamoxifen increased the relative amount of ROS production in MCF-7 cells more so than either drug on its own. Similar results were obtained in the ER- Hs578-T cell line (figure **3-6b**) as combined treatment of 0.5 μ M PST and 5 μ M increased the relative amount of ROS in greater amount than either drug alone. Furthermore to test the effect of combined PST and Tamoxifen in normal human fibroblast (NHF) cells we treated them with higher doses of PST and Tamoxifen to determine if there are any changes in the total ROS production. As was observed in figure **3-6c**, there was no significant increase from control upon the addition of 1 μ M PST, 10 μ M Tamoxifen and a combination of both, at these concentrations.

Figure 3-6a: Whole Cell ROS of MCF-7 Cells Treated With PST and Tamoxifen

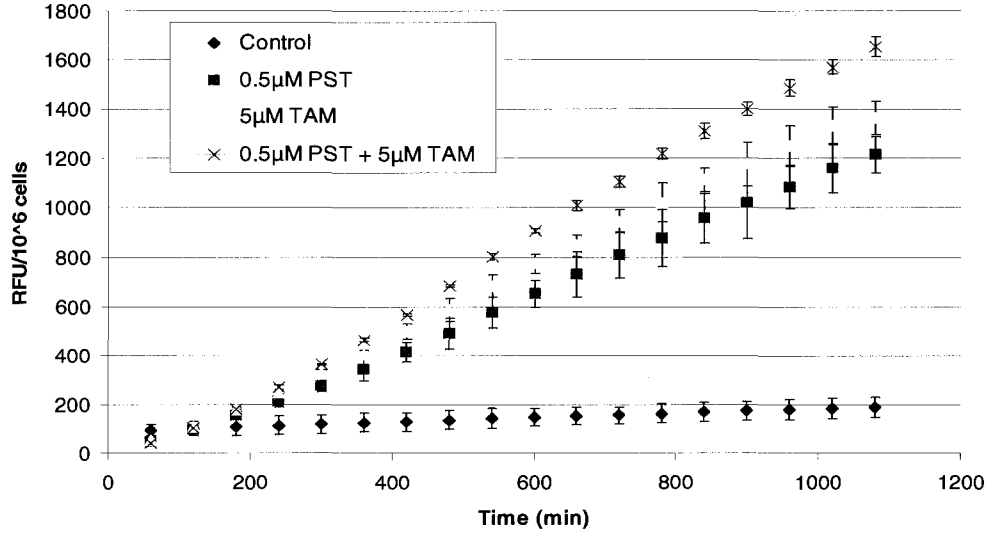


Figure 3-6a: Whole Cell ROS of MCF-7 cells treated with PST and Tamoxifen. MCF-7 cells were incubated with 0.5µM PST, 5µM Tamoxifen and a combination of both for a period of 24 hours then incubated with H₂DCFDA dye and monitored by a fluorometer for a period of 18 hours. Readings were taken in intervals of 10 minutes. Error bars were generated by the standard deviation between 3 separate trials of the experiment.

Figure 3-6b: Whole Cell ROS of Hs578-T Cells Treated With PST and Tamoxifen

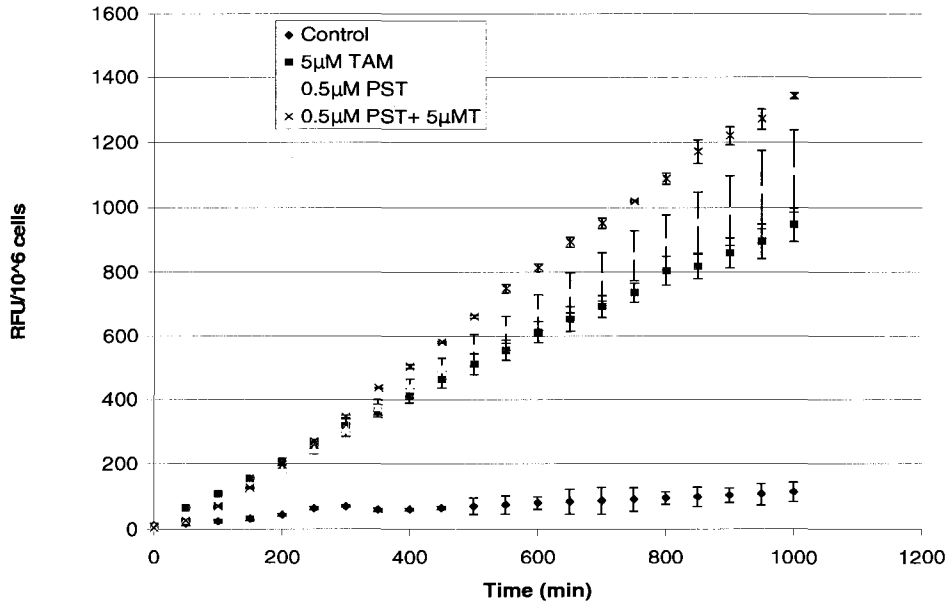


Figure 3-6b: Whole Cell ROS of Hs578-T cells treated with PST and Tamoxifen. Hs578-T cells were incubated with 0.5µM PST, 5µM Tamoxifen and a combination of both for a period of 24 hours then incubated with H₂DCFDA dye and monitored by a fluorometer for a period of 18 hours. Readings were taken in intervals of 10 minutes. Error bars were generated by the standard deviation between 3 trials of the experiment.

Figure 3-6c: Whole Cell ROS of NHF cells treated with PST and Tamoxifen

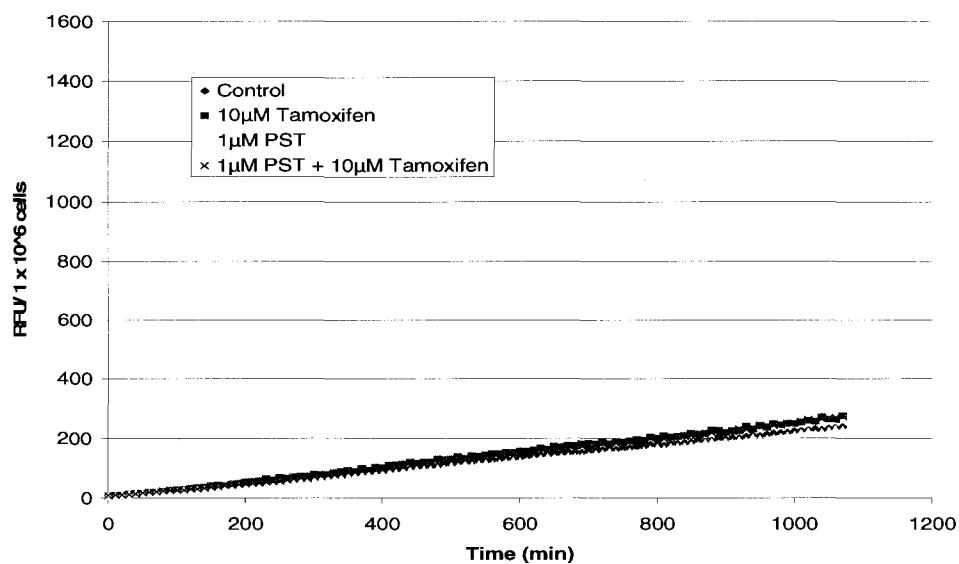


Figure 3-6c: Whole Cell ROS of NHF cells treated with PST and Tamoxifen. NHF cells were incubated with 1µM PST, 10µM Tamoxifen and a combination of both for a period of 24 hours then incubated with H₂DCFDA dye and monitored by a fluorometer for a period of 18 hours. Readings were taken in intervals of 10 minutes. Error bars were generated by the standard deviation between 3 trials of the experiment.

3.1.8 Mitochondrial membrane potential collapse upon treatment of PST and Tamoxifen

As previously mentioned, increase in ROS generation is indicative of mitochondrial dysfunction within the cell. In order to determine if mitochondria are destabilized following treatment we used a mitochondria permeable assay. This assay uses a cationic JC-1 dye, which localizes to mitochondria with adequate mitochondrial membrane potential and is retained within this membrane where it gives off a red fluorescent stain, when not localized to mitochondria JC-1 dye will fluoresce green in the cytosol. Both ER⁺ and ER⁻ breast cancer cell lines were treated at the previously determined doses of PST (0.5 μ M) and Tamoxifen (5 μ M) which exhibit greatest synergistic behavior, for 48 hours. Normal human fibroblasts were treated as a control to compare the effect of the treatment.

In figure **3-7a** clear red punctuate staining is observed in both the control and 48h Tamoxifen treated MCF-7 cells. It is evident from figure **3-7a** that the red mitochondrial staining becomes relatively more diffuse in 0.5 μ M PST treated cells. Red punctuate mitochondrial staining is even more diffuse in the combinatorial treatment of 0.5 μ M PST and 5 μ M Tamoxifen as is evident by the increase in green background staining (figure **3-7a**).

As can be seen from figure **3-7b**, in Hs578-T cells, control and 10 μ M Tamoxifen exhibited approximately the same red punctuate staining; however, the JC-1 stain of the combined treatment of 0.5 μ M PST and 10 μ M Tamoxifen indicate greater diffuse red staining than either of the compounds separately. Furthermore normal human fibroblast cells did not exhibit substantial changes in the amount of red punctuate JC-1 staining as shown in figure **3-7c**, when treated with 0.5 μ M PST and 5 μ M Tamoxifen.

Figure 3-7a: Mitochondrial Membrane Permeability in MCF-7 Cells Treated by PST and Tamoxifen: JC-1 Staining

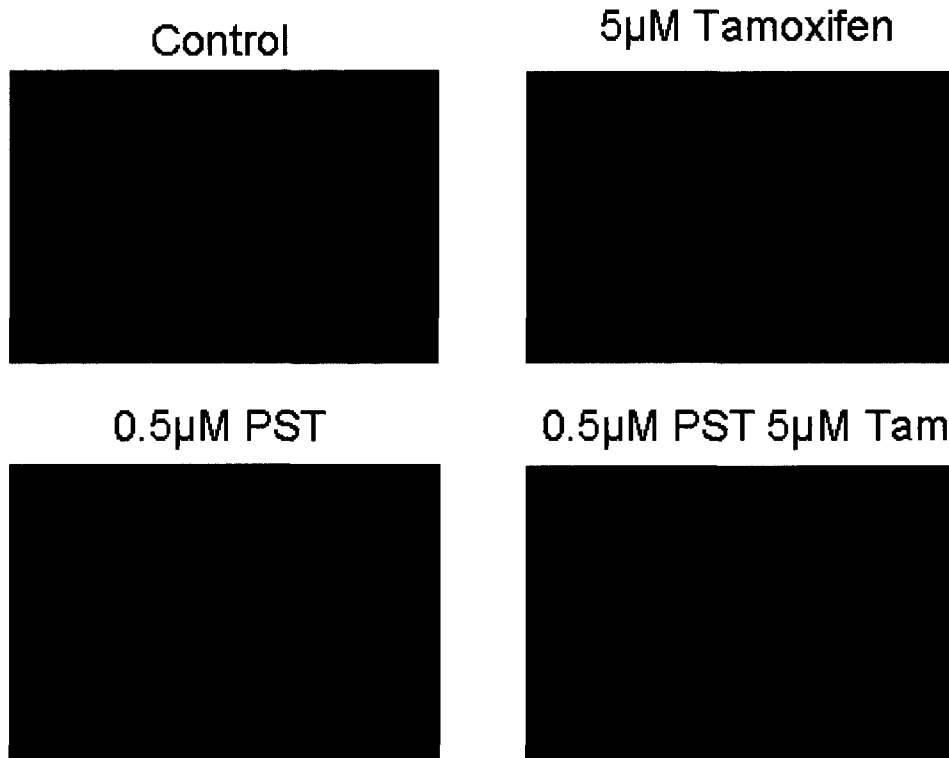


Figure 3-7a: Mitochondrial membrane permeability in MCF-7 cells treated by PST and Tamoxifen: JC-1 staining. MCF-7 cells were treated with 0.5µM PST and 5µM Tamoxifen for a period of 48 hours at which point JC-1 dye was applied to the cells to examine mitochondrial membrane potential. Fluorescent pictures were taken at 400x magnification. Bright red fluorescence is indicative of healthy mitochondria with intact membrane potential.

Figure 3-7b: Mitochondrial Membrane Permeability in Hs578-T Cells Treated by PST and Tamoxifen: JC-1 Staining

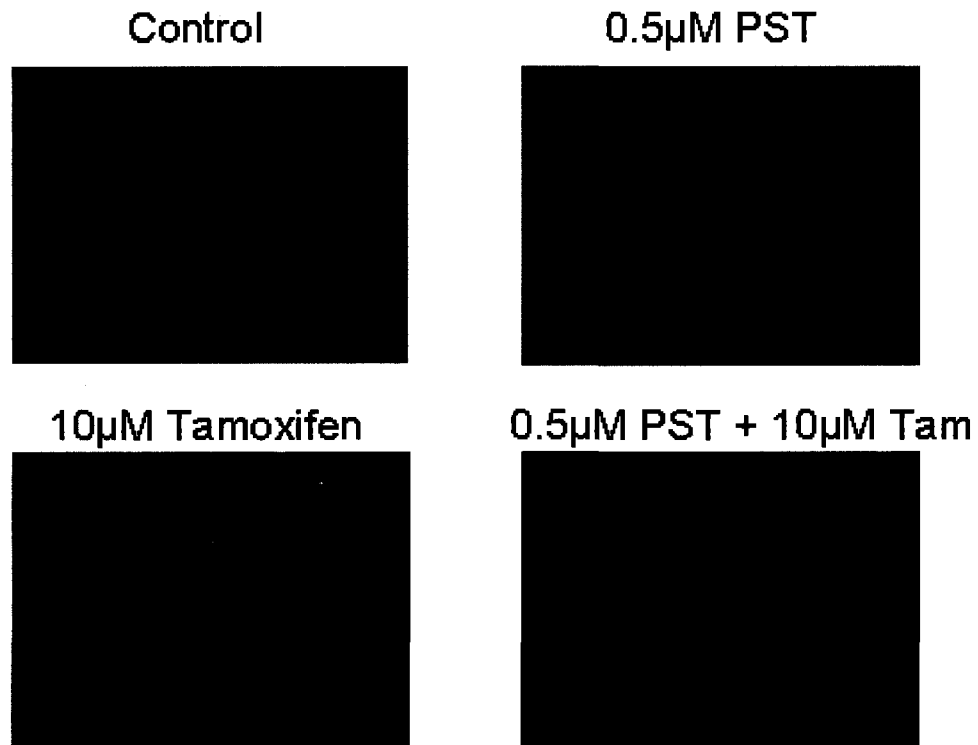


Figure 3-7b: Mitochondrial membrane permeability in Hs578-T cells treated by PST and Tamoxifen: JC-1 staining. Hs578-T cells were treated with 0.5µM PST and 10µM Tamoxifen for a period of 48 hours at which point JC-1 dye was applied to the cells to examine mitochondrial membrane potential. Fluorescent pictures were taken at 400x magnification. Bright red florescence is indicative of healthy mitochondria with intact membrane potential.

Figure 3-7c: Mitochondrial Membrane Permeability in NHF Cells Treated by PST and Tamoxifen: JC-1 Staining

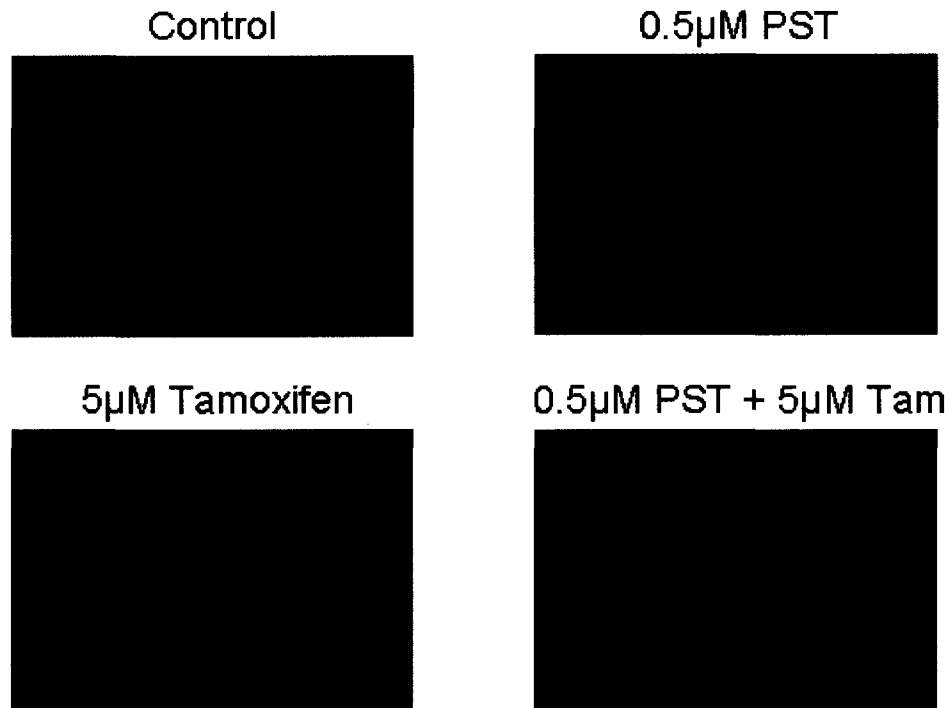


Figure 3-7c: Mitochondrial membrane permeability in NHF cells treated by PST and Tamoxifen: JC-1 staining. NHF cells were treated with 0.5µM PST and 5µM Tamoxifen for a period of 48 hours at which point JC-1 dye was applied to the cells to examine mitochondrial membrane potential. Fluorescent pictures were taken at 400x magnification. Bright red florescence is indicative of healthy mitochondria with intact membrane potential.

3.1.9 Mitochondria as the Target for PST and Tamoxifen Induced Apoptosis

PST has previously been shown to exhibit its activity directly on the mitochondria of cancerous cells and Tamoxifen has been observed to have mitochondrial targets independent of estrogen receptor activity. Therefore, to test the effect of both compounds on the mitochondria directly, we isolated mitochondria from MCF-7, Hs578-T and NHF cell lines and treated their isolated mitochondria directly with PST, Tamoxifen and a combination of both for a total of 1.5 hours. Paraquat which increases mitochondrial ROS was used as a positive control. Upon treatment of mitochondria with the compounds a fluorometric assay was utilized. This assay works by coupling a reaction involving: reduction of Amplex Red dye reagent with oxidation of hydrogen peroxide through the action of horse radish peroxidase enzyme.

Figure 3-8a shows that the treatment of MCF-7 mitochondria with 5 μ M Tamoxifen did not generate significant mitochondrial ROS increases when compared to control and MCF-7 mitochondria treated with 0.5 μ M PST increases the relative amount of mitochondrial ROS. Figure 3-8a demonstrates that 5 μ M Tamoxifen and 0.5 μ M PST significantly increase the relative amount of mitochondrial ROS, more so than either compound separately.

To test the mitochondrial response in estrogen receptor negative cells, we isolated mitochondria from Hs578-T cells and incubated them with the various treatments. As can be seen in figure 3-8b the mitochondrial ROS response in Hs578-T cells is similar to that observed in the estrogen receptor positive MCF-7 mitochondria, where the addition of the

double treatment 5 μ M Tamoxifen and 0.5 μ PST increased the relative ROS in greater amount than either compound separately.

To investigate the response of normal “healthy” mitochondria, we isolated mitochondrial fractions from normal human fibroblast cells and treated them in the same manner as the ER- and ER+ cell lines. As clearly shown in figure **3-8c**, there was no significant ROS increase from control when isolated mitochondria from NHF cells were treated with 0.5 μ M PST, 5 μ M Tamoxifen and both. To observe increased mitochondrial ROS response from the mitochondrial preparations, we treated them with 100 μ M Paraquat, which was observed to increase the ROS significantly (figure **3-8c**).

Figure 3-8a: Mitochondrial ROS Measurement Isolated From MCF-7 Cells

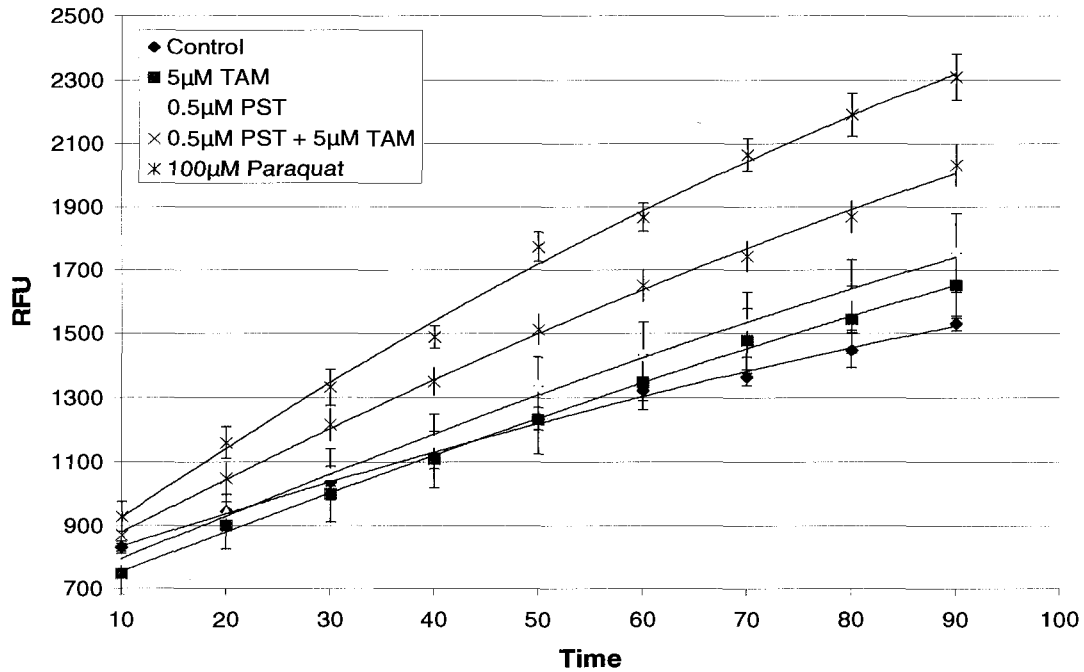


Figure 3-8a: Mitochondrial ROS measurement isolated from MCF-7 cells. Isolated MCF-7 cell mitochondria were incubated directly with 0.5µM PST, 5µM Tamoxifen and a combination of both. The amplex red/HRP mitochondrial ROS detection assay was performed over a period 1.5 hours. Readings were taken every 2 minutes using a fluorometer. Standard deviations were calculated upon the completion of 3 separate experiments.

Figure 3-8b: Mitochondrial ROS measurement isolated from Hs578-T cells

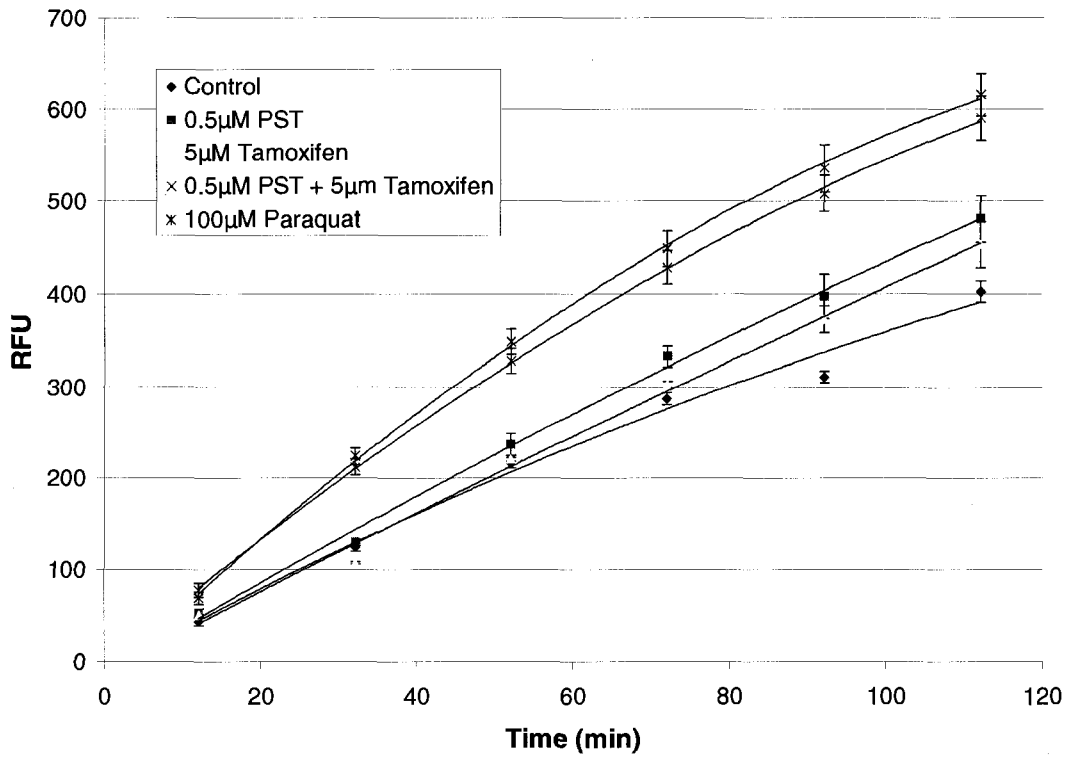


Figure 3-8b: Mitochondrial ROS measurement isolated from Hs578-T cells. Isolated Hs578-T cell mitochondria were incubated directly with 0.5µM PST, 5µM Tamoxifen and a combination of both. The amplex red/HRP mitochondrial ROS detection assay was performed over a period 1.5 hours. Readings were taken every 2 minutes using a fluorometer. Standard deviations were calculated upon the completion of 3 separate experiments.

Figure 3-8c: Mitochondrial ROS Measurement Isolated From NHF Cells

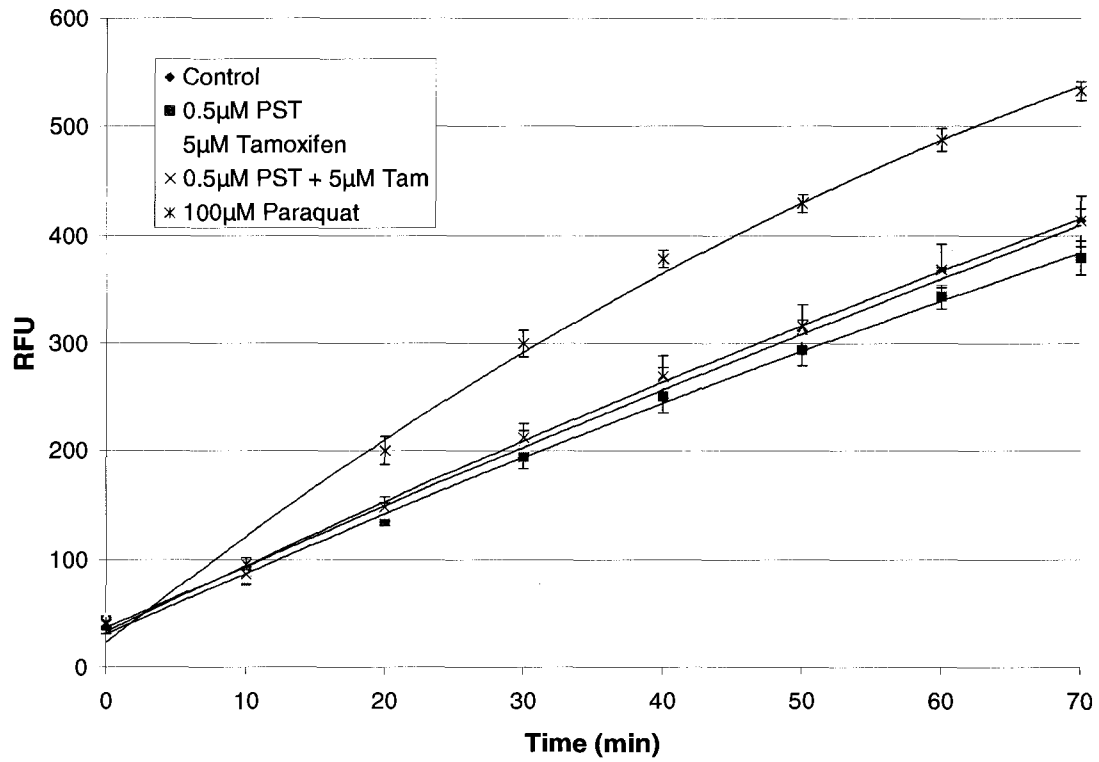


Figure 3-8c: Mitochondrial ROS measurement isolated from NHF cells. Isolated NHF cell mitochondria were incubated directly with 0.5µM PST, 5µM Tamoxifen and a combination of both. The amplex red/HRP mitochondrial ROS detection assay was performed over a period 1.5 hours. Readings were taken every 2 minutes using a fluorometer. Standard deviations were calculated upon the completion of 3 separate experiments.

3.1.10 PST and Tamoxifen Cause Release of Cytochrome *c* Synergistically in Isolated MCF-7 Mitochondria

To investigate Cytochrome *c* release from isolated mitochondria after PST treatment, we prepared isolated mitochondrial fractions from MCF-7 cells. Polyclonal anti-Cytochrome *c* antibody was used to probe for Cytochrome *c* retained within the mitochondria after the 2 hour incubation period. Anti-Succinate dehydrogenase antibody was used as a mitochondrial loading control. The concentrations used to treat isolated mitochondrial fractions include: 0.5 μ M, 1 μ M, 2 μ M, 4 μ M and 8 μ M PST and figure shows **3-9a** that 0.5 μ M PST did not significantly reduce the amount of Cytochrome *c* retained within the mitochondria. Figure **3-9a** shows that concentrations of 1 μ M PST and greater were required to significantly reduce the amount of Cytochrome *c* retained in the mitochondrial pellets.

To study the relative effect of combined PST and Tamoxifen treatment on isolated mitochondria preparations, we incubated mitochondrial pellets prepared from MCF-cells, for a period of 2 hours, with 0.5 μ M PST and 5 μ M Tamoxifen. It was observed from figure **3-9b** that 0.5 μ M PST did not reduce the amount of Cytochrome *c* retained within the mitochondria when compared with the control. As shown in figure **3-9b** 5 μ M Tamoxifen did not significantly reduce the amount of Cytochrome *c* retained in the mitochondrial pellets, however the combined treatment of 0.5 μ M PST and 5 μ M Tamoxifen was sufficient to decrease the amount of Cytochrome *c* retained within the mitochondria.

Figure 3-9a: Retention of Cytochrome *c* Upon Treatment of PST Directly on Isolated MCF-7 Mitochondria.

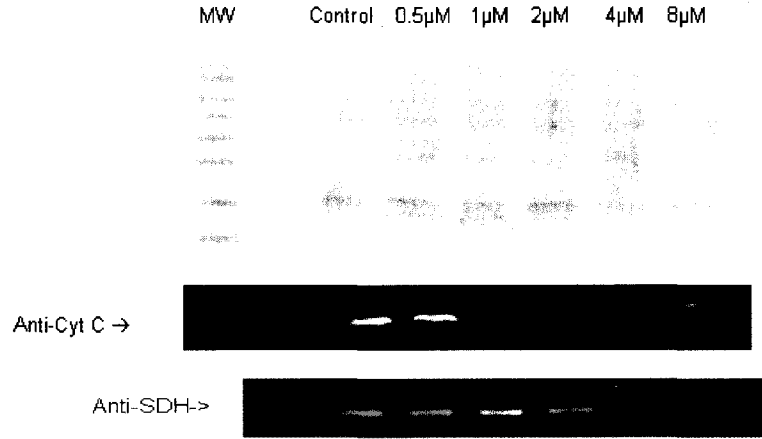


Figure 3-9a: Retention of Cytochrome *c* upon treatment of PST directly on MCF-7 isolated mitochondria. Approximately 100µg of mitochondrial protein was incubated with indicated concentrations of PST for a period of 2 hours upon which time mitochondrial pellets were loaded onto a polyacrylamid gel and blotted for cytochrome C and succinate dehydrogenase.

Figure 3-9b: Retention of Cytochrome *c* Upon the Combinatorial Treatment of PST and Tamoxifen Directly on Isolated MCF-7 Mitochondria.

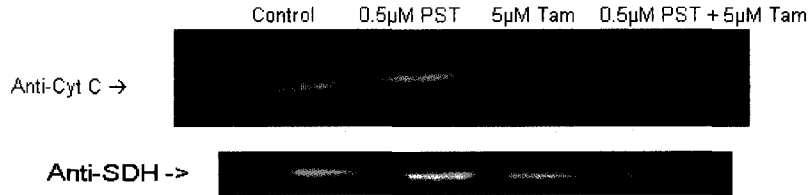


Figure 3-9b: Retention of Cytochrome C upon the combinatorial treatment of PST and Tamoxifen directly on MCF-7 isolated mitochondria. Approximately 100µg of mitochondrial protein was incubated with 0.5µM PST and 5µM Tamoxifen for a period of 2 hours upon which time mitochondrial pellets were loaded onto a polyacrylamid gel and blotted for cytochrome C and succinate dehydrogenase.

3.2 Insights into the Mechanism of PST Induced Apoptosis

Apoptosis induction caused by PST has been well established in our lab, however specific questions with respect to the internal biochemical response remain. We looked at levels of pro/anti-apoptotic proteins and caspase-8 activation in MCF-7, Hs578-T and NHF cells. Furthermore we examined MCF-7 cells for resistance over prolonged sub-lethal PST incubation.

3.2.1 Pro/Anti-apoptotic Protein Expression and Localization Upon PST Treatment in Hs578-T, MCF-7 and NHF Cells

To gain insights into biochemical mechanism of PST we probed cytosolic and mitochondrial fractions of MCF-7, Hs578-T and NHF cells with specific bcl-2 pro and anti-apoptotic protein antibodies to check for cellular expression and localization. Cells were treated with 1 μ M PST for 48 hours, homogenized and fractionated as per protocol, 40 μ g of proteins from the separate fractions were analyzed by western blot for the indicated antibody as per protocol. The polyclonal antibodies used for the western blot analysis include: anti-Bax, anti-Bad, anti-Bcl-2, anti-Bcl-xl, anti-Cytochrome C and anti-Succinate dehydrogenase.

We investigated the response of MCF-7 cells to 1 μ M PST treatment with respect to localization and expression of pro/anti-apoptotic proteins in cytosolic and mitochondrial fractions. Figure **3-10a** shows that the cytosolic fraction of MCF-7 cells treated with 1 μ M PST for 48 hours exhibited significantly higher amounts of Bad pro-apoptotic protein and significantly lower amounts of Bax pro-apoptotic protein as compared to the control un-treated cells. The mitochondrial fraction was probed for

Cytochrome *c* and Bax and it was observed in figure **3-10b** that the levels of cytochrome *c* decreased and the levels of Bax increased in the treated cells.

The breast cancer cell line Hs578-T was also analyzed for the expression anti/pro-apoptotic proteins under the same conditions as the MCF-7 cells to co-relate the overall response to treatment with 1 μ M PST for 48 hours. As observed in figure **3-10b** the cytosolic fraction levels of Bcl-2 are decreased and the levels of both Bax and Bad increased. In addition figure **3-10b** shows that in mitochondrial fractions the levels of Cytochrome *c* is decreased and levels of Bax are increase in the treated Hs578-T cells.

Analysis of pro/anti-apoptotic proteins in normal human fibroblast cells (NHF) revealed no significant changes in protein expression and localization as can be seen in figure **3-11a** and **3-11b**.

Figure 3-10a: Cytosolic Fraction of MCF-7 Cells Treated with 1 μ M PST



Figure 3-10a: Cytosolic fraction of MCF-7 cells treated with 1 μ M PST. MCF-7 cells were treated for a period of 48 hours. Cells were harvested and cytosolic fractions were isolated as per protocol. Western blots were then run as per protocol and blotted for specified antibodies. ImageJ was used to analyze the relative treated to control ratio (right column).

Figure 3-10b: Mitochondrial Fraction of MCF-7 Cells Treated with 1 μ M PST

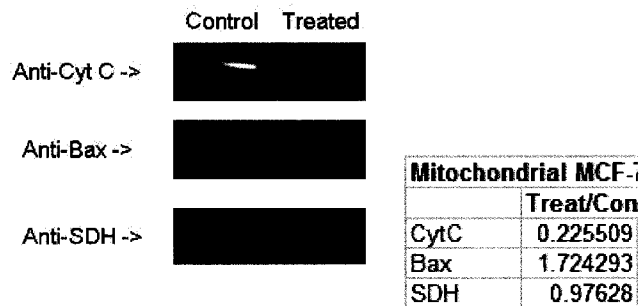


Figure 3-10b: Mitochondrial fraction of MCF-7 cells treated with 1 μ M PST. MCF-7 cells were treated for a period of 48 hours. Cells were harvested and mitochondrial fractions were isolated as per protocol. Western blots were then run as per protocol and blotted for specified antibodies. ImageJ was used to analyze the relative treated to control ratio (right column).

Figure 3-11a: Cytosolic fraction of Hs578-T Treated with 1 μ M PST

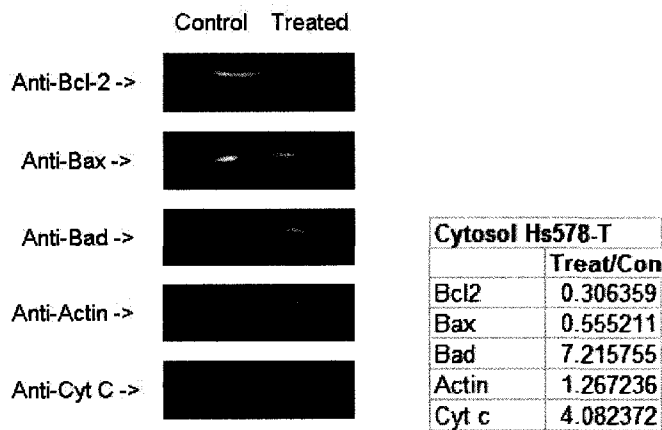


Figure 3-11a: Cytosolic fraction of Hs578-T cells treated with 1 μ M PST. Hs578-T cells were treated for a period of 48 hours. Cells were harvested and cytosolic fractions were isolated as per protocol. Western blots were then run as per protocol and blotted for specified antibodies. ImageJ was used to analyze the relative treated to control ratio (right column).

Figure 3-11b: Mitochondrial Fraction of Hs578-T Cells Treated with 1 μ M PST

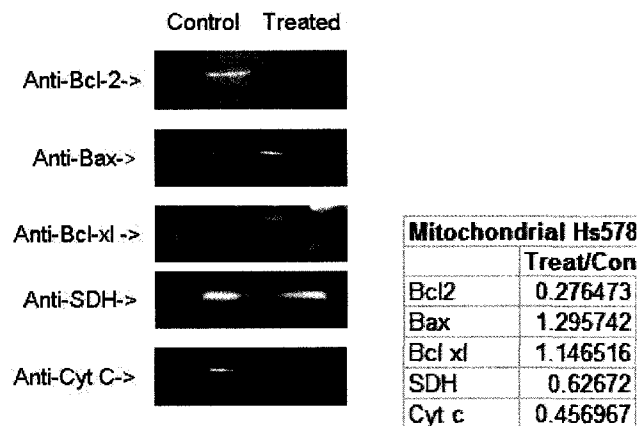


Figure 3-11b: Mitochondrial fraction of Hs578-T cells treated with 1 μ M PST. Hs578-T cells were treated for a period of 48 hours. Cells were harvested and mitochondrial fractions were isolated as per protocol. Western blots were then run as per protocol and blotted for specified antibodies. ImageJ was used to analyze the relative treated to control ratio (right column).

Figure 3-12a: Cytosolic Fraction of NHF Treated with 1 μ M PST

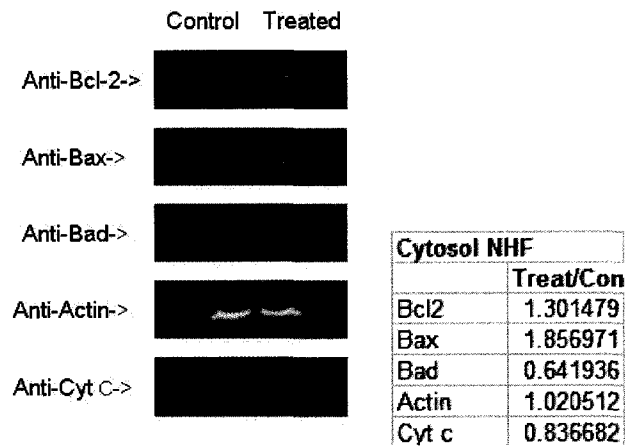


Figure 3-12a: Cytosolic fraction of NHF cells treated with 1 μ M PST. NHF cells were treated for a period of 48 hours. Cells were harvested and cytosolic fractions were isolated as per protocol. Western blots were then run as per protocol and blotted for specified antibodies. ImageJ was used to analyze the relative treated to control ratio (right column).

Figure 3-12b: Mitochondrial Fraction of NHF Cells Treated with 1 μ M PST

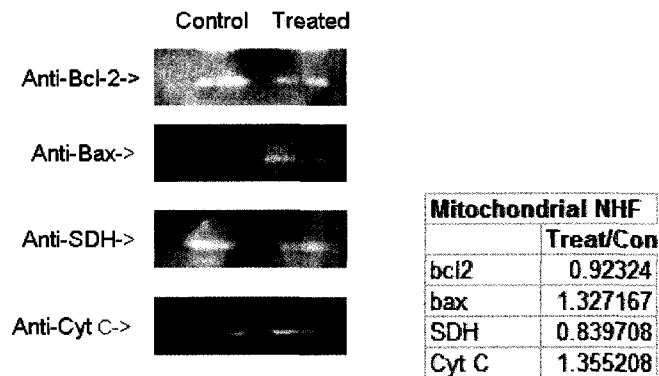


Figure 3-12b: Mitochondrial fraction of NHF cells treated with 1 μ M PST. NHF cells were treated for a period of 48 hours. Cells were harvested and mitochondrial fractions were isolated as per protocol. Western blots were then run as per protocol and blotted for specified antibodies. ImageJ was used to analyze the relative treated to control ratio (right column).

3.2.2 Hs-578-T and MCF-7 Cells Exhibit Late Caspase-8 Activation

The analysis of live cell caspase-8 activation was investigated in MCF-7, Hs578-T and NHF cells. The incubation of 1 μ M PST for the indicated time points revealed late caspase-8 activation in both cancer cell lines (MCF-7 and Hs578-T). Figure **3-13a** shows that MCF-7 cells exhibit late (24 hour) caspase-8 activation. As can be observed in figure **3-13b** the Hs578-T cells exhibit significant caspase-8 activation at 48 hours. Furthermore, as shown in figure **3-13c**, no caspase-8 activation was observed in 1 μ M PST treated NHF cells.

Figure 3-13a: MCF-7 Caspase-8 Live Assay

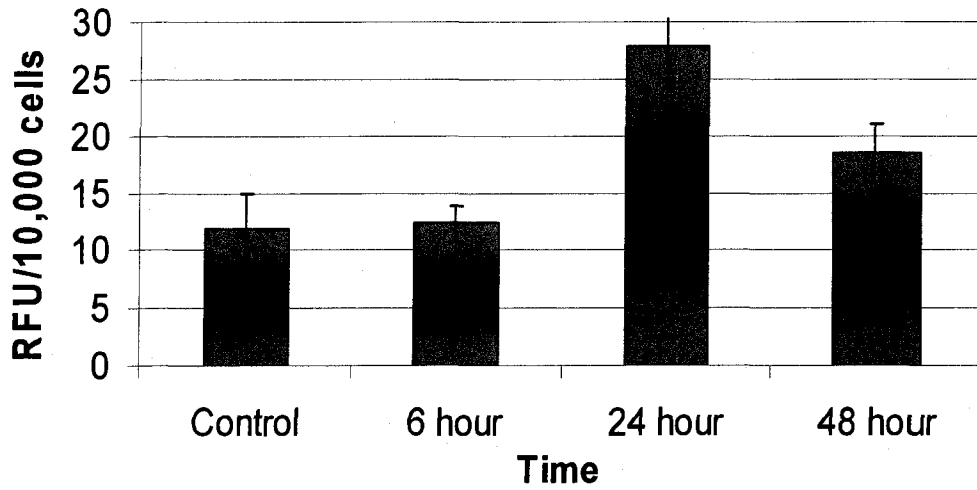


Figure 3-13a: MCF-7 caspase-8 live assay. MCF-7 cells were incubated with 1 μ M PST for the indicated times at which point a cell permeable FAM-LETD-FMK substrate was added to detect the relative fluorescence using a flourimeter set at excitation 488nm and emission 520nm. After the assay cells were counted and the relative fluorescent units per 10,000 cells was expressed.

Figure 3-13b: Hs578-T Caspase-8 Live Assay

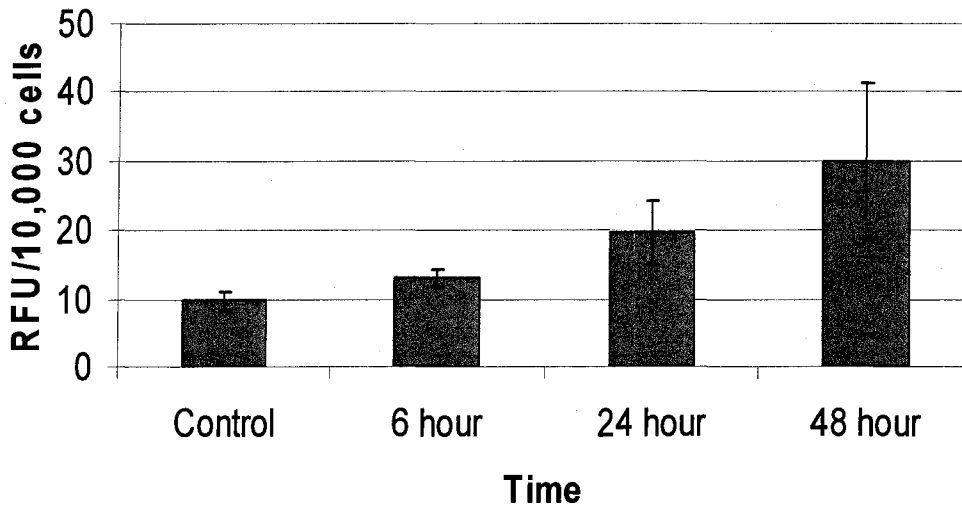


Figure 3-13b: Hs578-T caspase-8 live assay. Hs578-T cells were incubated with 1 μ M PST for the indicated times at which point a cell permeable FAM-LETD-FMK substrate was added to detect the relative fluorescence using a flourimeter set at excitation 488nm and emission 520nm. After the assay cells were counted and the relative fluorescent units per 10,000 cells was expressed.

Figure 3-13c: NHF Caspase-8 Live Assay

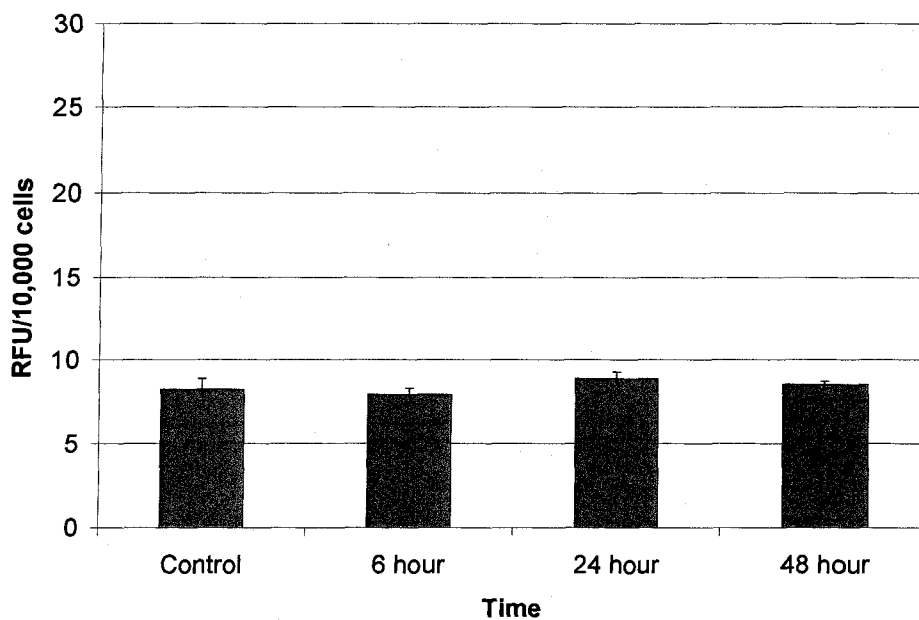


Figure 3-13c: NHF caspase-8 live assay. NHF cells were incubated with 1 μ M PST for the indicated times at which point a cell permeable FAM-LETD-FMK substrate was added to detect the relative fluorescence using a fluorimeter set at excitation 488nm and emission 520nm. After the assay cells were counted and the relative fluorescent units per 10,000 cells was expressed.

3.2.3 MCF-7 Cells Do Not Exhibit Resistance to PST

While the overall response rate to treatment can be high in breast cancer cells, the duration of response is relatively short, and it has been observed that initially responsive breast tumors acquire a multidrug resistance phenotype (Trock *et. al.* 1997). This phenotype is frequently characterized by a cross-resistance to drugs to which the tumors have not been exposed. The development of a multidrug resistant phenotype in metastatic breast cancer is primarily responsible for the failure of current treatment regimens (Trock *et. al.* 1997).

To test the potential of resistance to PST by MCF-7 cells we pre-incubated these cells with sub-lethal doses of PST and after a period of time we challenged these cells with the lethal 1 μ M dose. MCF-7 cells were treated with 25nM and 50nM PST for 20 days upon which the cells were challenged with 1 μ M PST for 72 hours. After the 72 hour incubation period MCF-7 cells were treated with the lethal dose of 1 μ M PST. Cells were then incubated with Hoechst 33342 dye and stained nuclei counted. Figure 3-14 shows that there was no difference in the degree of apoptosis induction between MCF-7 cells pre-treated with sub-lethal doses of PST and MCF-7 control (not pre-treated), as both types of cells exhibited the same apoptotic response upon 72 hour incubation with 1 μ M PST.

Figure 3-14: Apoptotic Index of Resistance to PST Treatment

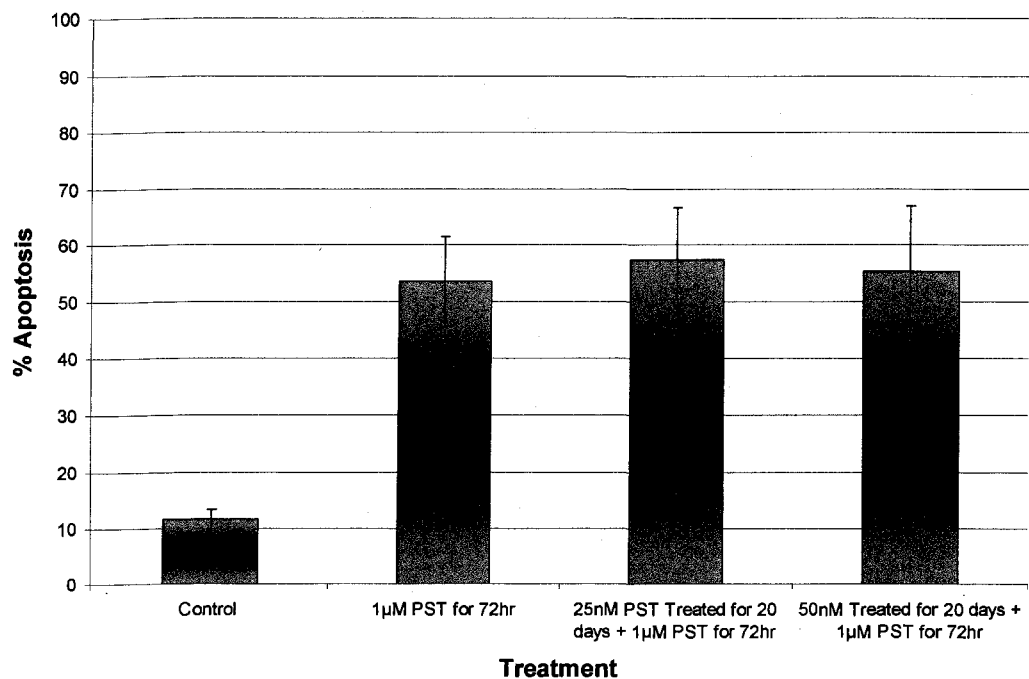


Figure 3-14: Apoptotic Index of Resistance to PST Treatment. MCF-7 cells were pre-treated for 20 days with sub-lethal 25 and 50nM PST treatments. After 20 days cells were re-plated and treated with lethal dose of 1µM PST for 72 hours. Hoechst 33342 dye was added and the number of cells exhibiting apoptotic nuclear morphology was counted.

3.3 Preliminary Study of *in-vivo* PST and Tamoxifen Induced Apoptosis

To test the effect of PST and Tamoxifen *in-vivo*, a RAG 2M mouse model was developed. Ten immunocompromised RAG 2M mice with disrupted recombination activating gene-2 were used in the model. Time release 17 β -estradiol pellets were injected sub-cutaneously into the neck of each mouse using a trochar device to achieve maximum tumor growth (Webb *et. al.* 2007). Tumors were generated by injecting 6 x 10⁶ MCF-7 cells subcutaneously into hind flank each mouse. Tumors were allowed to grow for approximately 2 weeks after initial injection until an approximate size of 5mm in diameter was visible. Mice were then selected and grouped according to relative tumor size for treatments. Four groups were generated with placebo (peanut oil), PST (3mg/kg), Tamoxifen (25mg/kg), and both PST (3mg/kg) and Tamoxifen (25mg/kg). Intra tumoral PST injections were given twice a week and intra peritoneal Tamoxifen injections were given 3 times up to a total of 10 PST injections and 14 Tamoxifen injections over 5 weeks on the 6th week the mice were put down. Over the course of the experiment 2 mice died in their cage unexpectedly (PST and Tamoxifen) and therefore the data presented is based on results from the remaining mice.

3.3.1 Breast Cancer Tumors Successfully Generated In RAG 2M Mice

We attained a 100% success rate in the development of human breast cancer tumors in each of the mice injected in the study. Figure 3-15 shows clearly visible subcutaneous tumors. Due to the hair on the mice it was difficult to measure the progression of tumor size over the course of treatment and so therefore only gross weight measurements were recorded during the treatment phase of the experiment. A total of six

weight measurements were taken over the course of the study as observed in figure **3-16** there were no significant changes in the gross weights of the mice. This data is preliminary and needs to be repeated to generate accurate results.

Figure 3-15: Tumorigenesis in RAG 2M Mouse Model



Figure 3-15: Tumorigenesis in RAG 2M mouse model established by the injection of 6×10^6 MCF-7 cells subcutaneously as per protocol.

Figure 3-16: Gross weight Measurements of Mice

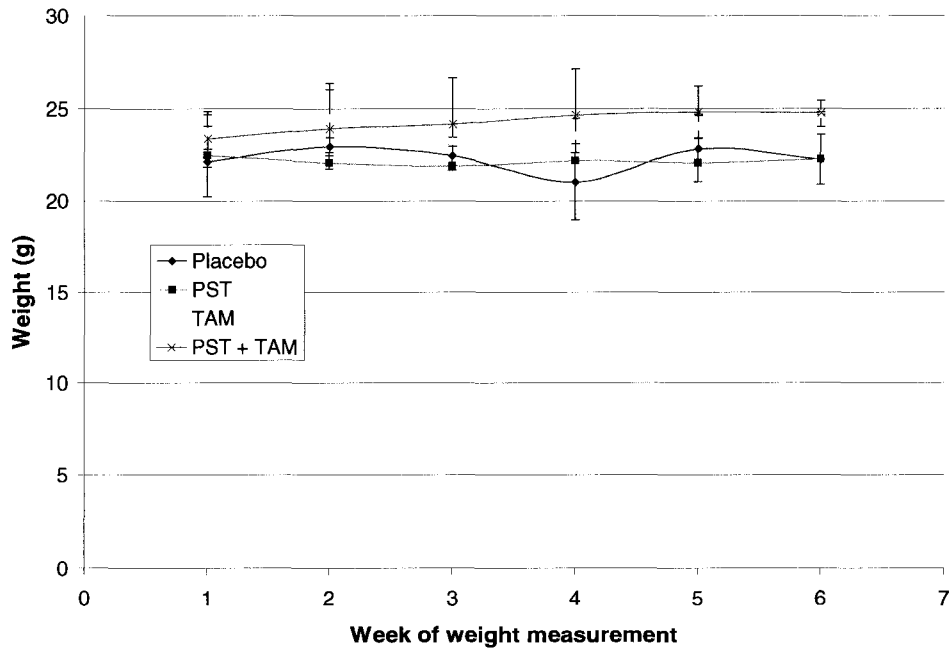


Figure 3-16: Gross weight measurements of mice. RAG 2M Mice were weighed 6 times over a 5 week period as part of handling procedure to record the total weight of the mouse over the course of treatment. Plotted is the weight of mice in the experimental groups which include: Placebo, PST, Tamoxifen (TAM) and PST + TAM.

3.3.2 TUNEL and DAPI Staining Reveal No Toxicity To Kidney and Liver

To evaluate genotoxicity of the treatments to organ tissue, the kidney and liver of each mouse was removed and prepared in wax blocks at which point 8 micron sections were prepared on slides as per protocol. Terminal Uridine Nick End Labeling assay was carried out as mentioned in materials and methods in order to evaluate the integrity of DNA. Each slide was also stained with DAPI to evaluate the nuclear morphology of the cells. All results are preliminary and will require further testing to validate.

The liver of each mouse was analyzed and figure **3-17a** shows that there was no positive TUNEL staining for any of the treatment groups. The DAPI stains revealed that the nuclear morphology of the tissues appeared consistently healthy across all test groups (figure **3-17a**).

The kidneys of each mouse were also removed and sectioned as per protocol to check for potential genotoxicity. Figure **3-17b** shows that no apparent genotoxic effects were observed when analyzing the TUNEL stains qualitatively. The lack of TUNEL staining in these tissues (figure **3-17b**) directly indicates the lack of nicks in the nuclear DNA which co-relates to the lack of genotoxicity in all samples analyzed. From qualitative analysis of the DAPI stains in **3-17b** it was revealed that the nuclear morphology does not change between the 3 treatments (PST, Tamoxifen, and PST + Tamoxifen) when compared to the placebo.

3.3.3 TUNEL and DAPI Staining Reveal Toxicity to Treated Tumor Samples

From our preliminary data it was observed that tumor samples from the treated groups (PST, Tamoxifen and PST + Tamoxifen) exhibited positive TUNEL labeling when compared to placebo. As observed in figure 3-17c there appears to be TUNEL DNA labeling particularly in the PST + Tamoxifen treated tumors (as denoted by bright green fluorescence). There also seems to be a greater intensity of DAPI staining in the PST + Tamoxifen treated tumors (figure 3-17c). TUNEL labeling was also observed to a lesser extent in PST or Tamoxifen alone; however these observations are only preliminary and more testing will be required to validate the findings.

Figure 3-17a: TUNEL Labeling and DAPI Staining of Liver Tissue Samples

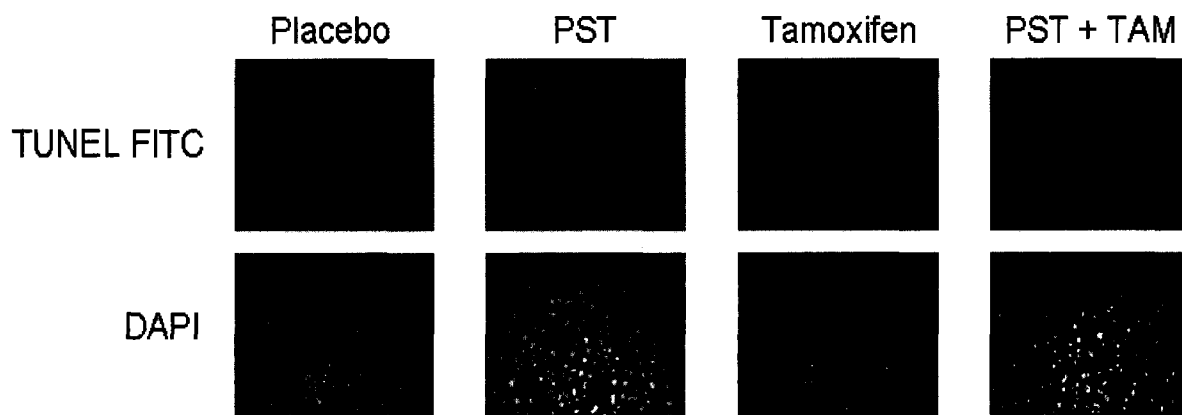


Figure 3-17a: TUNEL labeling and DAPI staining of liver tissue samples. Liver sections for each treatment group were stained by TUNEL and DAPI as per protocol to visualize apoptotic features. Bright TUNEL staining indicated DNA nicks.

Figure 3-17b: TUNEL Labeling and DAPI Staining of Kidney Tissue Samples

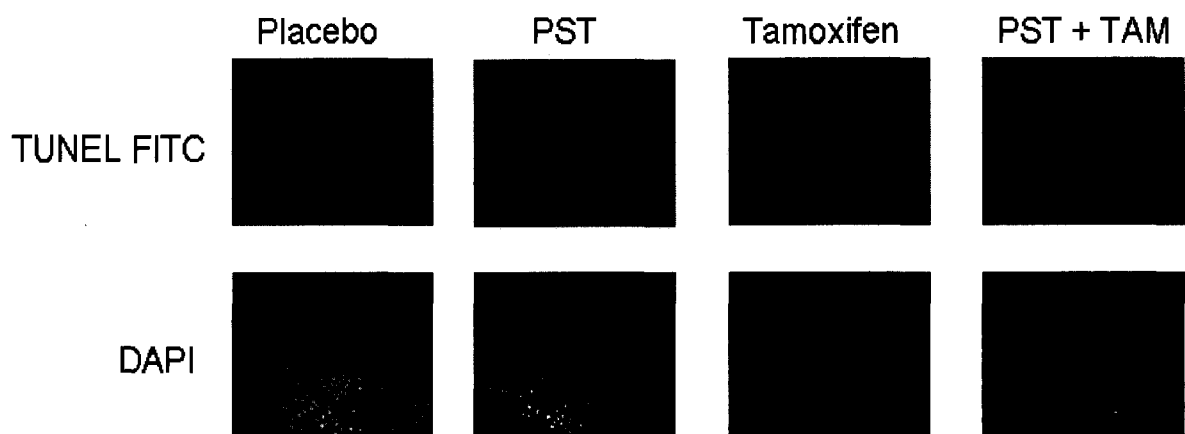


Figure 3-17b: TUNEL labeling and DAPI staining of kidney tissue samples. Kidney sections for each treatment group were stained by TUNEL and DAPI as per protocol to visualize apoptotic features. Bright TUNEL staining indicated DNA nicks.

Figure 3-17c: TUNEL Labeling and DAPI Staining of Tumor Tissue Samples

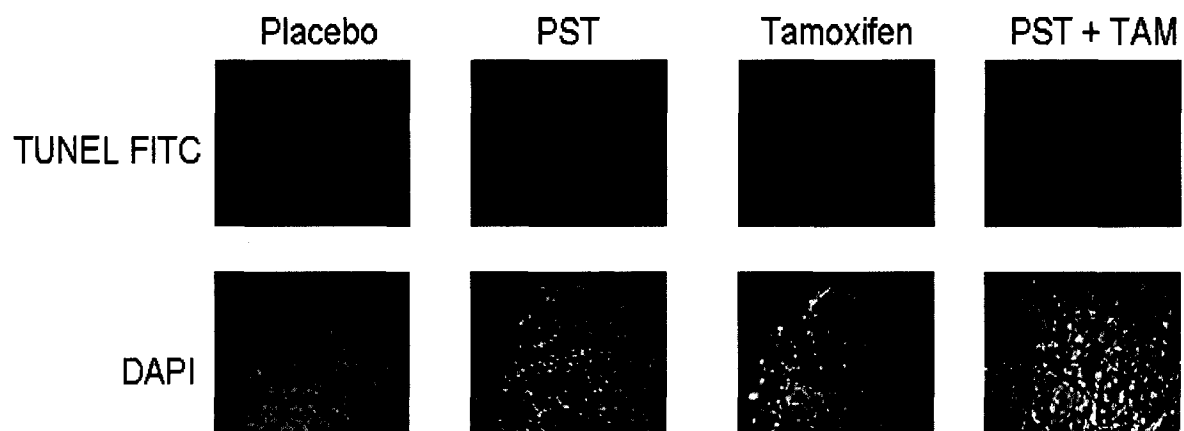


Figure 3-17c: TUNEL labeling and DAPI staining of Tumor tissue samples. Tumor sections for each treatment group were stained by TUNEL and DAPI as per protocol to visualize apoptotic features. Bright TUNEL staining indicated DNA nicks.

3.3.4 Histological Analysis of Tissues Using Hematoxylin and Eosin

To analyze the overall morphology of the tissue samples, we analyzed the sectioned liver, kidney and tumor samples using hematoxylin and eosin staining. Hematoxylin stains the nucleus and eosin stains the cytoplasm thus visualization of the morphological features of a cell becomes possible. Proper histochemical analysis will have to be performed by a trained pathologist these observations are only qualitative and preliminary.

Figure 3-18a shows that the liver samples in all treatments appear to be relatively same in consistency with respect to nuclear and cellular morphology. As observed in figure 3-18a there does not appear to be any morphological changes when compared to placebo. Furthermore, analysis of the kidney samples exhibited similar staining in all the treatment samples studied (figure 3-18b). Therefore no severe liver and kidney cellular changes were observed when comparing the treatment groups to placebo indicating minimal effect towards treatment.

Tumor samples analyzed by hematoxylin and eosin revealed interesting morphological features in the different treatment groups. It was found that the density of cells appeared to be higher in placebo and Tamoxifen groups (figure 3-18c). It is observed that the morphology of the treatment groups, in particular the combined treatment of PST + Tamoxifen, had drastic effects on the morphology of the cells (figure 3-18c). Tamoxifen + PST treated tumors exhibit inconsistencies in nuclear shape and cellular density (figure 3-18c). These insights are preliminary observations and the slides must be properly analyzed by a trained pathologist.

Figure 3-18a: Hematoxylin and Eosin Stain: Liver Morphology

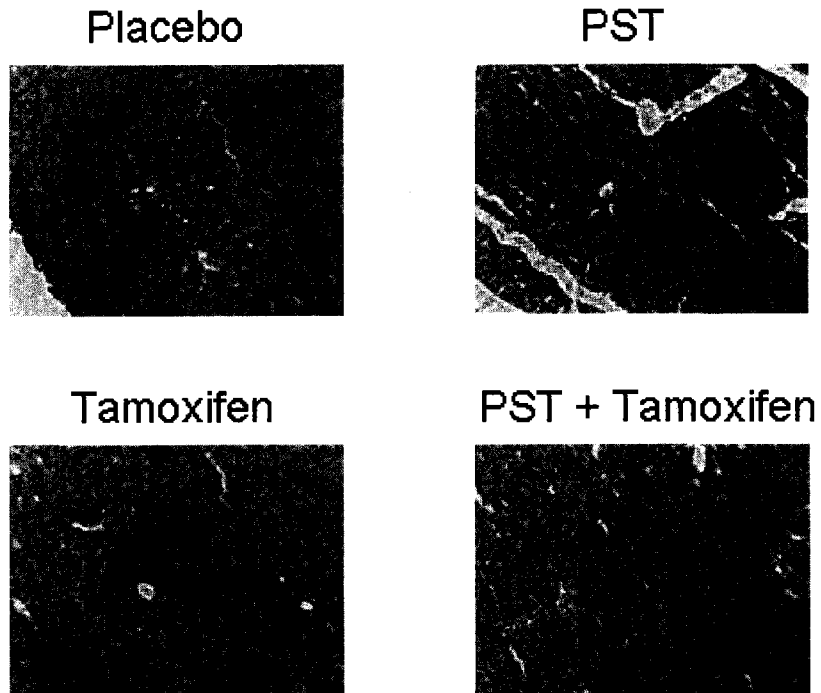


Figure 3-18a: Hematoxylin and eosin stain: liver morphology. Tissue morphology was analyzed by staining the nucleus with eosin and the cytosol with hematoxylin. Pictures were taken at 200x magnification using a phase-contrast light microscope and observed by motic imaging software.

Figure 3-18b: Hematoxylin and Eosin Stain: Kidney Morphology

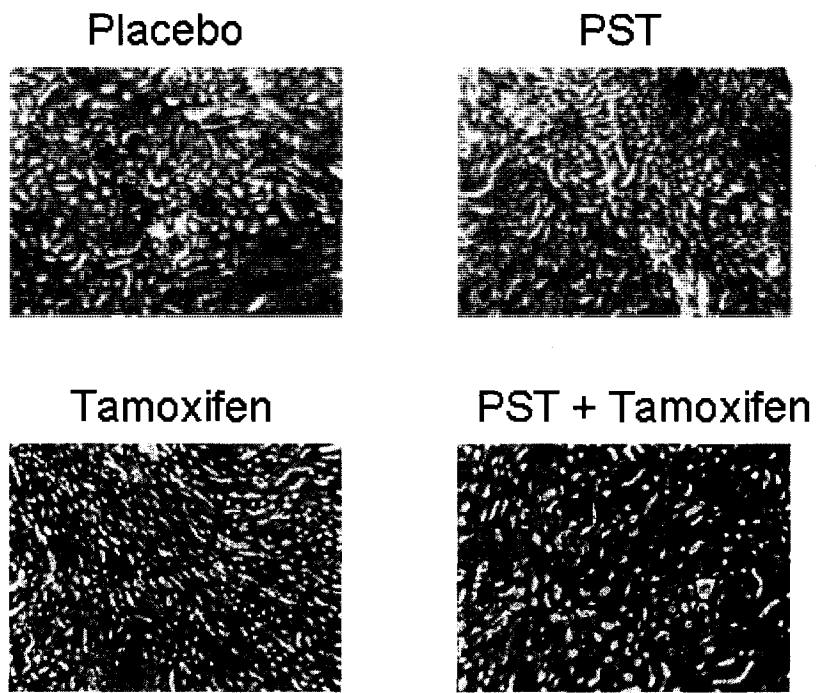


Figure 3-18b: Hematoxylin and eosin stain: kidney morphology. Tissue morphology was analyzed by staining the nucleus with eosin and the cytosol with hematoxylin. Pictures were taken at 200x magnification using a phase-contrast light microscope and observed by motic imaging software.

Figure 3-18c: Hematoxylin and Eosin Stain: Tumor Morphology

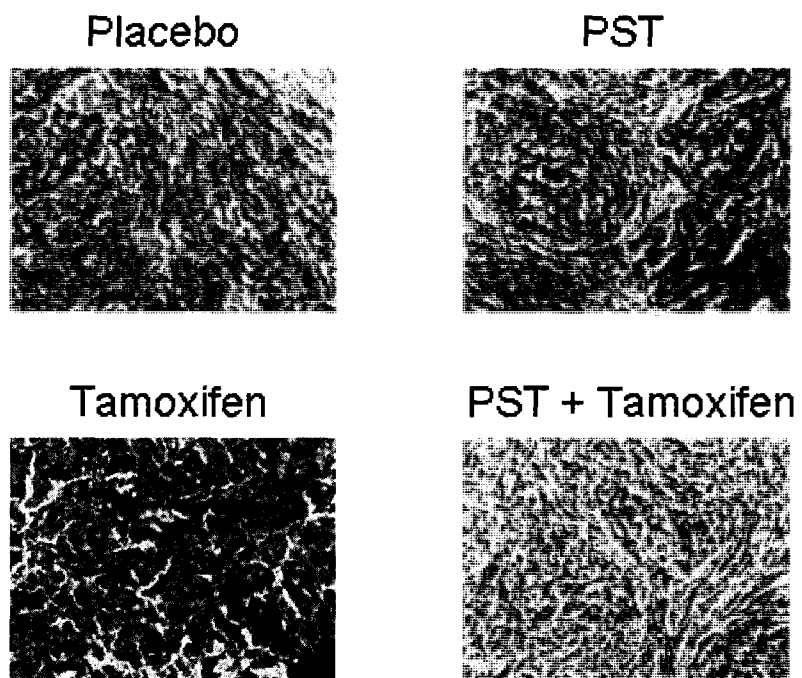


Figure 3-18c: Hematoxylin and eosin stain: tumor morphology. Tissue morphology was analyzed by staining the nucleus with eosin and the cytosol with hematoxylin. Pictures were taken at 200x magnification using a phase-contrast light microscope and observed by motic imaging software.

3.3.5 Western Blot Analysis: Kidney, Liver and Tumor Samples

To determine the expression and localization of key apoptotic factors, western blot analysis was performed on flash frozen tissue samples from the *in-vivo* studies. Tissue samples included liver, kidneys and tumor, of each mouse. The tissues were homogenized and fractionated into nuclear, cytoplasmic and mitochondrial fractions (as described in materials and methods). Western blot analysis was carried out with 50µg of protein from cytosolic and mitochondrial fractions and the use of Bax, Bad, Cytochrome *c* and actin antibodies allowed for qualitative comparisons of the levels of these proteins in each tissue and fraction.

Liver samples were prepared into cytosolic and mitochondrial fractions and probed for key apoptotic factors as mentioned previously. As shown in figure 3-19a no changes in the levels of apoptotic factors (Bax, Bad and Cytochrome *c*) were observed in the cytoplasmic fraction. Furthermore, figure 3-19b demonstrates that the mitochondrial fractions did not exhibit any changes in the levels of Bax and Cytochrome *c*.

Kidney samples were then analyzed by western blot analysis, from figure 3-20a shows that the cytosolic component did not have any drastic changes in the levels of Bax, Bad, and Cytochrome *c*. As observed in figure 3-20b the kidney mitochondrial fraction did not show significant changes in the level of Bax and Cytochrome *c*.

Tumor samples analyzed by western blot demonstrated interesting preliminary results. In particular, figure 3-21a shows that the cytosolic fraction of tumor cells has an increase in the level of Cytochrome *c* in the Tamoxifen and the PST + Tamoxifen treated tissues. The pro-apoptotic Bad protein had increased levels in the cytosol of PST treated tumors more so than any other treatment (figure 3-21a). Mitochondrial fractions prepared

from tumor samples exhibit a distinct increase in the level of Bax protein in the PST + Tamoxifen treated tumor (figure 3-21b).

Figure 3-19a: Mouse Liver Cytosolic Fraction

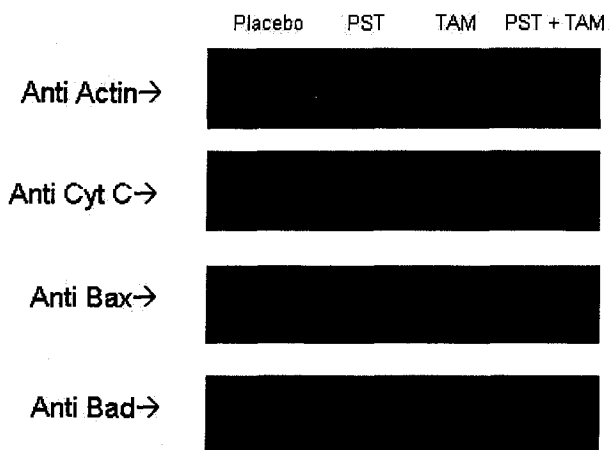


Figure 3-19a: Mouse liver cytosolic fraction. Liver tissue was homogenized and cytosolic fractions were isolated as per protocol. Approximately 50 μ g of protein were loaded on polyachrylamide gel and immunoblotted for Bad, Bax, Cyt *c* and Actin.

Figure 3-19b: Mouse Liver Mitochondrial Fraction

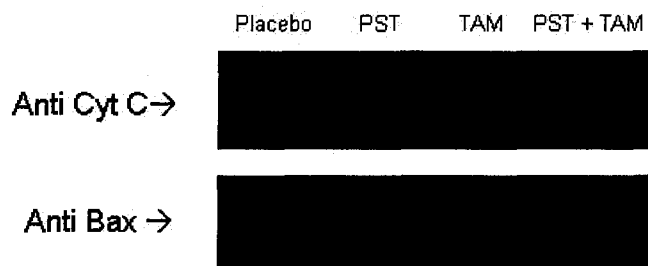


Figure 3-19b: Mouse liver mitochondrial fraction. Liver tissue was homogenized and mitochondrial fractions were isolated as per protocol. Approximately 50 μ g of protein were loaded on polyachrylamide gel and immunoblotted for Bax and Cyt *c*.

Figure 3-20a: Mouse Kidney Cytosolic Fraction

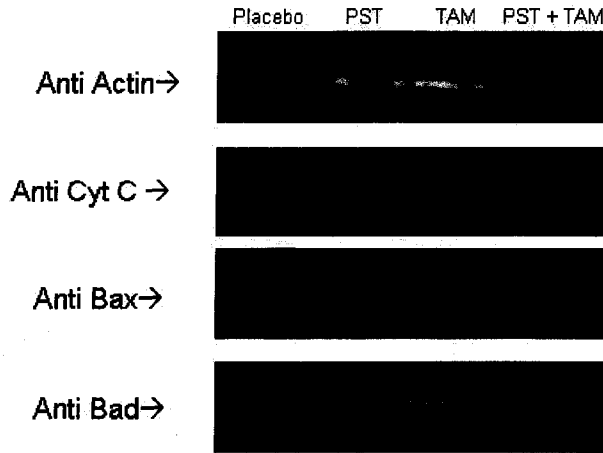


Figure 3-20a: Mouse kidney cytosolic fraction. Kidney tissue was homogenized and cytosolic fractions were isolated as per protocol. Approximately 50 μ g of protein were loaded on polyachrylamide gel and immunoblotted for Bad, Bax, Cyt *c* and Actin.

Figure 3-20b: Mouse Kidney Mitochondrial Fraction

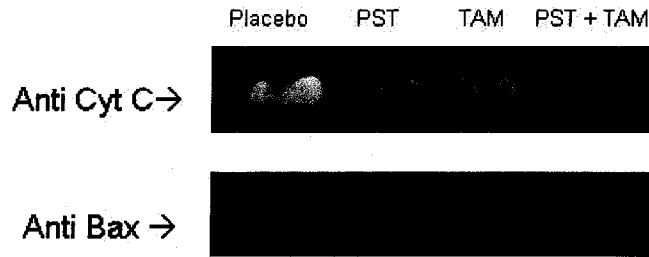


Figure 3-20b: Mouse kidney mitochondrial fraction. Kidney tissue was homogenized and mitochondrial fractions were isolated as per protocol. Approximately 50 μ g of protein were loaded on polyachrylamide gel and immunoblotted for Bax and Cyt *c*.

Figure 3-21a: Mouse Tumor Cytosolic fraction

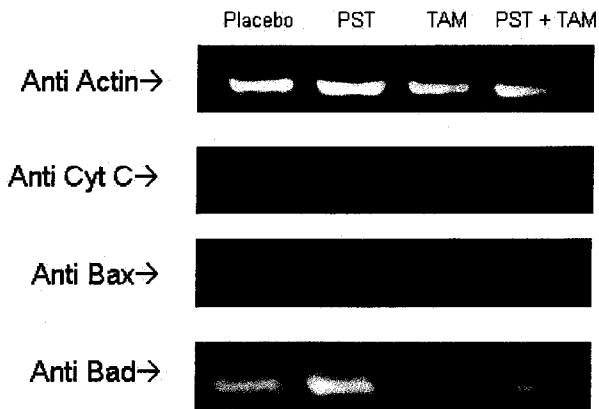


Figure 3-21a: Mouse tumor cytosolic fraction. Tumor tissue was homogenized and cytosolic fractions were isolated as per protocol. Approximately 50µg of protein were loaded on polyacrylamide gel and immunoblotted for Bad, Bax, Cyt *c* and Actin.

Figure 3-21b: Mouse Tumor Mitochondrial Fraction

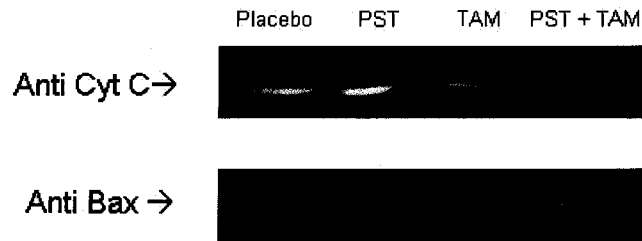


Figure 3-21b: Mouse tumor mitochondrial fraction. Tumor tissue was homogenized and mitochondrial fractions were isolated as per protocol. Approximately 50µg of protein were loaded on polyacrylamide gel and immunoblotted for Bax and Cyt *c*.

CHAPTER 4: DISCUSSION

The holy grail of anti-cancer therapy is selective elimination of cancer cells without affecting normal tissues. In the present work we demonstrate that PST is very selective and efficient in inducing apoptotic cell death in two different breast cancer cell lines without affecting the non-cancerous cells. In addition, we observed that treatment with low doses of Tamoxifen and PST had a synergistic effect in inducing apoptosis in cancerous MCF-7 and Hs578-T cells. Furthermore our results suggest that both these compounds may be inducing apoptosis by synergistically destabilizing mitochondria in cancer cells selectively.

4.1 Synergy between PST and Tamoxifen is Estrogen Receptor Pathway Independent

Tamoxifen, is a well established antagonist to estrogen receptor that primarily induces apoptosis in ER positive breast cancer cells by modulation of gene expression. Interestingly, recent research has indicated that besides ER-mediated genomic effects, Tamoxifen induces mitochondrial destabilization and apoptosis in an ER- independent manner in several ER negative cancer cell lines (Mandlekar, Kong 2001).

We used Tamoxifen in combination with PST to see if there is a synergistic effect. Indeed, our results using Hoechst staining clearly indicated that lower concentrations of 0.5 μ M PST and 5 μ M Tamoxifen together induced apoptosis in higher numbers than either compound alone in breast cancer MCF-7 cells. At a period of 72 hours the apoptotic index of 0.5 μ M PST increased by approximately 20% when incubated along with 5 μ M Tamoxifen. We validated this result by quantifying the synergistic effect using flow cytometry and observed that annexin V binding gave similar

synergistic profiles in the MCF-7 cells, were in which the apoptosis inducing potential of PST at a low dose of 0.5 μ M increased by 20% upon combined 5 μ M Tamoxifen incubation. The TUNEL assay carried by flow cytometry revealed that 0.5 μ M PST exhibited a approximate 4% increase in apoptotic induction when combined with 5 μ M Tamoxifen, this is far less than the result obtained in the annexin-V result, however it can be explained as DNA knicks are a later stage event in apoptosis, when cells undergo membrane blebbing, however phosphatidyl serine flipping (as observed by annexin-V binding) is an early stage apoptotic marker were cells are still in-tact. Therefore at 72 hours it is expected that most cells will exist in the later stage of apoptosis, in which condensation of DNA, membrane blebbing and cell shrinking occurs (Duke *et. al.* 1996). This therefore would pose challenges in the gating of these cells in the flow cytometry machine. It would be interesting to look at these stains at earlier time points, however due to access restrictions we were only able to gain accurate data for the 72 hour time period.

Our result show that the synergistic effect was also observed in ER negative breast cancer cells (Hs578-T). This effect however was observed at higher Tamoxifen concentrations. Specifically we found that the apoptotic index of 0.5 μ M PST was increased by 20% when incubated in combination with 10 μ M Tamoxifen, where as 10 μ M Tamoxifen treatment on its own did not induce any apoptosis in the Hs578-T cell line. This result therefore demonstrated that the synergistic effect is ER independent and potentially plays a role on mitochondria.

4.2 Role of Mitochondria in Synergistic Response

Differences between the mitochondria of cancerous versus normal cells have been researched intensely (Don, Hogg 2004, Villa, Doglia 2004). As previously discussed,

many cancerous cells have an altered metabolism, mitochondrial DNA mutations and altered membrane compositions (Green, Kroemer 2004, Villa, Doglia 2004, Modica-Napolitano, Singh 2002, Polyak *et. al.* 1998).

Increases in the total whole cell ROS have been linked to destabilization of mitochondria (Fluery *et. al.* 2002). We looked at total ROS production in both MCF-7 (ER+) and Hs578-T (ER-) cells. We found that the combined treatment of 0.5 μ M PST and 5 μ M Tamoxifen induced greater total ROS than either compound separately in both the ER+ MCF-7 (ER+) and Hs578-T (ER-) cells.

Depolarization of the mitochondrial membrane potential is essential for mitochondrial induced apoptosis (Green, Kroemer 2004, Yuan *et. al.* 2001). We confirmed this effect by JC-1 staining to observe the collapse of the mitochondrial membrane potential upon PST and Tamoxifen treatment. It was found that the combined treatment of PST and Tamoxifen reduced mitochondrial membrane potential in both MCF-7 (ER+) and H-578-T (ER-) cells upon 48 hour treatment.

Previous work has indicated that PST has mitochondrial targets which allow for selective induction of apoptosis (McLachlan *et. al.* 2005). Furthermore current research indicates that Tamoxifen has the ability to induce apoptosis through mitochondrial dysfunction, independently of its function as an estrogen receptor antagonist (Mandlekar, Kong 2001, Moreire *et. al.* 2006). To verify if mitochondria are being affected by the combined treatment of PST and Tamoxifen we performed ROS measurements directly on isolated mitochondria. Mitochondria from MCF-7 (ER+) and Hs578-T (ER-) cells were isolated and a HRP/Amplex Red ROS assay was carried out. Furthermore, we used Paraquat as a positive control. Paraquat induces ROS by disruption of the electron

transport chain (Mollace *et. al.* 2003). We found that the combined treatment of 0.5 μ M PST and 5 μ M Tamoxifen induced mitochondrial ROS increases in greater amount than either compound alone and to the same extent in both cell lines investigated. Indicating that both compounds (Tamoxifen and PST) target specific regions of the mitochondria and inducing increases in ROS production.

Mitochondrial membrane permeabilization plays a key role in apoptosis by releasing caspase activators such as Cytochrome *c* (Fernandez-Chenca 2003, Duchon 2004, Green, Reed 1998). We observed Cytochrome *c* leakage from isolated MCF-7 mitochondria. We found that a minimum of 1 μ M PST was required to induce cytochrome *c* leakage from isolated mitochondria. Interestingly 0.5 μ M PST was found to be insufficient to cause cytochrome C release, however when treated in combination with 5 μ M Tamoxifen we began to see mitochondrial Cytochrome *c* leakage. This result further supported the previous observation that the mitochondria seem to be targets of both PST and Tamoxifen in inducing destabilization of mitochondrial membrane leading to apoptosis.

4.3 PST and Tamoxifen Treatment Does Not Induce Apoptosis In Normal Cells

The observations of synergy between PST and Tamoxifen on whole cells as well as isolated mitochondria supports the hypothesis that vulnerability of cancer cell mitochondria could be used as cancer specific target to induce apoptosis selectively in cancer cells. However to verify the selectivity we chose to work with NHF cell model, NHF cells were chosen because of the relative ease of use and maintenance, we

encountered problems with contamination from company stocks of normal breast fibroblast cells (Hs578-Bst).

Previous work with anticancer compounds has led to the discovery of many clinically used chemotherapeutics which target cancerous cells non-selectively and therefore have drastic side-effects (Yeung *et. al.* 1999, Boos, Stopper 1999). PST has been previously observed to exhibit little toxicity to normal cell lines (McLachlan *et. al.* 2005). We therefore tested the combined effect of PST and Tamoxifen on normal human fibroblasts to evaluate any potential toxic effects.

From our analysis of Hoechst staining it was found that no clear indication was observed of apoptotic induction in NHF cells at all concentrations of PST and Tamoxifen studied. Observing the whole cell ROS we found that there was no apparent increase in whole cell ROS when compared to control untreated NHF cells. Furthermore it was found that upon treatment of isolated mitochondria from NHF cells we did not see any significant increase in ROS production from control. Likewise JC-1 staining indicated that the mitochondrial membrane potential in these cells remains intact even when challenged at the high 1 μ M PST and 10 μ M Tamoxifen concentrations. Therefore we observed that the synergistic effect is specific towards cancer cells.

4.4 Localization of Key Apoptotic Factors in PST Induced Apoptosis

The localization and expression of pro/anti-apoptotic proteins dictate whether a cell undergoes apoptosis or survives. Some Bcl-2 proteins localize to different compartments within the cell. During survival and cell proliferation, pro-apoptotic proteins such as Bax are generally compartmentalized in the cytosol while the anti-

apoptotic proteins such as Bcl-2 and Bcl-xl are found on the mitochondrial membrane and endoplasmic reticulum (Kuwana, Newmeyer 2003). Upon encountering a stress signal, the pro-apoptotic protein Bax will migrate to the outer mitochondrial membrane and cause the dysfunction of mitochondrial membrane potential (Goping *et. al.* 1998). One of the key stresses imposed on a cell that tips the balance between pro/anti-apoptotic state is the level of reactive oxygen species present within the cell. It is thought that ROS increases can be tolerated in cancer cells by the up-regulation of proteins such as Bcl-2 and Bcl-xl, which protect the mitochondria from mitochondrial membrane collapse (Harris, Thompson 2000). However if the ROS condition inside a cell is too high then apoptotic cell death is mediated by the up-regulation and activation of anti-apoptotic proteins such as Bax, this in turn causes Bax to migrate to the mitochondrial membrane where it is thought to interact with the protein transition pore complex (MPTP) and cause mitochondrial apoptotic factors such as Cytochrome *c* to be released (Harris, Thompson 2000).

Here we found Bax localization to the mitochondria following PST treatment and direct evidence for Cytochrome *c* leakage. In both MCF-7 and Hs578-T cells we found localization of Bax protein to the mitochondria, as well as Cytochrome *c* leakage after 48 hours of 1 μ M PST treatment. This may be attributed to increases in reactive oxygen species caused by direct PST interaction with mitochondria. Interestingly, we found that levels of Bad protein were increased in the treated cytosolic fraction of both cell lines. This result is particularly interesting because it suggests that there is up-regulation of Bad protein expression in both cell lines since Bad does not have a mitochondrial binding domain and predominantly resides in the cytosol. Bad protein acts by sequestering and in-

activating Bcl-2 protein (Kuwana, Newmeyer 2003). When looking at the relative levels of pro/anti-apoptotic proteins in the normal NHF cell line we did not see any significant differences in any of the protein levels. Due to the previous result that PST can directly cause release of Cytochrome *c* at concentrations of 1 μ M we therefore reason that PST both increases levels of ROS leading to apoptotic susceptibility as well as directly permeabilizing the mitochondrial membrane.

In future studies it should be noted that both Actin and Succinate Dehydrogenase controls should be run in both treated and control samples to give a reflection of relative purity in the sample.

Caspases are apoptotic messengers; their role is to propagate the apoptotic signal towards a state of cell suicide. Caspase-8 activation indicates extrinsic apoptotic signaling when occurring at early time points (Plesnila *et. al.* 2001). Using a cell membrane permeable caspase-8 substrate we found that late activation of caspase-8 occurs in both Hs578-T (48 hour) and MCF-7 (24 hour) cells indicating that caspase-8 activation occurs in a later stage of apoptosis induction. The difference in time of activation of caspase-8, we reason, is due to the fact that MCF-7 cells are caspase-3 deficient (Essmann *et. al.* 2004), and therefore a greater reliance on caspase-8 and other apoptogenic factors is required to bi-pass caspase-3 induced apoptosis in MCF-7 cells.

4.5 MCF-7 Cells Do Not Become Resistant to PST Treatment

Resistance to treatment is a major obstacle in chemotherapeutic development and research. Cancer cells have the capacity to up-regulate ATP-binding cassette transporter (ABC transporters) genes which give it the ability to reduce the amount of xenobiotics (drugs, toxins), as well as endobiotics within the cell and therefore reduce the effect of a

specific drug (Trock *et. al.* 1997). Therefore, to observe any resistance of MCF-7 cells to PST treatment we exposed these cells to prolonged sub-lethal dose of 25nM or 50nM PST for a period of 20 days, we did not observe any changes in the sensitivity of MCF-7 cells to the lethal dose of 1 μ M PST treatment. This result indicates that PST does not induce mechanisms of resistance in MCF-7 cells.

4.6 *In-vivo* Study of PST and Tamoxifen Synergy

Previous athymic nude mouse models that were used to establish colon tumors would not allow for MCF-7 tumorigenesis. We used a mouse model for breast cancer consisting recombinase deficient RAG 2M mice as described by Webb *et. al.* 2007. Each mouse had to be injected with a slow release 60-day 17- β estradiol tablet 24 hours prior to cancer cell injection. Approximately 6 X 10⁶ human breast cancer (MCF-7) cells were injected in the right hind flank. We were successful in establishing tumors in all the mice in our study and injected them with PST or Tamoxifen accordingly. At this point all data is preliminary since the experimental procedure had to be standardized for these mice.

Specific problems were encountered over the course of the experiment. For instance these mice contained fur making it difficult to measure tumor size progression using calipers. Also, over the course of the experiment two of the mice died in their cage (one PST and one Tamoxifen), therefore reducing the number of mice in the experiment. Tamoxifen was prepared in peanut oil as described previously (Paine-Murrieta *et. al.* 1997) because it is lipid soluble. However, this method of administering Tamoxifen gave rise to complications with respect to absorption. When dissecting the mice, oil pockets were found in the subcutaneous portions indicating that the oil had not properly absorbed into the body. Furthermore, growth rates of the tumors varied: some mice exhibited

tumors before others; the mice were treated accordingly to when tumor sizes reached approximately 5mm in diameter. Therefore, these preliminary results must be repeated with a larger sample of mice in order to make the findings statistically significant.

Despite complications, certain changes to the protocol are proposed here to enhance the reproducibility of the experiment. Nude mice were not used for modeling breast cancer because it is notoriously difficult to establish hormone dependent tumors through subcutaneous injections (Giovanella, Fogh 1985). RAG 2M mice were used because injected MCF-7 cells were reported to establish into tumors (Webb *et. al.* 2007). However, It has been reported that the use of matrigel greatly increases the tumorigenicity of MCF-7 cells in nude athymic mice (Fridman *et. al.* 1991). Therefore an alternate approach would be to use matrigel to establish MCF-7 tumors, which are relatively same size prior to insertion into immunocompromised mice. This model would have the advantage of increasing the ability to monitor tumor progression over the course of treatment, since the tumors would be relatively the same size and clearly visible.

Work by Yue *et. el* 1994. showed that once injected into the subcutaneous cavity, MCF-7 cells transfected with human placental aromatase gene (MCF-7a) provide a non-ovarian source of estrogen in nude BALB/c athymic mice. Furthermore, this work showed that these transfected cells (MCF-7a) developed into tumors rapidly and consistently when mice were given androstenedion (aromatase substrate) at a concentration of 0.1mg/per mouse/per day (injected subcutaneously) when compared with mice transfected with a control vector (MCF-7c). Therefore these considerations could be taken into account when developing future mouse models in our *in-vivo* study to establish more accurate and reliable data.

CHAPTER 5: FUTURE PERSPECTIVES

Critical hurdles exist in the research of PST as an anticancer compound. One of the major obstacles is the development of a synthetic compound produced by an organic process. Our collaborator Dr. McNaulty, an organic chemist at McMaster University is currently working on ways to simplify the organic synthesis of PST and has successfully developed structural analogues of PST, which help to deduce the minimum pharmacophore required for activity (McNulty *et. al* 2005). It is possible that an active derivative of PST may retain synergistic properties, and when combined with Tamoxifen may be used to treat a variety of cancer types.

The development of a synthetic PST derivative will allow for tritium or carbon-14 labeling. Radioactive labeling will allow us to therefore pinpoint the exact biochemical target of PST, and therefore expand our knowledge in cancer cell susceptibility.

The ability of Tamoxifen to destabilize the mitochondria enables testing of combinatorial treatment (PST and Tamoxifen) in a variety of cell lines, not just breast carcinoma. Currently, exactly that is being applied to a human melanoma cell line, and in the future, we will investigate the synergistic response in a host of different cancer cells (ex. Lymphoma, Colon, Pancreatic, Prostate, Lung...etc.) in order to observe any relevant increases in the apoptotic index of combined treatment versus single treatment alone.

Changes in protein expression and localization caused by PST treatment can be further investigated by 2-dimensional in gel electrophoresis (2-DIGE). Control and treated cellular fractions (cytosolic and mitochondrial) can be fluorescently labeled with separate dyes which incorporate into either lysine or cysteine residues and give two

distinct colors green or red. The fractions can then be run together on the same 2-dimensional gel and the relative intensity of each spot, with respect to their color, can determine the relative amount of up-regulation or down-regulation of the proteins in specified cellular fractions (mitochondrial and cytosolic).

CHAPTER 6: Conclusions

We have clearly demonstrated the apoptosis-inducing activity of PST in breast cancer cells, with no detectable toxicity to non-cancerous cells. The intrinsic pathway of apoptosis was observed by mitochondrial destabilization through ROS increases and Cytochrome *c* release in both Hs578-T and MCF-7 breast cancer cell lines, without any indication of this occurrence in the normal counterpart NHF cell line. Interestingly, there was a synergistic apoptotic effect with combined treatment of PST and Tamoxifen in both estrogen receptor positive (MCF-7) and estrogen receptor negative (HS578-T) cell lines. More importantly it was established that both of these drugs target cancer cell mitochondria selectively indicating that the observed effect is independent of estrogen receptor. Furthermore, we developed for the first time in our lab, a human breast cancer (MCF-7) mouse model using RAG 2M mice, although the results are inconclusive, they do open the window for future experiments on the synergistic response of PST and Tamoxifen *in-vivo*. Therefore a new window of opportunity has now been opened to develop novel combination therapy for cancer treatment.

REFERENCES

1. Albanell J, Baselga J. Unravelling resistance to trastuzumab (herceptin): insulin-like growth factor-1 receptor, a new suspect. *Journal of the National Cancer Institute*. 2001; 93: 1830-1832.
2. Ames B N, Gold L S, Willett W C. The causes and prevention of cancer. *Proceedings of the National Academy of Sciences*. 1995; 92 (12): 5258-65.
3. Amundadottir L.T., Merlino G., Dickson R.B. Transgenic mouse models of breast cancer. *Breast Cancer Res Treat*. 1996; 39:119-135.
4. Ashkenazi A, Dixit V M. Death receptors; signaling and modulation. *Science*. 1998; 281: 1305-1308.
5. Baum M. Adjuvant endocrine therapy in postmenopausal women with early breast cancer: Where are we now? *European Journal of Cancer*. 2005; 41: 1667–1677.
6. Benedict M A, Hu Y, Inohara N, Nunez G. Expression and functional analysis of Apaf-1 isoforms: Extra Wd-40 repeat is required for cytochrome c binding and regulated activation of procaspase-9. *Journal of Biological Chemistry*. 2000; 275: 8461-8468.
7. Boose G, Stopper H. Genotoxicity of several clinically used topoisomerase II inhibitors. *Toxicology Letters*. 2000; 116: 7-16.
8. Canadian Cancer Society, National Cancer Institute of Canada, Statistics Canada, Provincial / Territorial Cancer Registries, Public Health Agency of Canada Canadian Cancer Statistics 2008. *Canadian Cancer Society*. 2008. www.cancer.ca
9. Carafoli E. Mitochondria and disease. *Mol Aspects Med*. 1980; 3: 295-429.
10. Cardiff RD. Validity of mouse mammary tumor models for human breast cancer: comparative pathology. *Microscopy Research and Technique*. 2001; 52:224-230.

11. Casciola-Rosen L, Nicholson D W, Chong T, Rowan K R, Thornberry N A, Miller D K, Rosen A. Apopain / CP32 cleaves proteins that are essential for cellular repair: a fundamental principle of apoptotic death. *Journal of Experimental Medicine*. 1996; 183: 1957-64.
12. Chabner B A, Roberts T G Jr. Timeline: Chemotherapy and the war on cancer. *Nature Reviews Cancer*. 2005; 5(1): 65-72.
13. Chernyak B V, Bernardi P. The mitochondrial permeability transition pore is modulated by oxidative agents through both pyridine nucleotides and glutathione at two separate sites. *European Journal of Biochemistry*. 1996; 238: 623-630.
14. Chinnadurai G, Lutz R J. A conserved domain in Bak, distinct from BH1 and BH2 mediates cell death and protein binding functions. *The EMBO Journal*. 1995; 14 (22): 5589-5596
15. Chou JJ , Li H, Salvesen G S, Yuan J, Wagner G. Solution structure of BID, an intracellular amplifier of apoptotic signaling. *Cell*. 1999; 96(5): 615-24.
16. Cunha KS., Reguly ML., Graf U., de Andrade HHR., Taxanes: the genetic toxicity of paclitaxel and docetaxel in somatic cells of drosophila melangaster. *Mutagenesis*. 2001; 16:79-84.
17. Debatin K M. Apoptosis pathways in cancer and cancer therapy. *Cancer Immunology Immunotherapy*. 2004; 53(3): 153-9.
18. Degtarev A., Boyce M., Yuan J. A decade of caspases. *Oncogene*. 2003; 22: 8543-8567.
19. Don A, Hogg P. Mitochondria as cancer drug targets. *Trends in Molecular Medicine*. 2004; 10(8): 372-377.

20. Dragowska W.H., Verreault M., Yapp D.T., Warburton C., Edwards L., Ramsey E.C., Huxham L.A., Minchinton A.I., Gelmon K., Bally M.B. Decreased levels of hypoxic cells in gefitinib treated ER+ HER-2 overexpressing MCF-7 breast cancer tumors are associated with hyperactivation of the mTOR pathway: therapeutic implications for combined therapy with rapamycin. *Breast Cancer Res Treat.* 2007; 106:319-331.
21. Duchon M R. Roles of mitochondria in health and disease. *Diabetes.* 2004; 53: 96-102.
22. Duffy MJ. Predictive markers in breast and other cancers: a review. *Clinical Chemistry.* 2005; 51: 494-503.
23. Duke RC, Ojcius DM, Young JD. Cell suicide in health and disease. *Scientific America.* 1996: 80-7.
24. Dunning AM., Healey CS., Pharoah PD., Teare MD., Ponder B., Easton DF. A systemic review of genetic polymorphisms and breast cancer risk. *Cancer Epidemiology.* 1999; 8:843-854.
25. Earnshaw C W, Martins M L, Kaufman H S. Mammalian caspases; structure, activation, substrates and functions during apoptosis. *Annual Reviews in Biochemistry.* 1999; 68: 383-424.
26. Essmann F., Engels IH., Totzke G., Schulze-Osthoff K., Janicke RU. Apoptosis resistance of MCF-7 breast carcinoma cells to ionizing radiation is independent of P53 and cell cycle control but caused by the lack of caspase-3 and a caffeine-inhibited event. *Cancer Research.* 2004; 64:7065-7072.
27. Fantin V R, Leder P. F16, a mitochondriotoxic compound, trigger apoptosis or necrosis depending on the genetic background of the target carcinoma cell. *Cancer*

Research. 2004; 64: 329-36.

28. Fernandez-Chenca C. Redox regulation and signaling lipids in mitochondrial apoptosis. *Biochemical and Biophysical Research Communications*. 2003; 304: 471-479.
29. Fluery C, Mignotte B, Vayssiere JL. Mitochondrial reactive oxygen species in cell death signaling. *Biochimie*. 2002; 84: 131-41.
30. Fridman, R., Kibbey, M. C., Royce, L S., Zain, M., Sweeney, T. M., Jicha, D. L, Yannelli, J. R., Martin, G. R., and Kleinman, H. K. Enhanced tumor growth of both primary and established human and murine tumor cells in athymic mice after coinjection with matrigel. *Journal of National Cancer Institute*. 1991; 83: 769-774.
31. Fulda S., Scaffidi C., Susin S.A., Krammer P.H., Kroemer G., Peter M.E., Debatin K.M. Activation of Mitochondria and Release of Mitochondrial Apoptogenic Factoris by betulinic acid. *The Journal of Biological Chemistry*. 1998; 273 (51): 33942-33948.
32. Gayther S., Warren W., Mazoyer S., Russel P., Harrington P., Chiano M., Seal S., Hamoudi R., van Rensburg E., Dunning A., Love R., Evans G., Easton D., Clayton D., Stratton M., Ponder B. Germline mutations of the BRCA1 gene in breast and ovarian cancer families provide evidence for a genotype-phenotype correlation. *Nature*. 1995; 11: 428-433.
33. Gelmann EP. Tamoxifen for the treatment of malignancies other than breast and endometrial carcinoma. *Semin Oncol*. 1997; 24: S65-S75.
34. Giovanella, B. C., and Fogh, J. The nude mice in cancer research. *Advancements in Cancer Research*. 1985; 44: 69-120.

35. Goping I S, Gross A, Lavoie J N, Nguyen M, Jemmerson R, Roth K, Korsmeyer S J, Shore GC. Regulated targeting of BAX to mitochondria. *Journal of Cell Biology*. 1998; 143(1): 207-15.
36. Green D, Kroemer G. The Pathology of Mitochondrial Cell Death. *Science*. 2004; 305: 626-629.
37. Green D R, Reed J C. Mitochondria and apoptosis. *Science*. 1998; 281 : 1309-1312.
38. Gross A, Mc Donald J M, Korsmeyer S J. Bcl-2 family members and the mitochondria in apoptosis. *Genes & Development*. 1999; 13: 1899-1911.
39. Hait WN., Yang JM. The individualization of cancer therapy: the unexpected role of P53. *Transactions of the American Clinical and Climatological Association*. 2006; 117: 85-101.
40. Haldar S., Negrini M., Monne M., Sabbioni S., Croce CM. Down-regulation of Bcl-2 by P53 in breast cancer cells. *Cancer Research*. 1994; 54: 2095-2097.
41. Harris M H, Thompson C B. The role of Bcl-2 family in the regulation of outer mitochondrial membrane permeability. *Cell Death and Differentiation*. 2000; 7: 1182-91.
42. Haslett C. Resolution of acute inflammation and role of apoptosis in the tissue fate of granulocytes. *Clinical Science*. 1992; 83:639-648.
43. Heerdt AS, Borgan PI. Current status of Tamoxifen use: An update for the surgicaloncologist. *Journal of Surgical Oncology*. 1999; 72: 42-49.
44. Hirsch T., Susin S.A., Marzo I., Marchetti P., Zamzami N., Kroemer G. Mitochondrial permeability transition in apoptosis and necrosis. *Cell Biology and Toxicology*. 1998; 14: 141-145.

45. Hickey J., Raje R., Reid E., Gross M., Ray D., Diclofenac induced in vivo nephrotoxicity may involve oxidative stress-mediated massive genomic DNA fragmentation and apoptotic cell death. *Free Radical Biology & Medicine*. 2001; 31: 139-152.
46. Hongtae K., Junjie C. New Players in the BRCA1-mediated DNA Damage Responsive Pathway. *Molecules and Cells*. 2008; 25: 457-461.
47. Hunter J J, Bond B L, Parslow T G. Functional dissection of the human Bcl-2 protein: sequence requirements for inhibition of apoptosis. *Molecular Cell Biology*. 1996; 16(3): 877-883.
48. Jeremic B. Radiation therapy. *Hematology / Oncology Clinics of North America*. 2004; 18: 1-12.
49. Josephine S. M., Singh K.K. Mitochondrial dysfunction in cancer. *Mitochondrion* 2004; 755-762.
50. Josephine S, Modica N, Sing K. Mitochondria as targets for detection and treatment of cancer. *Expert Reviews*. 2002; 1-19.
51. Kallio A, Zheng A, Dahllund J, Heiskanen KM, Harkonen P. Role of mitochondria in tamoxifen-induced cancer cells. *Apoptosis*. 2005; 10: 1395-1410.
52. Kerr J F, Wyllie A H, Currie A R. Apoptosis: A basic biological phenomenon with wide ranging implications in tissue kinetics. *British Journal of Cancer*. 1972; 26: 239-257.
53. Kim R. Recent Advances in Understanding the Cell Death Pathways Activated by Anticancer Therapy. *Cancer*. 2005; 103(8): 1551-1560.
54. Kleinsmith, L J. Principles of Cancer Biology. Pearson Benjamin Cummings: 2006

55. Kohler T., Schill C., Deininger MW., Krahl R., Borchert S., Hasenclever D., Leiblein S., Wagner O., Niederwieser D. High Bad and Bax mRNA expression correlate with negative outcome in acute myeloid leukemia (AML). *Nature*. 2002; 16: 22-29.
56. Korsmeyer S J, Wei M C, Saito M. Proapoptotic cascade activates BID which oligomerizes BAK or BAX into pores that result in the release of cytochrome *c*. *Cell death and Differentiation*. 2000; 7: 1166-1173.
57. Kroemer G, Reed J C. Mitochondrial control of cell death. *Natural Medicine*. 2000; 6: 513-519.
58. Kroemer, G. Mitochondrial control of apoptosis: an introduction. *Biochemistry and Biophysics Research Communications*. 2003; 302: 433-435.
59. Kroemer G., Galluzzi L., Brenner C. Mitochondrial membrane permeabilization in cell death. *Physiol Rev*. 2007; 87: 99-163.
60. Kuwana T, Mackey MR, Perkins G, Ellisman MH, Latterich M, Schneider R, Green DR, Newmeyer DD: Bid, Bax and lipids cooperate to form supramolecular openings in the outer mitochondrial membrane. *Cell*. 2002; 111: 331-342.
61. Kuwana T., Newmeyer D. Bcl-2 family proteins and the role of the mitochondria in apoptosis. *Current Opinion in Cell Biology*. 2003; 15: 691-699.
62. Lamarca HL., Rosen JM. Hormones and mammary cell fate: what will I become when I grow up? *Endocrinology*. 2008; 1-6.
63. Leist M, Nicotera P. The shape of cell death. *Biochemistry and Biophysics Research Communications*. 1997; 236: 1-9.
64. Levine B., Sinha S., Kroemer G. Bcl-2 family members. *Autophagy*. 2008; 4 : 600-606.

65. Li N, Ragheb K, Lawler G, *et al.* Mitochondrial complex-I inhibitor rotenone induces apoptosis through enhancing mitochondrial reactive oxygen species production. *The Journal of Biological Chemistry*. 2003; 278; 8516-8525.
66. Li P., Nijhawan D., Budihardjo I., Srinivasula M., Ahmed M., Alnemri S., Wang X. Cytochrome c and dATP – dependent formation of Apaf-1 / caspase-9 complex initiates an apoptotic protease cascade. *Cell*. 1997; 91: 479-489.
67. Lin EY., Jones JG., Li P., Zhu L., Whitney K., Muller W., Pollard JW. Progression to malignancy in the polyoma middle T oncoprotein mouse breast cancer model provides a reliable model for human disease. *American Journal of Pathology*. 2003; 163(5): 2113-2126.
68. Luduena R F, Roach M C, Prasad V, Pettit G R. *Biochemical Pharmacology*. 1992; 43: 539.
69. Mandlekar S, Kong ANT. Mechanisms of Tamoxifen-induced apoptosis. *Apoptosis*. 2001; 6: 469-77.
70. Martin NMB. DNA Repair Inhibition and Cancer Therapy. *Journal of Photochemistry & Photobiology*. 2001; 63: 162-70.
71. McCarthy S, Somayajulu M, Hung M, Sikorska M, Borowy-Borowski H, Pandey S. Paraquat Induces Oxidative Stress and Neuronal Cell Death; Neuro-protection by Water-Soluble Coenzyme Q₁₀. *Toxicology & Applied Pharmacology*. 2004; 201: 21-31.
72. McDonnell J M, Fushman D, Milliman C L, Korsmeyer S J, Cowburn D. Solution structure of the proapoptotic molecule BID: a structural basis for apoptotic agonists and antagonists. *Cell*. 1999; 96: 625-634.

73. McGuire WL, Carbone PP, Sears ME, Escher GC. Estrogen receptors in human breast cancer: an overview. In: McGuire WL, Carbone PP, Vollner EP, eds. Estrogen receptors in human breast cancer. *New York: Raven Press*. 1975; 1-8.
74. McLachlan A, Kekre N, McNulty J, Pandey S. Pancreatistatin: a natural anti-cancer compound that targets mitochondria specifically in cancer cells to induce apoptosis. *Apoptosis*. 2005; 10(3): 619-30.
75. McLachlan-Burgess A, McCarthy S, Griffin C, Richer J, Pandey S. The differential response induced by exposure to low-dose ionizing radiation in SHSY-5Y and normal human fibroblast cells. *Applied Biochemistry & Biotechnology*. 2006; *In Press*.
76. McNulty J, Larichev V, Pandey S. A synthesis of 3-deoxyhydrolycoricine: refinement of a structurally minimum Pancreatistatin pharmacophore. *Bioorganic & Medicinal Chemistry Letters*. 2005; 1: 15(23): 5315-5318.
77. Mendlekar S., Kong T. Mechanisms of Tamoxifen-induced apoptosis. *Apoptosis*. 2001; 6: 469-477.
78. Mense S., Hei T., Ganju R., Bhat H. Phytoestrogens and breast cancer prevention: possible mechanism of action. *Environmental Health Perspectives*. 2008; 116: 426-433.
79. Modica-Napolitano J S, Singh K. Mitochondria as targets for detection and treatment of cancer. *Expert Reviews in Molecular Medicine*. 2002; 11: 1-19.
80. Modica-Napolitano J S, Singh K. Mitochondrial dysfunction in cancer. *Mitochondrion*. 2004; 755-762.
81. Moll, U. M., Riori, G., and Lavine, A. J. Two distinct mechanisms alter p53 in breast cancer mutation and nuclear exclusion. *Proceedings National Academic Science*. 1992; 89: 7262-7266.

82. Mollace V., Iannone M., Muscoli C., Palma E., Granato T., Rispoli V., Nistico R., Rotiroti D., Salvemini D. The role of oxidative stress in paraquat-induced neurotoxicity in rats: protection by non peptidyl superoxide dismutase mimetic. *Neuroscience Letters*. 2002; 335: 163-166.
83. Moreira P, Custodio J, Morena A, Oliveira C, Santos M. Tamoxifen and Estradiol interact with the flavin mononucleotide site of mitochondrial complex 1 leading to mitochondrial failure. *Journal of Biological Chemistry* 2006; 281: 10143-52.
84. Naderi J, Hung M, Pandey S. Oxidative stress-induced apoptosis in dividing fibroblasts involves activation of p38 MAP kinase and over-expression of Bax: Resistance of quiescent cells to oxidative stress. *Apoptosis*. 2003; 8: 91-100.
85. Nazarewicz RR, Zenebe WJ, Parihar A, Larson SK, Alidema E, Choi J, Ghafourifar P. Tamoxifen induces oxidative stress and mitochondrial apoptosis via stimulating mitochondrial nitric oxide synthase. *Cancer Res*. 2007; 67: 1282-90.
86. Neuzil J., Tomasetti M., Zhao Y., Dong L., Birringer M., Wang X., Low P., Wu K., Salvatore B., Ralph S. Vitamine E analogues, a novel group of “mitocans”, as anticancer agents: the importance of being redox-silent. *Molecular Pharmacology*. 2007; 71: 1185-1199.
87. Nieves-Neira W., Pommier Y. Apoptotic response to camptothecin and 7-hydroxystaurosporine (ucn-1) in the 8 human breast cancer cell lines of the NCI anticancer drug screen: multifactorial relationships with topoisomerase I, protein kinase C, Bcl-2, p53, MDM-2 and caspase pathways. *Int. J. Cancer*. 1999; 82:396-404.
88. Orrenius S. Mitochondrial regulation of apoptotic cell death. *Toxicology Letters*. 2004; 149: 19-23.

89. Osborne C, Wilson P, Tripathy D. Oncogenes and tumor suppressor genes in breast cancer: potential diagnostic and therapeutic applications. *Oncologist*. 2004; 9(4): 361-77.
90. Olichon A, Baricault L, Gas N, Guillou E, Valette A, Belenguer P, Lenaers G. Loss of OPA1 perturbs the mitochondrial inner membrane structure and integrity, leading to cytochrome c release and apoptosis. *Journal of Biological Chemistry*. 2003; 278: 7743-7746.
91. Paine-Murrieta G.D., Taylor C.W., Curtis R.A., Lopez M.H., Dorr R.T., Johnson C.S., Funk C.Y., Thompson F., Hersh E.M. Human tumor models in the severe combined immuno deficient (scid) mouse. *Cancer Chemother Pharmacol*. 1997; 40: 209-214.
92. Pandey S, Smith B, Walker P R, and Sikorska M. Caspase-dependent and independent cell death in rat hepatoma 5123tc cells. *Apoptosis*. 2000; 5: 265-275.
93. Pandey S., Kekre N., Naderi J. Induction of apoptotic cell death specifically in rat and human cancer cells by pancratistatin. *Artificial Cells, Blood Substitutes, and Biotechnology*. 2001; 33: 1-17.
94. Parlo RA, Coleman PS. Enhanced rate of citrate export from cholesterol-rich hepatoma mitochondria. The truncated Krebs cycle and other metabolic ramifications of mitochondrial membrane cholesterol. *Journal of Biological Chemistry*. 1984; 259: 9997-10003.
95. Pedram A., Razandi M., Wallace D., Levin E. Functional estrogen receptors in the mitochondria of breast cancer cells. *Molecular Biology of the Cell*. 2006; 17: 2125-2137.
96. Pettit R., Backhaus A., Boyd R., Meerow W. Antineoplastic Agents 256: Cell Growth Inhibitory Isocarbostryls from *Hymenocallis*. *Journal of Natural Products*. 1993; 56:1682.

97. Plesnila N., Zinkel S., Le DA., Armin-Hanjani S., Wu Y., Qlu J., Chlarugi A., Thomas SS., Kohane DS., Korsmeyer SJ., Moskowitz MA. Bid mediates neuronal cell death after oxygen glucose deprivation and focal cerebral ischemia. *PNAS*. 2001; 98(26): 15318-15323.
98. Polyak K, Li Y, Zhu H, Lengauer C, Willson J K, Markowitz S D, Trush M A, Kinzler K W, Vogelstein B. Somatic mutations of the mitochondrial genome in human colorectal tumors. *Nature Genetics*. 1998; 20: 291-3.
99. Reed J C. Mechanisms of Bcl-2 family protein function and dysfunction in health and disease. *Behring Institute Mitteilungen*. 1996; 97: 72-100.
100. Reed J C. Warner-Lambert/Parke-Davis Award Lecture: Mechanisms of Apoptosis. *American Journal of Pathology*. 2000; 157(5): 1415-1426.
101. Reed J C. Apoptosis-based therapies. *Nature Reviews in Drug Discovery*. 2002; 1: 111-121.
102. Reedy S., Wang X., Samaha H., Lubet R., Steele E., Kelloff J., Rao V. *Cancer Research*. 1997; 57: 420-425.
103. Sattler M, Liang H, Nettesheim D, Meadows R P, Harlan J E, Eberstadt M, Yoon H S, Shuker S B, Chang B S, Minn A J, Thompson C B, Fesik S W. Structure of Bcl-xL-Bak Peptide Complex: Recognition Between Regulators of Apoptosis. *Science*. 1997; 275(5302): 983 – 986.
104. Selvanayagam, P., Rajaraman, S. Detection of mitochondrial genome depletion by a novel cDNA in renal cell carcinoma. *Lab. Invest*. 1996; 74: 592-599.
105. Shao W., Brown M. Advances in estrogen receptor biology: prospects for improvements in targeted breast cancer therapy. *Breast Cancer Res*. 2004; 6: 39-52.

106. Shimizu S, Narita M, Tsujimoto Y: Bcl-2 family proteins regulate the release of apoptogenic cytochrome c by the mitochondrial channel VDAC. *Nature*. 1999; 399: 483-487.
107. Smith CL., O'Malley BW. Coregulator Function: A Key to Understanding Tissue Specificity of Selective Receptor Modulators. *Endocrine Reviews*. 2004; 25(1): 45-71.
108. Somayajulu M, McCarthy S, Hung M, Sikorska M, Borowy-Borowski H, Pandey S. Role of mitochondria in neuronal cell death induced by oxidative stress; neuroprotection by Coenzyme Q₁₀. *Neurobiology of Disease*. 2005; 18: 618-627.
109. Soto-Cerrato V., Llagostera E., Montaner B., Scheffer G.L., Perez-Tomas R. Mitochondria-mediated apoptosis operating irrespective of multidrug resistance in breast cancer cells by the anticancer agent prodigiosin. *Biochemical Pharmacology*. 2004; 1345-1352.
110. Susin S A, Lorenzo H K, Zamzami N, Marzo I, Snow B E, Brothers G M, Mangion J, Jacotot E, Costantini P, Loeffler M, Larochette N, Goodlett D R, Aebersold R, Siderovski D P, Penninger J M, Kroemer G. Molecular characterization of mitochondrial apoptosis-inducing factor. *Nature*. 1999; 397(6718): 441-6.
111. Szabo C. Mechanisms of cell necrosis. *Critical Care Med*. 2005; 33: 530-534.
112. Trock BJ., Leonessa F., Clarke R. Multidrug resistance in breast cancer: a meta-analysis of MDR1/gp170 expression and its possible functional significance. *Journal of the National Cancer Institute*. 1997; 89(13): 917-931.
113. Verhagen AM., Ekert PG., Pakusch M., Silke J., Connolly LM., Reid GE., Moritz RL., Simpson RJ., Vaux DL. Identification of DIABLO, a mammalian protein that promotes apoptosis by binding to and antagonizing IAP proteins. *Cell*. 2000; 102:43-53.

114. Villa, A M, Doglia S M. Mitochondria in tumor cells studied by laser scanning confocal microscopy. *Journal of Biomedical Optics*. 2004; 9: 385-94.
115. Wang J., Barnes RO., West NR., Olson M., Chu JE., Watson PE. Jab1 is a target of EGFR signaling in ER α negative breast cancer. *Breast Cancer Research*. 2008; ahead of print.
116. Webb MS., Johnstone S., Morris TJ., Kennedy A., Gallagher R., Harasym N., Harasym T., Shew CR., Tardi P., Dragowski W., Mayor LD., Baley MB. In-vitro and in-vivo characterization of a combination chemotherapy formulation consisting of vinorelbine and phosphatidylserine. *European Journal of Pharmaceutics and Biopharmaceutics*. 2007; 65: 289-299.
117. Weinberg R A. How cancer arises. *Scientific America*. 1996; 40-48.
118. Willett W., The search for the causes of breast and colon cancer. *Nature*. 1989; 338: 389-394.
119. Wolter K., Hsu Y., Smith C., Nechushtan A., Xi X. G., Youle R. Movement of Bax from the cytosol to the mitochondria during apoptosis. *Journal of Cell Biology*. 1997; 139: 1281-1292.
120. Yang E., Zha J., Jockel J., Boise LH., Thompson CB., Korsmeyer SJ. Bad, a heterodimeric partner for Bcl-xl and Bcl-2 displaces Bax and promotes cell death. *Cell*. 1995; 80: 285-291.
121. Yeung T K, Germond C, Chen X, Wang Z The mode of action of taxol: apoptosis at low concentration and necrosis at high concentration. *Biochemistry and Biophysics Research Communications*. 1999; 263(2): 398-404.

122. Yin X., Luo Y., Cao G, Bai G., Pei W., Kuharsky D., Chen J. Bid-mediated Mitochondrial Pathway Is Critical to Ischemic Neuronal Apoptosis and Focal Cerebral Ischemia. *The Journal of Biological Chemistry*. 2002; 277(44): 42074-42081
123. Yuan H., Mutaomba M., Prinz I, Gottlieb R. Differential processing of cytosolic and mitochondrial caspases. *Mitochondrion*. 2001; 1: 61-69.
124. Yue W., Zhou D., Chen S., Brodie A. A new nude mouse model for postmenopausal breast cancer using MCF-7 cells transfected with the human aromatase gene. *Cancer Research*. 1994; 54: 5092-5095.
125. Zhang Y., McLaughlin R., Goodyer C., LeBlanc A. Selective cytotoxicity of intracellular amyloid beta peptide 1-42 through p53 and Bax in cultured primary human neurons. *Journal of Cellular Biology*. 2002; 156: 519-529.
126. Zhai Y.F., Esselman W.J., Oakley C.S., Chang C.C., Welsch C.W. Growth of MCF-7 human breast carcinoma in severe combined immunodeficient mice: growth suppression by recombinant interleukin-2 treatment and role of lymphokine-activated killer cells. *Cancer Immunology Immunotherapy*. 1992; 35: 237-245.
127. Zoratti M, Szabo I. The mitochondrial permeability transition. *International Journal of Biochemistry, Biophysics and Molecular Biology*. 1995; 1241: 139-179. Zou H, Henzel W J, Liu X, Lutschg A, Wang X. Apaf-1, a human protein homologous to C. elegans CED -4, participates in cytochrome c- dependent activation of caspase-3. *Cell*. 1997; 90: 405-413.

VITA AUCTORIS

NAME: Peter Siedlakowski

PLACE OF BIRTH: Gorzow, Poland

EDUCATION: University of Windsor

2006 – 2008 Master's of Science: Biochemistry

2002 – 2006 Bachelor's of Science: Honour's Biochemistry